University of Massachusetts Amherst

ScholarWorks@UMass Amherst

November 2015

Chemical Biology-Based Probes For The Labeling Of Targets On Live Cells

Amanda M. Hussey
University of Massachusetts - Amherst

Follow this and additional works at: https://scholarworks.umass.edu/dissertations_2

Part of the Biochemistry Commons, Molecular and Cellular Neuroscience Commons, and the Organic Chemistry Commons

**CHEMICAL BIOLOGY-BASED PROBES FOR THE LABELING OF TARGETS
ON LIVE CELLS**

A Dissertation Presented

by

AMANDA M. HUSSEY

Submitted to the Graduate School of the
University of Massachusetts Amherst in partial fulfillment
of the requirements for the degree of

DOCTOR OF PHILOSOPHY

September 2015

Department of Chemistry

CHEMICAL BIOLOGY BASED-PROBES FOR THE LABELING OF TARGETS ON
LIVE CELLS

A Dissertation Presented

by

AMANDA M. HUSSEY

Approved as to style and content by:

_____
James J. Chambers, Chair

_____
Richard W. Vachet, Member

_____
Nathan A. Schnarr, Member

_____
Peter Chien, Member

_____
Craig T. Martin, Department Head Department of Chemistry

DEDICATION

To my family and friends. Thank you all.

ACKNOWLEDGMENTS

ABSTRACT

CHEMICAL BIOLOGY-BASED PROBES FOR THE DETECTION OF RECEPTORS
ON LIVE CELLS

SEPTEMBER 2015

AMANDA M. HUSSEY

B.S., UNIVERSITY OF THE SCIENCES IN PHILADELPHIA

Ph.D., UNIVERSITY OF MASSACHUSETTS AMHERST

Directed by: Professor James J. Chambers

Proper detection is the key to studying any processes on the cellular scale. Nowhere is this more evident than in the tight space which confines the synaptic cleft. Being able to ascertain the location of receptors on live neurons is fundamental to our understanding of not only how these receptors interact and move inside the cell but also how neurons function. Most detection methods rely on significantly altering the receptor; both tagging with a fluorescent protein or targeting the receptor by a fluorescent reporter in the form of a small molecule causes significant difficulties. These localization techniques often result in forced dimerization, unnatural movement, and at worst inactivation of the receptor.

Small molecule organic dyes provide a potential advantage because they can be structurally functionalized to target the protein of interest in a non-perturbing fashion which allows for information to be gathered about the targeted receptor. The work I initiated in the Chambers lab first focused on using a ligand directed fluorophore connected via a photo-labile linker. Through the use of epifluorescence microscopy, I determined that this probe targets glutamate receptors, however questions about subtype inclusion could not be addressed.

The pharmacophore that our first probe is based on could be much more promiscuous than is presently appreciated in the field of neurobiology. Thus, we designed a new series of probes to allow for covalent modification and affinity purification of endogenous receptors. The second generation of probes set out to answer the questions left by the first. Purified proteins were subjected to SDS-PAGE analysis and could be applied to proteomic identification of receptors.

In addition to ligand directed probes, we have also initiated a project on a new, bimolecular photoaffinity probe in which the new methodology continues to develop. The initial studies were performed to ensure that our new strategy is able to be used in biological systems.

TABLE OF CONENTS

LIST OF FIGURES

LIST OF SCHEMES

CHAPTER 1

INTRODUCTION

Portions of this chapter have been published as Hussey, A.M. and Chambers, J.J. *ACS Chem.*

Neurosci. **2015** 6(1), pp189-98

1.1 Neuronal Structure

The brain is a complex organ composed of 1,000,000s of neurons which interface with each other in order for the body to function. Neurons are post-mitotic, highly polarized cells which transmit information through chemical and electrical signals. Neurons contain three major morphological regions: a soma, or cell body, which contains the nucleus and other cytoplasmic organelles, a single axon which extends from the cell body to transmit neuronal information, and numerous dendrites which may be spiny or non-spiny which receive information. (Figure 1.1)[1]
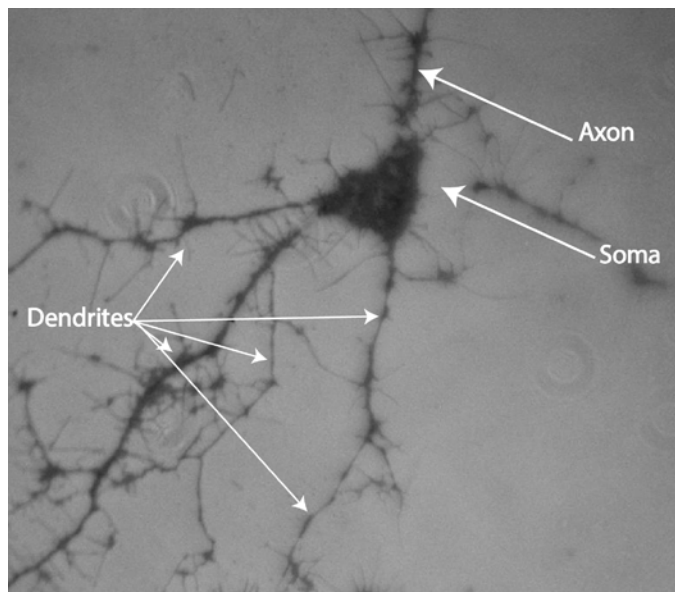
Figure 1.1: Annotated image of a neuron

Neurons communicate via transfer of electrochemical signals from the axon terminal to the dendrites. This area is called a synapse. The axon terminal of one neuron acts as the presynaptic portion of the synapse, while the dendrite acts as the post-synaptic portion. The space in-between is the synaptic cleft, which measures to be about 20 nm in

size.[2] It is in this area where neurotransmitter receptors reside and synaptic

communication takes place.

1.1.2 Synaptic Communication and Plasticity

Neuronal communication involves the transfer of neurotransmitter from the pre-

synaptic side of one neuron to the post-synaptic side of another neuron. It is on the post-

synaptic side where neurotransmitter receptors and ion channels reside. (Figure 1.2)
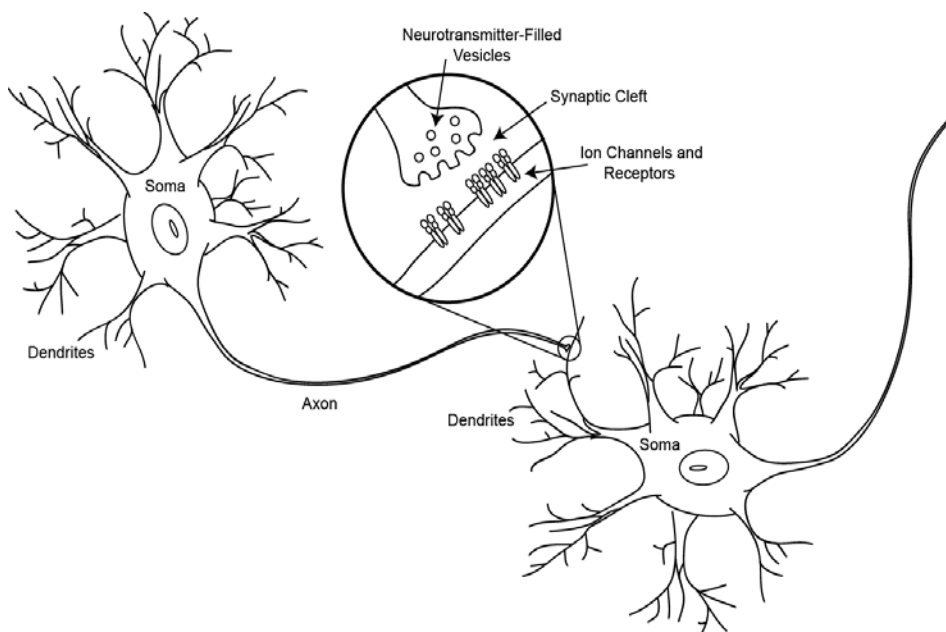
Figure 1.2: Cartoon image of synaptic communication. Neurotransmitter flows from the pre-synaptic side of one neuron to the post-synaptic side of another. Neuronal receptors reside on the postsynaptic side to receive the neurotransmitter. Reprinted with permission from Hussey, A.M. and Chambers, J.J. *ACS Chem. Neurosci.* **2015** 6(1), pp189-98. Copyright 2015 American Chemical Society.

How the synapse strengthens or weakens in response (e.g. the addition or

removal of neuronal receptors from synapse) to a chemical response is termed synaptic

plasticity, which can be controlled on either side of neuronal communication. On the

presynaptic side, the flow of neurotransmitter can be regulated. On the postsynaptic side,

the type and density of receptors is regulated. Regulation on the post synaptic side either

adds more neuronal receptors, known as long term potentiation (LTP), or removes

receptors, known as long term depression (LTD).[3] Both LTP and LTD are thought to underlie memory formation in the brain. α-amino-3-hydroxy-5-methyl-4-isoxazole propionic acid receptors (AMPARs) are the critical receptors which mediate fast excitatory synaptic processes during LTP. Thus, the mechanism of how these receptors are trafficked is of fundamental importance.

1.1.3 Long Term Potentiation

LTP involves the insertion into the plasma membrane and the rapid recycling of AMPARs through the endosomal systems (Figure 1.3). Until very recently, LTP was thought to be mediated by the insertion of GluA1-containing AMPARs into the synaptic membrane, thus, there is a large amount of characterization of these processes. The combination of calcium being tightly regulated by all cells and the low abundance of calcium permeable AMPARs on the surface lead to the thought that these receptors play a minor role in LTP. However, calcium permeable AMPARs have now been shown to play a larger role than originally thought in LTP, though the mechanism of how is not well understood.[4]

A key player in long term potentiation is phosphorylation of AMPARs by protein kinases.[5] One particular class of kinases thought to be important in LTP are the Ca^{2+}/calmodulin-dependent protein kinases (CaMK), specifically, CaMKII. AMPAR conductance is increased when CaMKII phosphorlylates GluA1 at S831 directly which may induce LTP.[6] Another key kinase is protein kinase A (PKA), which phosphorylates GluA1 at S845. Phosphorylation at this latter site allows for the increased chance of the channel opening, thus more neurotransmitter to go through the channel.[7] Phosphorylation of GluA1 S845 also allows for some of the delivery of GluA1 to synapses, as well as to the extrasynaptic membrane.[8] Synaptic associated protein 97 kDa (SAP97) is in the PSD95-like membrane-associated guanylate kinase family, and has been found to be

important during LTP. It binds to the C-teminus of GluA1 and plays a role in the phosphorylation of GluA1, leading to enhancement of LTP.[5b]
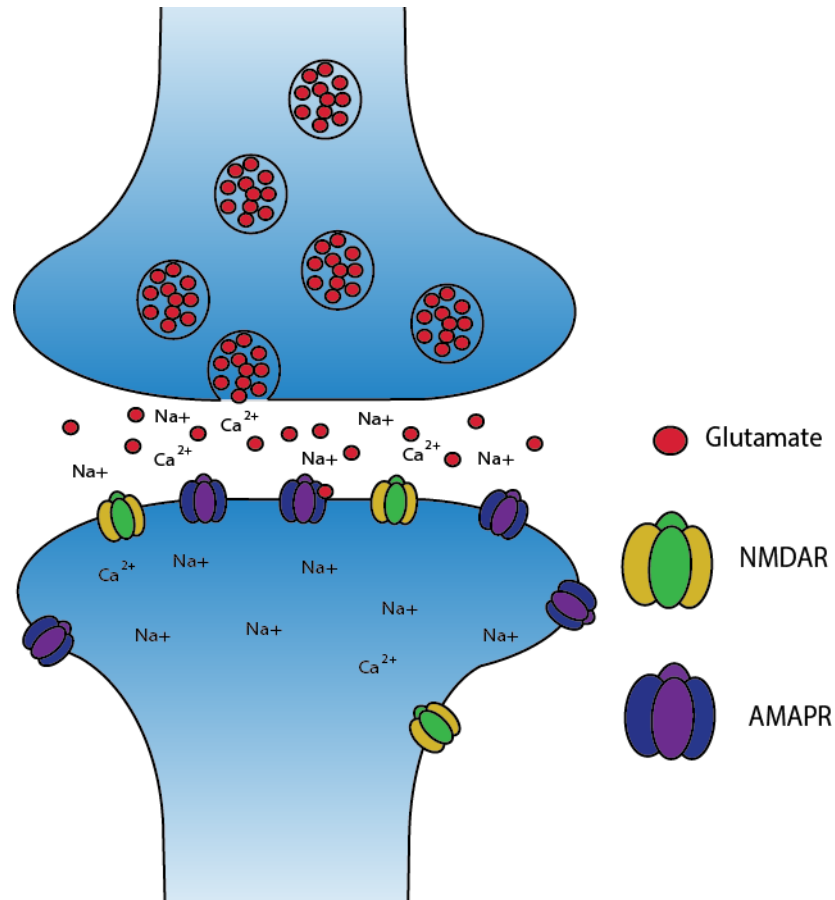
Figure 1.3: Cartoon of LTP. The pre-synaptic side of one neuron releases neurotransmitter to the post-synaptic side of another. This is thought to be pivotal in memory formation.

In pyramidal neurons, LTP induces transient and rapid insertion of GluA2-lacking calcium-permeable AMPARs into the membrane presumably to enhance the received signal from the presynaptic terminal.[9] The exact mechanisms of how calcium permeable AMPARs are trafficked to the surface are still under investigation. Addiction studies with cocaine in mice have shown there is an increase in the number of calcium permeable AMPARs found at the synaptic membrane after initial drug-dose exposure. It is believed that the overall number of AMPARs does not increase; rather, calcium

permeable ones replace calcium impermeable ones. This creates a long-lasting plasticity, even after a single injection, possibly underlying some of the addictive seeking behavior.[10]

1.1.4 Long Term Depression

LTD is the removal of AMPARs from the plasma membrane. This can be done through either endocytotic processes or internalization of the receptors. Endocytosis can be done through a clathrin–dependent method in which the AMPARs are removed for possible intracellular sorting.[11] The mechanisms of LTD are harder to pin down, as most evidence shows that LTD is caused by endocytosis of AMPARs. However, there are many factors that could cause endocytosis and internalization resulting from provocation from stimuli such as calcium influx, calcineurin, synaptic activity, ligand binding, and insulin influx. These stimuli can result in synaptic vesicle endocytosis and endocytosis of AMPARs to the early endosome, which can be hard to differentiate from that caused by LTD in cultured cells. [8, 11-12]
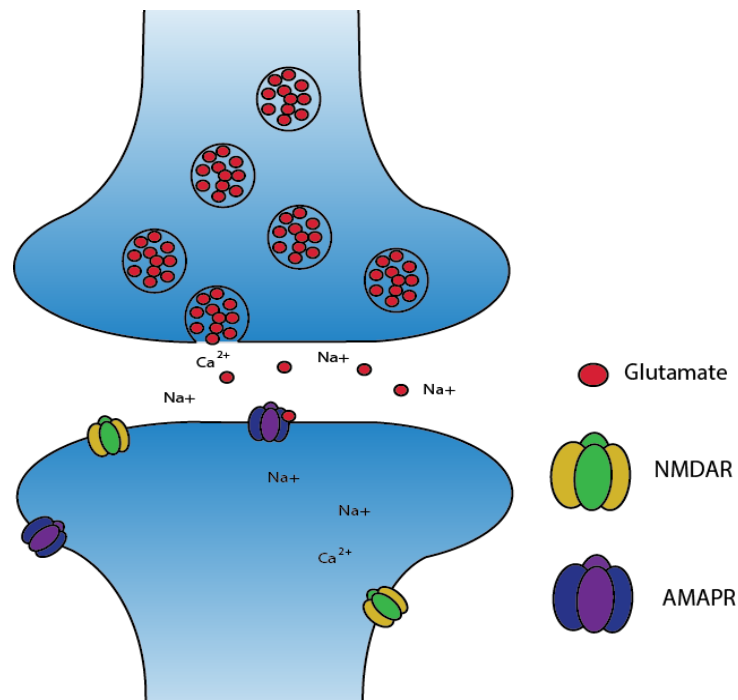
Figure 1.4: Cartoon of LTD. Fewer receptors are present on the surface of the post-synaptic side of the receptor. It is a synaptic pruning process which occurs during sleep.

5

Glutamate receptor interacting proteins (GRIP1 and GRIP2) are another class of proteins which aid in trafficking of AMPARs during synaptic plasticity. In LTD, phosphorylation of S880 and Y886 on GluA2 disrupt the binding of GRIP1, allowing for internalization of AMPARs, thus reducing the numbers in the synapse.[13] GluA2 can also interact with clathrin adaptor protein AP-2, which leads to the NMDA-induced internalization of AMPARs in an LTD like fashion.[8] PICK1 is another protein that plays a role in the LTP/LTD cascade. The interaction GluA2 and PICK1 is critical in leading to LTD [14], thus prompting the idea that PICK1 removes GluA2 containing AMPARs from the synapse.[15]

1.1.5 Glutamate Receptors

There are many classes of neurons including inhibitory, excitatory, and neuromodulary. Both inhibitory and excitatory neurons can be further broken down into neurons that make local contacts and those that make distant contacts.[1] Inhibitory neurons include GABAergic neurons, medium spiny neurons in the basal ganglia and Pukinje cells, just to name a few. These neurons are characterized by small, localized projections which help to regulate excitatory neurons. Excitatory neurons include pyramidal neurons and spiny stellate neurons found in the cortex. These cells project both locally in the cortex and make long range connections into different neuronal areas. They are responsible for carrying the electrochemical communications within the brain.[1]

Fast excitatory glutamatergic transmission is exclusively mediated in the central nervous system (CNS) by ionotropic glutamate receptors (iGluRs). These include kanaite receptors (KA), n-methyl-d-aspartate receptors (NMDARs), and α-amino-3-hydroxy-5-methyl-4-isoxazole propionic acid receptors (AMPARs). IGluRs are characterized as tetramers which are encoded by 18 genes. Several of these genes undergo alternative splicing and RNA editing. All iGluRs are encompassed by three distinct domains: an

extracellular N-terminus, a central transmembrane domain, and an intracellular C-terminus domain (Figure 1.5).[8, 16]
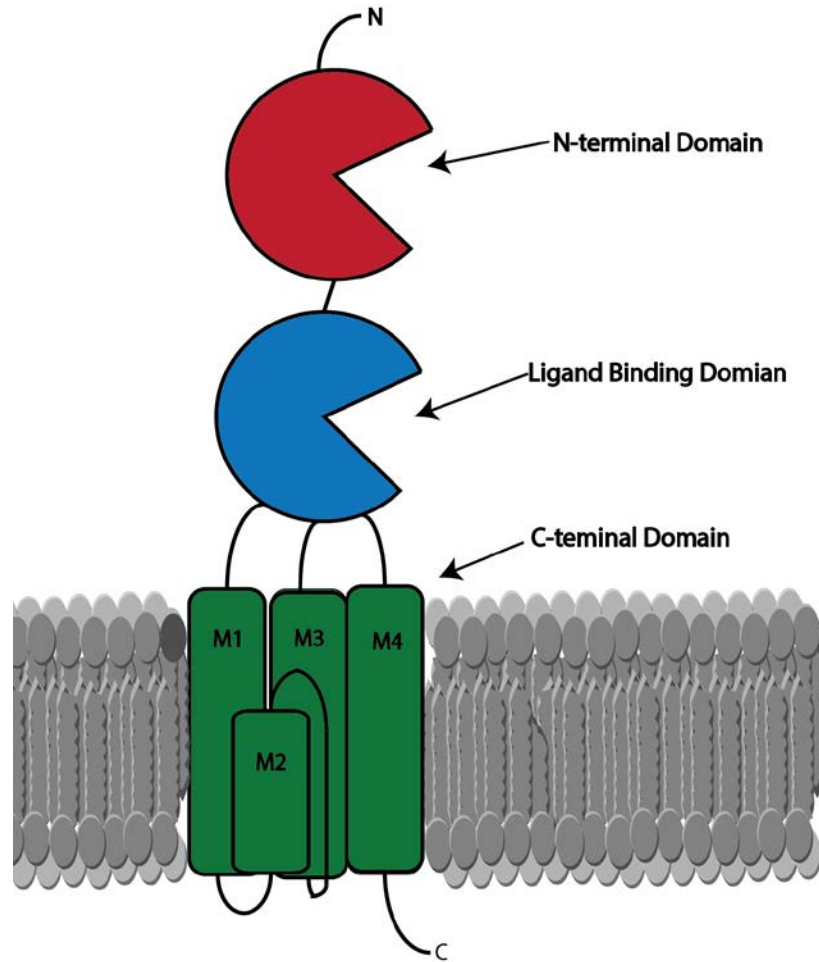
Figure 1.5: Cartoon representation of iontropic glutamate receptor in the membrane. All iGluRs follow the same orientation with the N-terminus and ligand binding domain in the extracellular space, four transmembrane domains, and the C-terminus in the intracellular space.

α−amino-3-hydroxy-5-methyl-4-isoxazolepropionic acid, AMPA

N-methyl-D-aspartic acid, NMDA
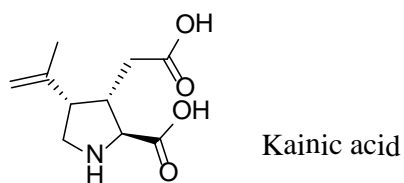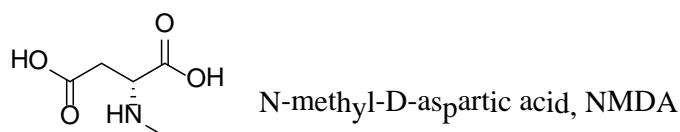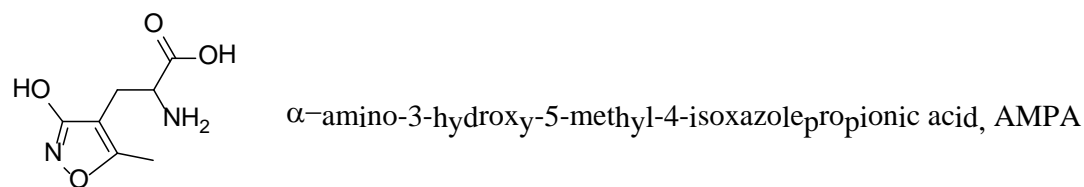
Kainic acid

Figure 1.6: Structures of glutamate analogues AMPA, NMDA, and kainic acid

1.1.6 Kainate Receptors

Kainate receptors are a subclass of glutamate receptors named for their activation by the synthetic agonist kainic acid (Figure 1.6). They are tetramers of GluK1-GluK5 and their main function is to modulate neuronal excitability and synaptic transmission. They differ from other ionotropic glutamate receptors, as they are located in pre-synaptic terminals rather than the post-synaptic terminals.[16a] Kainate receptors are generally calcium impermeable, but there is evidence of a calcium permeable form.

1.1.7 NMDARs

NMDARs are named for their activation by the synthetic analogue of glutamate, n-methyl-d-aspartate (Figure 1.6), and are important regulators of synaptic plasticity. They form obligate heteromers of GluN1, GluN2A-GluN2D, GluN3A, or GluN3B in a tetrameric fashion. Channel composition combinations include two GluN1 and two GluN2A-GluN2D subunits, and two GluN subunits with one GluN2A-D subunit and one GluN3 subunit. Once assembled, they act as Ca^{2+} permeable channels, which require both

glutamate and glycine for activation.[16a] NMDA receptors are blocked by extracellular Mg^{2+} ions which blocks the channel so that there is little ion flux through it in the absence of post-synaptic depolarization, allowing for a crucial role in activity dependent synaptic communication.[17]

1.1.8 AMPARs

AMPA receptors are named for their sensitivity towards the glutamate analogue α-amino-3-hydroxy-5-methyl-4-isoxazole propionic acid (Figure 1.6). They are the most abundant of the ionotropic glutamate receptors and mediate excitatory neurotransmission. They assemble as either homo or heterotetramers of GluA1-GluA4, which share 68-73% sequence identity.[18] The most common of the tetrameric pairings are those containing GluA1-GluA2 and GluA2-GluA3.[8] AMPARs have some calcium permeability (discussed in section 1.1.9) and are impermeable to Mg^{2+}.[16a] AMPARs have an inwardly rectifying current, which can be blocked by the application of polyamine toxins (described in section 1.1.11).

Like other glutamate receptors, AMPARs contain an extracellular N-terminus, central transmembrane domain, and intracellular C-terminus. The central transmembrane domain can be further broken down into three distinct transmembrane portions M1, M3, and M4, as well as an M2 hairpin structure which changes the direction so it returns to the intracellular side of the cell (Figure 1.5).[8, 18] There are two subforms of each subunit, referred to as "flip" and "flop", as they vary by an interchangeable 38 amino acid sequence before the M4 transmembrane portion.[18-19]

Assemblies of AMPARs start in either the endoplasmic reticulum (ER) or the Golgi apparatus and are trafficked to the plasma membrane. In the ER, the C-terminus is subjected to palmitoylation, phosphorylation, and ubiquination for regulation. The C-terminus is also the site where signaling molecules (such as protein interacting with kinase C, PICK) and cytoskeletal proteins (such as kinesin) bind, aiding in insertion into

either the soma or synapses.[3, 20] These receptors are then in a dynamic equilibrium with the synapse.[17, 20] The amount of receptors is variable dependent upon location and cell type, and is also dependent upon endo and exocytosis at the postsynaptic membrane.[3, 8] AMPARs are known to move in endosomes in a recycling process that first involves endocytosis of the receptor, then entry into the endosomal system, and then final movement back to the receptor surface.[4]

AMPAR assemblies are controlled not only by posttranslational modifications, such as phosphorylation of key residues on the individual subunits, but also by regulatory proteins. One of the key classes of proteins to act as AMPAR regulators are transmembrane AMPAR regulatory proteins (TARPs). There have been many TARPs identified, including stargazin (ɣ-2), ɣ-3,-4,-5,-7, and -8.[21] Each AMPAR is thought to contain 1-4 TARPs for stabilization of their pore, and each TARP influences the behavior of the particular AMPAR.[21a, 21c] Stabilization of synapses by TARPs is via interaction with PSD-95 and other membrane-associated guanylate kinases (MAGUKs) that are present, as TARPs bind to the PDZ domain on each.[22] TARPs influence AMPAR behavior in a variety of ways including increasing single channel conductance, slowing deactivation and desensitization, modification of pharmacological properties by making kainate a better agonist, and, perhaps most importantly to this dissertation, attenuating voltage-dependent blocks by endogenous polyamines.[21a, 23] TARPs are also involved in AMPAR trafficking, as they promote AMPAR maturation, cellular delivery and clustering, and are most likely involved in both LTP and LTD.[21a-c]

AMPARs can insert themselves into the membrane in a couple of different fashions. First is through kinesin directing endosomes containing AMPARs, and the second is through vesicle fusion events with SNARE proteins on the surface of the membrane.[24] Once the AMPAR cargo is delivered, the receptor can travel to an active spine via lateral diffusion.[25]

10

1.1.9 Calcium Permeability in AMPARs

AMPA receptors can either be calcium permeable or calcium impermeable. Those receptors that contain GluA1, GluA3, and Glu4 combinations are calcium permeable. Ones which contain GluA2 are generally calcium impermeable. There is a subclass of calcium permeable AMPA receptors which contain unedited GluA2 receptors, which have been thought to be pivotal in some disease states, such as amyotrophic lateral sclerosis (ALS). The calcium permeability of GluA2 is mediated by a single RNA codon edit known as the Q/R site inside the M2 domain of the subunit. Here, an encoded glutamine is changed to an arginine via a single nucleoside edit. In the nucleotide code, CAG (glutamine), the encoded adenosine is changed to inosine (CIG), which is read as CCG (arginine). This edit is mediated by the enzyme adenosine deaminase acting on RNA (ADAR2), as it recognizes the Q/R site through the formation of a duplex structure of the editing site and the editing site of the complimentary sequence.[26] This edit occurs postnatally and accounts for only about 1% of the GluA2 RNA. ADAR2 activity is important as ADAR2 knock out (KO) mice die very young from epilepsy due to the increased amount of calcium influx from the larger population of unedited GluA2. [18, 27] It is important to note that AMPARs which do contain unedited forms of GluA2 may be very effective at inducing neurotoxicity, suggesting their role in the disease states mentioned in section 1.4. [28]

The populations of calcium permeable AMPA receptors are not consistent or uniform, but are highly dependent on developmental stage of the neurons as well as cell type. For example, inhibitory interneurons contain larger amounts than that of mature excitatory neurons.[17, 29] However, immature excitatory neurons (e.g. postnatal culture) have high populations of calcium permeable AMPARs.[30] The number of calcium permeable AMPARs can increase due to pathological and physiological conditions found in the brain, meaning that in times of stress and disease, their numbers can increase

greatly. This induced stress from the extra calcium makes it harder for the neuron to regain normal function thus they might perish.

Calcium permeable AMPARs, unlike NMDARs, are not subject to blocks by extracellular cations, such as Mg^{2+}, but are subject to voltage dependent block by polyamines. They are also permeable towards other divalent cations, specifically Zn^{2+}. Zn^{2+} is toxic to neurons and can enter through calcium permeable channels. The entry of Zn^{2+} can lead to ischemic like injury and neurodegeneratation.[17, 31]

1.1.10 Calcium Permeable AMPA Receptors in Excitatory Disease

AMPA receptors are involved in a number of disease states. This is influenced by a number of factors including influx of calcium, certain drugs (such as cocaine), disease progression, and ischemic trauma.

Forty percent of patients, who are being treated with l-DOPA for Parkinson's disease, and other similar diseases, will develop l-DOPA induced dyskinesia which is linked to pathological corticostriatal synaptic plasticity such as altered expression of striatal opioid peptides. This presents enhanced corticostriatal glutamatergic transmission by which the mechanism and expression of l-DOPA induced dyskinesia plays a critical role. Animal studies have shown that AMPARs may be present during these induced dyskinesias as enhanced trafficking and phosphorylation of AMPARs in the striatum was present.[32]

More recently, GluA2 containing calcium permeable AMPA receptors have been implicated as a potential cause of ALS. ALS has a couple of different disease phenotypes; the most well studied being the familial form which has defects in copper zinc superoxide dismutase 1 (SOD1) known as ALS1. Familial cases of ALS only compose 10% of all new ALS diagnoses, so there is ultimately another mechanism, or mechanisms, of how the disease initiates and progresses. It is also noteworthy that the death inducing molecular mechanisms differ between sporadic ALS and ALS1, as those

who have sporadic ALS do not share the same disease causative mutations that are characteristic of ALS1. Also, those who have ALS1 lack the accumulation of TDP-43 (transactive response DNA binding protein 43 kDa), a transcriptional protein whose ubiquinated, phosphorylated form is a marker for ALS [33] which is seen in patients having sporadic ALS. [27] Transgenic animal studies have suggested a role of GluA2 containing calcium permeable AMPA receptors as there is a large amount of motor neuron loss in these animals. Crosses of SOD1 mutant mice and mice which contain a nonlethal calcium permeable GluA2 edit (asparagine in the Q/R site) lead to acceleration in the disease.[27, 34] Analysis of brain samples from ALS patients after autopsy show a decreased amount of ADAR2 mRNA in the ventral grey matter compared to those of who are non-symptomatic for ALS, thus showing a possible correlation of ADAR2 reduction and motor neuron death due to inefficient editing of the Q/R site.[27]

Calcium permeable AMPARs are involved in brain ischemias, or loss of blood flow to the brain leading to reduced metabolic rates, and ultimately total neuronal death. When present in early brain development, there is an increased rate of neuronal death in the white and grey matter coinciding with the times that there are a marked increase in the numbers of calcium permeable AMPARs present, suggesting the link of these receptors to ischemic susceptibility.[35] Ischemia can also be present after cardiac arrest, resulting in damage to, and potential loss of, of neurons. Pyramidal neurons in the hippocampus are particularly vulnerable to this type of injury. The amount of calcium permeable AMPARs rises after ischemia, resulting in a greater injury due to the ischemic event, and ultimately neuronal death due to the induction of Ca^{2+} permeability.[17, 36]

1.1.11 Polyamine Toxins as Tools in Neurobiology

Polyamine toxins have become a key tool as antagonists of calcium permeable AMPA receptors. AMPA receptors, specifically calcium permeable ones, are subjected to

voltage dependent blocks by polyamines, but are not blocked by extracellular cations. This allows for the free flow of Ca^{2+} through the channel.[37]

Polyamine toxins (Figure 1.7) are low molecular weight secondary metabolites which have mainly been isolated from the venom of spiders and wasps. These toxins are not deadly; rather they have a reversible paralytic effect. Argiotoxin-636 (Arg-TX-636) was the first isolated polyamine toxin isolated from the venom of the orb weaver spider. Next came Joro spider toxin (JSTX-3), isolated from the spider of the same common name. The venom of the Egyptian digger wasp was known to block iGluRs since the early 1980's, its isolation of the active component, philanthotoxin-433, provided another toxin.[38] All of these toxins share two structural moieties in common; an aromatic head group and a polyamine tail, which then enabled the synthesis of napthylacetylspermine, a synthetic polyamine.[39] All act as open-channel ion blockers of iGluRs, are use-dependent, and voltage-dependent coming from the polyamine blocking the inward current of the AMPAR channel. The use-dependence comes from the ion channel needing to be open for targeting by the exogenous polyamine application. It is important to re-iterate that this is true of all AMPARs which do not contain an edited GluA2 subunit. The presence of the arginine in the channel will not allow for binding of the polyamine into the ion channel due to charge repulsion.[38a, 40]
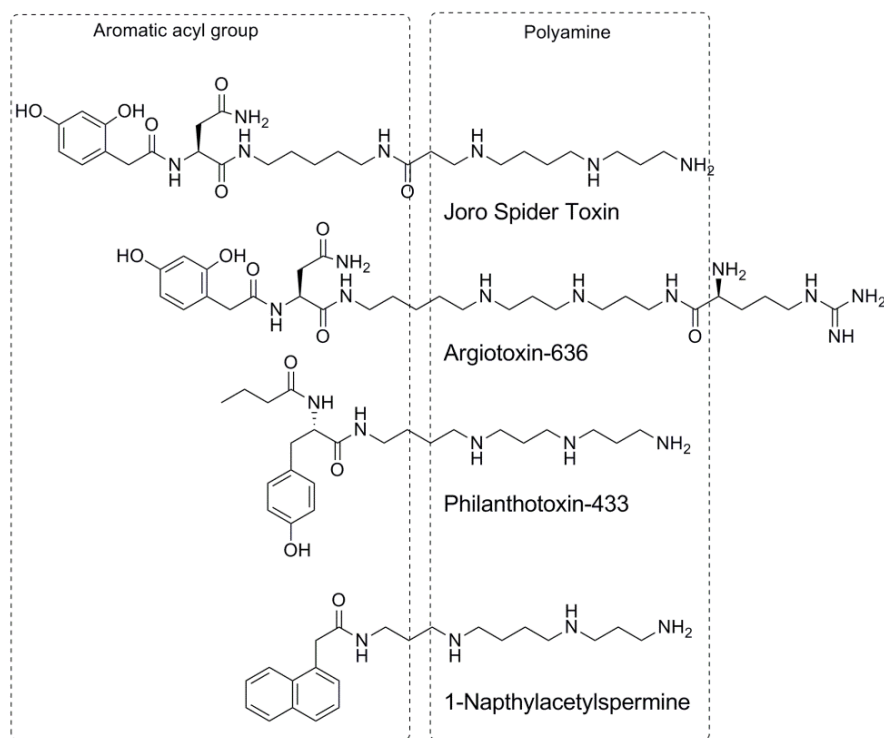
Figure 1.7: Structures of polyamine toxins with activity towards AMPARs.
The common moieties of the aromatic acyl head group and the
polyamine tail are pointed out in the box

Binding of polyamine toxins to ion channel pores has been explored through a
variety of molecular modeling and structure-activity experiments as there is no X-ray
crystal structure data available for precise details of the full AMPA receptor. However, a
crystal structure is available of the GluA2 subunit.[41] From the collected data, polyamine
toxins are suggested to bind so that the polyamine tail binds into the ion pore and the
acryl head acts as a block to the ion channel.[42]

1.2 Imaging Techniques
Small molecule fluorophores and proteinaceous fluorophores have been the main
tools used in the visualization of ion channels, neuronal receptors, and other targets on
live neurons. The main methods for visualization can be divided into two broad
categories; genetic methods and non-genetic methods. Genetic methods involve encoding
the receptor of interest to produce either a fluorescent reporter or a small tag for

attachment of a fluorophore. Non-genetic methods involve the delivery of biological or

small molecule reporters for visualization. This can be summarized by Figure 1.8
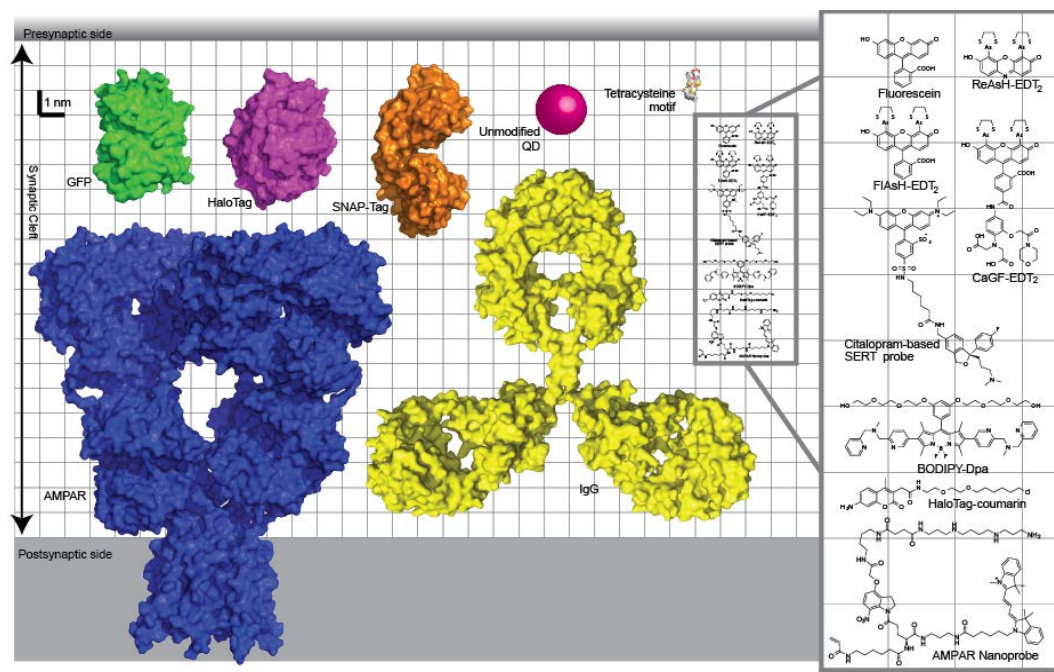
Figure 1.8: Size comparison of common protein tag**s.** All of the common protein tags for visualization of neuronal receptors (antibodies, GFP, HaloTag, Snap Tag, quantum dots, and tetracysteine motifs) have been scaled relative to the size of an AMPAR. The size comparisons for small molecule organic probes are in the right panel. Reprinted with permission from Hussey,A.M. and Chambers, J.J. *ACS Chem. Neurosci.* **2015** 6(1), pp189-98. Copyright 2015 American Chemical Society.

1.2.1 Genetic Imaging Techniques

Genetic imaging techniques have benefited greatly from the discovery of

fluorescent proteins (FPs). FPs can be encoded into to the DNA of a protein of interest

which can then be transfected into a cell. Recently, FPs have been used to visualize

neurons and glia in 90 different colors in zebrafish, drosophila, and mice in a technique

known as Brainbow, which allows for the serial reconstruction of connectivity through

the stochastic expression of cytosolic FPs. This is done through a Cre/Lox recombination

which determines the pattern and colors that are expressed, allowing for the visualization

of neuronal connectivity in a given system.[43] FPs are more commonly used as fluorescent

fusion proteins which are then transfected into a particular system of interest, thus

allowing for the visualization of the receptor of interest as the protein is covalently tagged to the protein of interest. This has been done numerous times to determine receptor surface expression, how receptors are endo/exocytosed, and to interrogate the biophysical properties of a particular ion channel.[43b, 44] Fusion proteins can be quite small, but most are based on the GFP (green fluorescent protein) template developed by Tsein et al.[45]

1.2.2 Fluorescent Proteins

GFP ushered in a new age in which many biological advances have and can be made. GFP, itself, is a 28 kDa protein which is added to the receptor of interest in a fashion which allows for the particular receptor to still remain functional. This is done by adding GFP as either a fusion to the N or C terminus or added into a loop on the protein. This can then result in non-native heteromultimers or homomultimers when the receptors assemble. Also, the addition of GFP (and variants) can disrupt normal receptor motion, which will provide no information about receptor dynamics.[43b, 46]

1.2.3 Enzymatically Active Tags

One way to circumvent some of the issues presented by FPs, is to use enzymatically active tags such as SNAP, CLIP, and Halo tags. SNAP and CLIP tags involve the incorporation of a derivative of O^6-alkyl guanine-DNA alkyltransferase (AGT), a 20 kDa DNA repair protein, which can be inserted to the protein of interest. For SNAP-tag technology, modifications to the protein are delivered via the intrinsic activity of the tag and synthetic derivatives of O^6-benzylguanine that have been modified to contain cargo such as fluorophores.[47] O^6-benzylguanine probes act as a substrate to the tag, delivering cargo to a reactive cysteine in the AGT active site. CLIP-tag reacts in the same fashion, but contains mutations to AGT so that it will interact with derivatives of O^2-benzylcytosine.[48] SNAP and CLIP tags have been used in numerous systems to track subunit assembly and stoichiometry. Much like FPs, SNAP and CLIP tags suffer from the same issues of complications in the natural assembly and protein dynamics.

HaloTag is a labeling technology that is derived from modified bacterial

haloalkane dehalogenase. It is a large tag, approximately 34 kDa, and needs to be

attached to the protein of interest via a 16 amino acid linker derived from the tobacco

mosaic virus.[49] Once fused to the protein of interest, HaloTag is targeted by a separate

reporter probe containing a haloalkane. HaloTag works by alkylation of the reporter

probe to the protein of interest affixed with HaloTag, resulting in the formation of an

ester bond at a catalytic aspartate on the carboxylate. The modification that allows for

this to happen is a mutation of a crucial histidine near the catalytic aspartate leaves the

transient covalent ester intact, allowing for the reporter probe to attach to HaloTag.[50] The

linker length between the haloalkane and the reporter (fluorescein, tetramethylrhodamine,

Alex 288, Dy633, Oregon green, etc.) is crucial for the optimum performance of

HaloTag. The optimal linker length was found to be six carbons, when terminated with a

chloride. HaloTag has been utilized to measure retrograde axonal transport and to look at

some of the basis of cell mediated autophagy.[43b, 51] HaloTag suffers from the same

disadvantages as FPs, SNAP and CLIP tag, however it has been reported that the large

tag size does not disrupt protein function.[52]

Similar to enzymatically active tags are enzymatic substrate tags. This

technology was pioneered by the Ting lab and involves the attachment of a 15 amino acid

acceptor peptide to the protein of interest and then is targeted by a substrate sequence that

is exogenously expressed biotin ligase resulting in bioconjugation of a peptide with biotin

which then can be targeted by a streptavidin labeled moiety. This biotin ligase based

strategy has been used in conjunction with HaloTag for use in single molecule live cell

imaging.[53]

1.2.4 Small, peptide-based tags

The use of small, peptide based tags is another genetic technique that averts the

need for FPs or enzymatic tags. These include tetracysteine motifs, poly-histidine tags,

18

and Ni-NTA tags. The most widely used of the small, peptide tags are tetracysteine motifs. Tetracysteine motifs, as the name suggests, insert a small peptide sequence which contains four cysteines (C-C-X-X-C-C) to the protein of interest in a non-perturbing fashion. The added tetracysteine sequence can then be targeted by a fluorophore which contains a biarsenical core, taking advantage of the high affinity between the sulfurs in the cysteine and the arsenic. This can then allow for the location and dynamics of the protein to be measured. Tetracysteine motifs are also used because there is generally a lack of arsenic in proteins, and the multivalency that is given between the four encoded cysteines to a single arsenic in the reporter.[54] The biarsenical reporter tag comes in a variety of colors, including green, red, and blue (FlAsH, ReAsH, and XoXAsH).[54-55] In 2007, Bhunia et al expanded the pallet even further through the use of SplAsH, which can incorporate a fluorophore of any color on to the arsenic core.[56]

Tetracysteine motifs have been used in conjunction with FlAsH in imaging using either chromophore-assisted laser inactivation (CALI) or fluorophore-assisted laser inactivation (FALI), which allows for perturbations to the system and collect observations from that set time point.[57] FlAsH and ReAsH have been used in combination to examine the intracellular trafficking of GluA1 and GluA2 subunits. This was done by inserting the tetracysteine motif on the C-terminus and thus could report on protein synthesis in these two subunits.[58]

Tetracysteine motifs do have some caveats, chiefly that there is a low level of specificity when using the whole system in cysteine rich environments. The biarsenical detection ligand does not discriminate between that of the added tetracysteine motif and the endogenous cysteine rich areas on the protein. This can lead to misdirection of the biarsenical targeting ligand; thus confounding the imaging outcome as it will be a mixture of the desired protein and the non-desired cysteine rich one.[43b]

1.2.5 Antibodies

Antibodies are exquisitely specific towards their target of interest and thus are an extremely useful diagnostic tool for protein interactions. Antibodies are the bridge between genetic and non-genetic techniques as they contain aspects from each. Antibodies are genetic in the sense that they are derived from proteins raised to label a specific epitope on the protein of interest. Antibodies are non-genetic as they need to be exogenously applied to label the protein of interest, and also may need a secondary detection for visualization.[43b]

The use of antibodies mostly involves no genetic manipulation to the protein of interest when the antibody is raised towards a particular epitope on the receptor. Antibodies have been used in both live and fixed cell imaging with neuronal targets providing information on location, quantification, and observation of the dynamic movements of the neuronal receptors. Antibodies are large proteins, typically measuring 10-15 nanometers in size.[59] Primary antibodies typically need to be conjugated with a secondary antibody for visualization. The synaptic cleft is approximately 20 nanometers,[2] so when the antibody complex is placed onto the neurotransmitter of interest and then targeted by a secondary antibody for visualization, this complex is typically larger than that of the synaptic cleft. This will then limit the use of antibodies in providing information about receptor movement at the synapse.

1.2.6 Non-Genetic Imaging Techniques

Non-genetic imaging techniques compose a wide range of molecules that deliver a fluorophore to the neurotransmitter receptor of interest. This is typically done in a ligand-directed method that either uses a small molecule, or small peptide, as the delivery method. Antibodies can also be used as a targeting method. Since non-genetic techniques are partially synthetic in nature, a wide rainbow of fluorophore colors and properties can be made available for targeting and subsequent imaging. When designing a

probe for targeting of neural proteins, many factors need to be considered. The ideal probe should be selective, non-toxic, water soluble, and robust enough to withstand the environment inside the cell if used towards intracellular targets. Fluorophore attachment to either an antibody or the small molecule probe must have the above properties, and also be able to maintain brightness when bound to the system of interest.[43b, 60]

1.2.7 Quantum Dots

Quantum dots, QDs, are nano-sized colloid semiconductors which have properties that are tuned during their synthesis, and thus, can be targeted to a biomolecule of interest by graphing certain ligands to the surface of the QD. This often relies on the interaction of biotin and streptavidin [61], acid-base interactions [62], and covalent ligand attachment to a polymer on the surface of the QD.[63] QDs are more photostable than organic fluorophores and as a result, are brighter. However, QDs are subject to blinking and this can lead to complications during tracking experiments. Considerations also need to be made with size, as QDs can vary from 2 nanometers up to 20 nanometers in size once fully decorated. This would then make QDs the same size as the synaptic cleft.[64]

Antibodies and QDs have been used in conjunction for long term tracking of proteins involved in synaptic transmission. This was demonstrated in work tracking glycine receptors. Antibodies were raised against the glycine receptor and then targeted with a secondary biotinylated antibody. Visualization of the receptor location in the soma and dendrites was then achieved by the addition of streptavidin coated QDs. [65] Single particle tracking has been used to observe changes NMDA receptor subtypes [66], and in live cell imaging of AMPARs via fluorescence-recovery after photoinactivation experiments.[67]

1.2.8 Ligand-Based Detection

Ligands, in conjunction with other chemical entities such as fluorophores, have been used extensively to deliver cargo to the receptor of interest. This can be achieved

through bioconjugation to the target receptor after directed targeting via a ligand that has

been affixed with a fluorophore for visualization. The modification by the probe can

either be covalent or non-covalent in nature. Ligand based techniques are extremely

useful in helping to determine receptor expression in native culture. Discoveries made by

these techniques may be closer to what is occurring inside the brain.

Our group [68] has designed such a probe for the detection of calcium permeable

AMPA receptors, which is further discussed in detail in Chapter 2. Other ligand-directed

methods for cargo delivery to neurotransmitter receptors of interest modify existing drug

molecules to be decorated with fluorophores via a linker chain that does not interfere with

target binding. Amy Hauck Newman and coworkers at the NIH have developed two such

ligand-directed probes, one for the dopamine transporter (DAT) and one for the serotonin

transporter (SERT), using this method. These probes take an analogue of an agonist for

the particular receptor and decorated it with a fluorophore for visualization. This then

allows for information to be gathered about proteins synthesized inside the native

receptor.[69] The Strømgaard group at the University of Copenhagen employed a similar

technique in the development of a NMDA receptor probe by using a NMDA antagonist

attached to a fluorophore. Using this technique, they were able to visualize native, active

NMDA receptors in culture.[70]

1.2.9 Peptide-Based Ligand Delivery

Much like small molecule ligand delivery, peptide-based ligand delivery has

allowed for gains in knowledge about how receptors traffic inside the brain. Small

peptides can easily be synthesized thus leading to a plethora of peptide-based ligands that

can be optimized rapidly. A synthetic biomimetic peptide based probe was designed by

Choquet and Imperiali to target the PDZ domains at synapse. These domains, located on

the postsynaptic side of the synapse, are believed to govern the general dynamics of

receptors and ion channels to look at the dynamics of AMPA and NMDA receptors. The

use of these probes provided insight into the 2-4 stoichiometry of the anchoring proteins of the AMPA receptor.[71] As for NMDA receptors, the dynamics of the 2A and 2B subunits were interrogated via the PDZ biomimetic probe. The results suggest the anchoring mechanism is different between the two subunits as the 2A subunit was blocked, but the 2B subunit was not affected. [72]

Ligand directed probes, whether small molecule or peptide based, have the advantage that the ligand drives the specificity of labeling towards the target. The main limitation of this method is that the ligand may not be as completely specific as designed and can have known interactions with alternate subunits on the same receptor as well as interactions with off-target receptors. There are also limitations due to cell permeability and target location. Some probes will be difficult to deliver inside of cells, some may be less optimal for visualization, and some may suffer from lack of optimization. A lot of probes are tested in heterologous systems which lack the complexity and nuance of the downstream pathways which are found in the native system.

However, small molecule probes offer advantages over genetic techniques. The targeted receptors do not need to be genetically modified to contain either the FP or a protein tag. Transfection of these genes cannot always be done efficiently in neurons. Also, the palate of fluorophores that can be used in combination with small molecule probes is much wider, as organic fluorophores come in a plethora of colors and photostablities. Small molecule probes can also be designed in a fashion that should not disturb the receptor of interest, something that cannot always be said of genetic techniques. Due to these reasons, we decided to make small molecule probes to target towards AMPARs.

1.3 Bioorthogonal Chemistry

Bioorthogonal chemistry is any chemical reaction which occurs inside living biological systems, such as a cell, that does not interfere with normal biochemical

processes (Figure 1.9).[73] This allows for the study of proteins, lipids, glycans, and other

metabolites inside of the host system and gives an idea of how they act in real time.

Bioorthogonal chemistry is an umbrella term which covers a wide subset of reactions

which must have fast reaction rates and be biologically inert. These include 1,3-dipolar

cycloadditions (Click reactions), hydrazine/oxime formation from aldehydes and ketones,

tetrazine ligation, isocyanide based click reactions, and quadricyclane ligations.[73]

Use of bioorthogonal reagents is generally done in a two-step process. First, the

biological host, such as cells or living organisms, is incubated with a reporter, a

metabolic precursor which contains a unique bioinert functional group. Then, the host is

treated with a probe that has a complimentary tag for bioorthogonality. These reactions

are second order, so the rates of reaction are dependent upon the concentrations of the

reactants and second order reaction kinetics.[73]
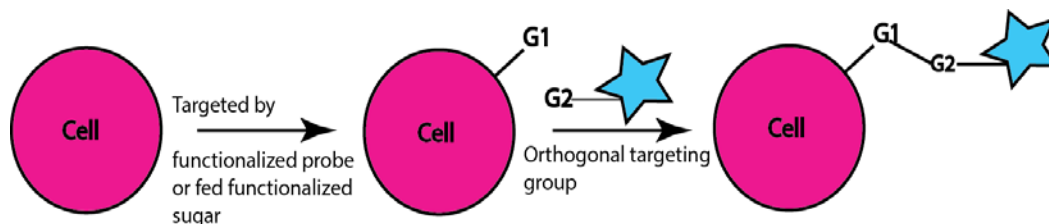
Figure 1.9: Cartoon of bioorthogonal targeting. In bioorthogonal chemistry, the cell is first either targeted by a probe containing a functionalized group, or fed a functionalized sugar (G1). This is then targeted by a reporter tag (G2) which contains either a fluorophore or biotin. G1 and G2 covalently bond, leaving the cell covalently tagged.

1.3.1 Staudinger Ligation

The Staudinger ligation was developed by the Bertozzi lab at UC Berkley in

2000 as a modification to the Staudinger reduction for use with azides and

triarylphosphines.[74] Strategic placement of an ester on the aryl substituent of the

phosphate allows for the formation of an amide bond via an intermediate aza-ylide.[73]

The Staudinger ligation has been particularly useful in biological imaging

experiments as fluorophores can be incorporated. This can be as simple as using a

coumarin for the aryl ring [75] or installing a FRET quencher into the ester group. When

cleaved, the quencher can provide an alternate way for activation of fluorescence.[76]

The Staudinger ligation does have some issues with biocompatibility as azides

and phosphines have reactivity towards both thiols and disulfides. This can be mitigated

slightly by using TCEP, tris (2-carboxyethyl) phosphine, to reduce disulfides on the

surface of the protein.[77] The Staudinger ligation suffers from slow reaction kinetics, and,

thus, excess amounts of triarylphosphine are needed to have the reaction go to

completion, causing issues when studying sensitive biological systems.[78]

1.3.2 Click Chemistry
The application of click chemistry in biology has been revolutionary in

determining the functions of different biomolecules that are not accessible by standard

antibody and genetic methods. Click reactions are those which are selective, high

yielding, have preferable reaction kinetics, simple to preform, and can be conducted in

benign solvents such as water. The term "click chemistry" was coined by Sharpless in

reference to the development of the copper-catalyzed [3+2] cycloaddition of an azide to

an acylic alkyne.[79] Sharpless did not come up with the [3+2] cycloaddition, only

improved upon the chemistry that was discovered in the 1960's by Huisgen.[80] As such,

terminal azides have become the most popular functional group to add for

bioorthogonality as they are small in size and inert towards endogenous biological

functionalities.

Copper catalyzed click chemistry works well in most biological circumstances,

unless cell viability is needed. Copper is extremely toxic to living cells so there is a need

for copper free methods that retain the same fast reaction kinetics that are needed inside

the cellular environment. The Bertozzi lab has, once again, been one of the pioneering

labs in developing this technology by using molecules which contain a large amount of

ring strain, specifically cyclooctenes. Borrowing from president set by Huisgen [81],

Wittig, and Krebol [82], Bertozzi used the information that cyclooctenes react explosively with phenylazides and sought to lower the LUMO of the alkyne by withdrawing electron density away from the triple bond. [83] Bertozzi's group went on to synthesize difluronated cylcooctene (DIFO), which has reaction kinetics similar to that of the copper catalyzed click chemistry. Fluorophore functionalized versions of DIFO have since been synthesized which allows for live imaging in cells, *C.elegans*, and zebrafish without the worry of the toxic effects of copper.[84]

1.3.3 Activity Based Protein Profiling (ABPP)

One key development in the identification of protein interactions has been the discovery and use of activity based protein profiling (ABPP). ABPP is used to visualize the active form of any enzyme or protein by using chemical probes to tag it. The prototype was first described in 1961 using a radioactive probe against esterases.[85] This technique was then refined by the Cravatt group at Scripts for use with enzymes using a directed small molecule probe.[86] Probes are directed towards an active site residue for covalent attachment and then visualization can be achieved. These probes can be used to detect proteins in a variety of complex biological environments including cell culture, cell lysates, and even living cells.[87]

A typical activity based probe contains three parts: a targeted reactive group, or warhead, a recognition element for selectivity, and some sort of detectable reagent. The warhead is typically an electrophilic moiety that is used for covalent attachment to the protein of interest. This electrophilic element needs to be reactive enough to quickly bind to the protein of interest, yet should not be able to interact with offsite proteins. The recognition element acts to direct the warhead to a willing nucleophile on the surface of the protein. It also serves to be selective towards the targeted protein. The recognition element is typically either a fluorophore, an affinity based tag, such as biotin, resin for solid phase mass spec analysis, or some combination of all three. [87]

1.4 Conclusions

Taking everything into account that was presented in the introduction, it is clear that what is sorely lacking is a small-molecule probe which can target towards, and identify, calcium permeable AMPARs *in situ*. Use of this type of probe would allow for identification of calcium permeable AMPARs in different neuronal subtypes and answer questions about their inclusions during LTP. To do so, we need to design a probe that is both specific and able to be used in a variety of cellular environments. We also need to be able to incorporate a reporter tag, such as a fluorophore, so we can visualize the motion of the AMPAR as it moves along the dendrite. This could have implications on how signaling in LTP occurs through calcium permeable AMPARs and how calcium permeable AMPARs are trafficked to the surface. This probe could also fill in some of the gaps in LTP, such as AMPAR recycling.

A probe towards calcium permeable AMPARs could also lead to a better understanding of why neurons switch between calcium-impermeable AMPARs and calcium permeable AMPARs after traumatic brain events, such as ischemia, or chemically induced trauma, such as addiction. If we are able to have a better grasp of what is occurring, then better and more targeted treatments could be developed.

To do so, we designed nanoprobe **1** as a functionalized probe for the detection of calcium permeable AMPARs. Subsequent testing with nanoprobe **1** showed that nanoprobe 1is directed towards glutamate receptors, however we are not able to answer questions about subtype. Nanoprobe **2** was then designed to more closely resemble the natural polyamine antagonists of calcium permeable AMPARs, specifically philanthotoxin-433. Nanoprobe **2** also could be used in a more refined method to answer questions about subtype inclusion through pull-down experiments. However, nanoprobe **2** was not able to bind to any receptors. We then designed nanoprobe **3** off of the same scaffold and added a more promiscuous electrophile, which could be activated using

photochemistry. Ultimately, the same result was seen as with nanoprobe **2**. We then

moved into new methods for bioorthogonal chemistry by using a two-step delivery

system. This new method does not rely on incorporation of an azide into the protein of

interest and will ultimately be further tested for ligand directed experiments.

1.5 References

1.Squire, L. R.; Darwin, B.; Bloom, F. E.; su Lac, S.; Ghosh, A.; Spitzer, N. C., *Fundamental Neuroscience Third Edition*. 3 ed.; Elisver: Burlington, 2008.

2.Zuber, B.; Nikonenko, I.; Klauser, P.; Muller, D.; Dubochet, J., The mammalian central nervous synaptic cleft contains a high density of periodically organized complexes. *Proc. Natl. Acad. Sci. U. S. A.* **2005,** *102* (52), 19192-19197.

3.Anggono, V.; Huganir, R. L., Regulation of AMPA receptor trafficking and synaptic plasticity. *Current Opinion in Neurobiology* **2012,** *22* (3), 461-469.

4.Hanley, J. G., Subunit-specific trafficking mechanisms regulating the synaptic expression of Ca2+-permeable AMPA receptors. *Seminars in Cell & Developmental Biology* **2014,** *27*, 14-22.

5.(a) Thomas, G. M.; Huganir, R. L., Mapk cascade signalling and synaptic plasticity. *Nature Reviews Neuroscience* **2004,** *5* (3), 173-183; (b) Lee, H. K.; Takamiya, K.; Han, J. S.; Man, H. Y.; Kim, C. H.; Rumbaugh, G.; Yu, S.; Ding, L.; He, C.; Petralia, R. S.; Wenthold, R. J.; Gallagher, M.; Huganir, R. L., Phosphorylation of the AMPA receptor GluR1 subunit is required for synaptic plasticity and retention of spatial memory. *Cell* **2003,** *112* (5), 631-643.

6.Benke, T. A.; Luthi, A.; Isaac, J. T. R.; Collingridge, G. L., Modulation of AMPA receptor unitary conductance by synaptic activity. *Nature* **1998,** *393* (6687), 793-797.

7.(a) Roche, K. W.; Obrien, R. J.; Mammen, A. L.; Bernhardt, J.; Huganir, R. L., Characterization of multiple phosphorylation sites on the AMPA receptor GluR1 subunit. *Neuron* **1996,** *16* (6), 1179-1188; (b) Banke, T. G.; Bowie, D.; Lee, H. K.; Huganir, R. L.; Schousboe, A.; Traynelis, S. F., Control of GluR1 AMPA receptor function by cAMP-dependent protein kinase. *Journal of Neuroscience* **2000,** *20* (1), 89-102.

8.Shepherd, J. D.; Huganirl, R. L., The cell biology of synaptic plasticity: AMPA receptor trafficking. In *Annual Review of Cell and Developmental Biology*, 2007; Vol. 23, pp 613-643.

9.Man, H.-Y., GluA2-lacking, calcium permeable AMPA receptors-inducers of plasticity? *Current Opinion in Neurobiology* **2011,** *21*, 291-298.

10.(a) Bellone, C.; Luscher, C., Cocaine triggered AMPA receptor redistribution is reversed in vivo by mGluR-dependent long-term depression. *Nature Neuroscience* **2006,** *9* (5), 636-641; (b) Wolf, M. E.; Tseng, K. Y., Calcium-permeable AMPA receptors in the VTA and the nucleus accumbens after cocaine exposure: when, how, and why? *Frontiers in Molecular Neuroscience*

2012, *5* (72), 1-27; (c) Ungless, M. A.; Whistler, J. L.; Malenka, R. C.; Bonci, A., Single cocaine exposure in vivo induces long-term potentiation in dopamine neurons. *Nature* **2001,** *411* (6837), 583-587.

11. Ehlers, M. D., Reinsertion or degradation of AMPA receptors determined by activity-dependent endocytic sorting. *Neuron* **2000,** *28* (2), 511-525.

12. (a) Beattie, E. C.; Carroll, R. C.; Yu, X.; Morishita, W.; Yasuda, H.; von Zastrow, M.; Malenka, R. C., Regulation of AMPA receptor endocytosis by a signaling mechanism shared with LTD. *Nature Neuroscience* **2000,** *3* (12), 1291-1300; (b) Lin, J. W.; Ju, W.; Foster, K.; Lee, S. H.; Ahmadian, G.; Wyszynski, M.; Wang, Y. T.; Sheng, M., Distinct molecular mechanisms and divergent endocytotic pathways of AMPA receptors internalization. *Nature Neuroscience* **2000,** *3* (12), 1282-1290.

13. (a) Kim, C. H.; Chung, H. J.; Lee, H. K.; Huganir, R. L., Interaction of the AMPA receptor subunit GluR2/3 with PDZ domains regulates hippocampal long-term depression. *Proc. Natl. Acad. Sci. U. S. A.* **2001,** *98* (20), 11725-11730; (b) Seidenman, K. J.; Steinberg, J. P.; Huganir, R.; Malinow, R., Glutamate receptor subunit 2 serine 880 phosphorylation modulates synaptic transmission and mediates plasticity in CA1 pyramidal cells. *Journal of Neuroscience* **2003,** *23* (27), 9220-9228.

14. Chung, H. J.; Steinberg, J. P.; Huganir, R. L.; Linden, D. J., Requirement of AMPA receptor GluR2 phosphorylation for cerebellar long-term depression. *Science* **2003,** *300* (5626), 1751-1755.

15. Hanley, J. G., PICK1: A multi-talented modulator of AMPA receptor trafficking. *Pharmacology & Therapeutics* **2008,** *118* (1), 152-160.

16. (a) Uzunova, G.; Hollander, E.; Shepherd, J., The Role of Ionotropic Glutamate Receptors in Childhood Neurodevelopmental Disorders: Autism Spectrum Disorders and Fragile X Syndrome. *Current Neuropharmacology* **2014,** *12* (1), 71-98; (b) Hollmann, M.; Heinemann, S., Cloned glutamate receptors. *Annual Review of Neuroscience* **1994,** *17*, 31-108.

17. Weiss, J. H., Ca^{2+} permeable AMPA channels in disease of the nervous system. *Frontiers in Molecular Neuroscience* **2011,** *4* (42), 1-7.

18. Wright, A.; Vissel, B., The essential role of AMPA receptor GluA2 subunit RNA editing in the normal and diseased brain. *Frontiers in Molecular Neuroscience* **2012,** *5* (34), 1-13.

19. Hollmann, M.; Hartley, M.; Heinemann, S., CA2+ permeability of KA-AMPA gated glutamate channels depends on subunit composition. *Science* **1991,** *252* (5007), 851-853
.
20. Shephard, J. D., Memory, plasticity, and sleep- a role for calcium-permeable AMPA receptors? *Frontiers in Molecular Neuroscience* **2012,** *5* (49), 1-5.

21. (a) Bats, C.; Farrant, M.; Cull-Candy, S. G., A role of TARPs in the expression and plasticity of calcium-permeable AMPARs: Evidence from cerebellar neurons and glia. *Neuropharmacology* **2013,** *74*, 76-85; (b) Chen, L.; Chetkovich, D. M.; Petralia, R. S.; Sweeney, N. T.; Kawasaki, Y.; Wenthold, R. J.; Bredt, D. S.; Nicoll, R. A., Stargazin regulates synaptic targeting of AMPA receptors by two distinct mechanisms. *Nature* **2000,** *408* (6815), 936-943; (c) Kato, A. S.; Siuda, E. R.; Nisenbaum, E. S.; Bredt, D. S., AMPA receptor subunit-specific regulation by a distinct

family of type II TARPs. *Neuron* **2008,** *59* (6), 986-996; (d) Soto, D.; Coombs, I. D.; Kelly, L.; Farrant, M.; Cull-Candy, S. G., Stargazin attenuates intracellular polyamine block of calcium-permeable AMPA receptors. *Nature Neuroscience* **2007,** *10* (10), 1260-1267; (e) Tomita, S.; Chen, L.; Kawasaki, Y.; Petralia, R. S.; Wenthold, R. J.; Nicoll, R. A.; Bredt, D. S., Functional studies and distribution define a family of transmembrane AMPA receptor regulatory proteins. *Journal of Cell Biology* **2003,** *161* (4), 805-816.

22.(a) Jackson, A. C.; Nicoll, R. A., Stargazin (TARP γαμμα-2) is required for compartment-specific AMPA receptor trafficking and synaptic plasticity in cerebellar stellate cells. *The Journal of Neuroscience* **2011,** *31* (11), 3939-3952; (b) Jackson, A. C.; Nicoll, R. A., The Expanding Social Network of Ionotropic Glutamate Receptors: TARPs and Other Transmembrane Auxiliary Subunits. *Neuron* **2011,** *70* (2), 178-199.

23.Straub, C.; Tomita, S., The regulation of glutamate receptor trafficking and function by TARPs and other transmembrane auxiliary subunits. *Current Opinion in Neurobiology* **2012,** *22* (3), 488-495.

24.Correia, S. S.; Bassani, S.; Brown, T. C.; Lise, M.-F.; Backos, D. S.; El-Husseini, A.; Passafaro, M.; Esteban, J. A., Motor protein-dependent transport of AMPA receptors into spines during long-term potentiation. *Nature Neuroscience* **2008,** *11* (4), 457-466.

25.Adesnik, H.; Nicoll, R. A.; England, P. M., Photoinactivation of native AMPA receptors reveals their real-time trafficking. *Neuron* **2005,** *48* (6), 977-985.

26.Higuchi, M.; Stefan, M.; Single, F. N.; Hartner, J.; Rozov, A.; Burnashev, N.; Feldmeyer, D.; Sprengel, R.; Seeburg, P. H., Point mutation in an AMPA receptor gene rescues lethality in mice deficient in the RNA-editing enzyme ADAR2. *Nature* **2000,** *406* (6791), 78-81.

27.Kwak, S.; Hideyama, T.; Yamashita, T.; Aizawa, H., AMPA receptor-mediated neuronal death in sporadic ALS. *Neuropathology* **2010,** *30* (2), 182-188.

28.Mahajan, S. S.; Ziff, E. B., Novel toxicity of the unedited GluR2 AMPA receptor subunit dependent on surface trafficking and increased Ca2+-permeability. *Molecular and Cellular Neuroscience* **2007,** *35* (3), 470-481.

29.Jonas, P.; Racca, C.; Sakmann, B.; Seeburg, P. H.; Monyer, H., Differences in Ca2+ permeablity of AMPA-type glutamate-receptor channels in neocortical neurons cuased by differential GluR-B subunit expression. *Neuron* **1994,** *12* (6), 1281-1289.

30.Kumar, S. S.; Bacci, A.; Kharazia, V.; Huguenard, J. R., A developmental switch of AMPA receptor subunits in neocortical pyramidal neurons. *Journal of Neuroscience* **2002,** *22* (8), 3005-3015.

31.Yin, H. Z.; Weiss, J. H., Zn2+ permeates Ca2+ permeable AMPA kainate channels and triggers selective neural injury. *Neuroreport* **1995,** *6* (18), 2553-2556.

32.Kobylecki, C.; Cenci, M. A.; Crossman, A. R.; Ravenscroft, P., Calcium-permeable AMPA receptors are involved in the induction and expression of l-DOPA-induced dyskinesia in Parkinson's disease. *J. Neurochem.* **2010,** *114* (2), 499-511.

33.Neumann, M.; Sampathu, D. M.; Kwong, L. K.; Truax, A. C.; Micsenyi, M. C.; Chou, T. T.; Bruce, J.; Schuck, T.; Grossman, M.; Clark, C. M.; McCluskey, L. F.; Miller, B. L.; Masliah, E.; Mackenzie, I. R.; Feldman, H.; Feiden, W.; Kretzschmar, H. A.; Trojanowski, J. Q.; Lee, V. M. Y., Ubiquitinated TDP-43 in frontotemporal lobar degeneration and amyotrophic lateral sclerosis. *Science* **2006,** *314* (5796), 130-133.

34.Tateno, M.; Sadakata, H.; Tanaka, M.; Itohara, S.; Shin, R. M.; Miura, M.; Masuda, M.; Aosaki, T.; Urushitani, M.; Misawa, H.; Takahashi, R., Calcium-permeable AMPA receptors promote misfolding of mutant SOD1 protein and development of amyotrophic lateral sclerosis in a transgenic mouse model. *Hum. Mol. Genet.* **2004,** *13* (19), 2183-2196.

35.Talos, D. M.; Fishman, R. E.; Park, H.; Rebecca, D. F.; Follett, P. L.; Volpe, J. J.; Jensen, F. E., Developmental regulation of alpha-amino-3-hydroxy-5-methyl-4-isoxazole-propionic acid receptor subunit expression in forebrain and relationship to regional susceptibility to hypoxic/ischemic injury. I. Rodent cerebral white matter and cortex. *Journal of Comparative Neurology* **2006,** *497* (1), 42-60.

36.Liu, S. H.; Lau, L.; Wei, J. S.; Zhu, D. Y.; Zou, S. W.; Sun, H. S.; Fu, Y. P.; Liu, F.; Lu, Y. M., Expression of Ca2+-Permeable AMPA receptor channels primes cell death in transient forebrain ischemia. *Neuron* **2004,** *43* (1), 43-55.

37.Bowie, D.; Mayer, M. L., Inward rectification of both AMPA and kainate subtype glutamate receptors generated by polyamine-mediated ion-channel block. *Neuron* **1995,** *15* (2), 453-462.

38.(a) Stromgaard, K.; Mellor, I., AMPA receptor ligands: Synthetic and pharmacological studies of polyamines and polyamine toxins. *Medicinal Research Reviews* **2004,** *24* (5), 589-620; (b) Xiong, X.; Strømgaard, K., Polyamine Toxins from Spiders and Wasps. In *Polyamines*, Kusano, T.; Suzuki, H., Eds. Springer Japan: 2015; pp 201-214.

39.Asami, T.; Kagechika, H.; Hashimoto, Y.; Shudo, K.; Miwa, A.; Kawai, N.; Nakajima, T., Acylpolyamines mimic the action of joro spider toxin (jstx) on crustacean muscle glutamate receptors. *Biomedical Research-Tokyo* **1989,** *10* (3), 185-189.

40.(a) Herlitze, S.; Raditsch, M.; Ruppersberg, J. P.; Jahn, W.; Monyer, H.; Schoepfer, R.; Witzemann, V., Argiotoxin detects molecular differences in AMPA receptor channels. *Neuron* **1993,** *10* (6), 1131-1140; (b) Blaschke, M.; Keller, B. U.; Rivosecchi, R.; Hollmann, M.; Heinemann, S.; Konnerth, A., A single amino-acid determines the subunit-specific spider toxin block of alpha-amino-3-hydroxy-5-methylisoxazole-4-propionate kainate receptor channels. *Proc. Natl. Acad. Sci. U. S. A.* **1993,** *90* (14), 6528-6532.

41.Sobolevsky, A. I.; Rosconi, M. P.; Gouaux, E., X-ray structure, symmetry and mechanism of an AMPA-subtype glutamate receptor. *Nature* **2009,** *462* (7274), 745-66.

42.(a) Andersen, T. F.; Tikhonov, D. B.; Bolcho, U.; Bolshakov, K.; Nelson, J. K.; Pluteanu, F.; Mellor, I. R.; Egebjerg, J.; Stromgaard, K., Uncompetitive antagonism of AMPA receptors: Mechanistic insights from studies of polyamine toxin derivatives. *Journal of Medicinal Chemistry* **2006,** *49* (18), 5414-5423; (b) Barygin, O. I.; Grishin, E. V.; Tilchonov, D. B., Argiotoxin in the Closed AMPA Receptor Channel: Experimental and Modeling Study. *Biochemistry* **2011,** *50* (38), 8213-8220; (c) Tikhonov, D. B., Ion channels of glutamate receptors: structural modeling. *Molecular Membrane Biology* **2007,** *24* (2), 135-64.

43. (a) Livet, J.; Weissman, T. A.; Kang, H.; Draft, R. W.; Lu, J.; Bennis, R. A.; Sanes, J. R.; Lichtman, J. w., Transgenic strategies for combinatoral expression of fluorescent proteins in the neurvous system. *Nature* **2007,** *450*, 56-64; (b) Hussey, A. M.; Chambers, J. J., Methods To Locate and Track Ion Channels and Receptors Expressed in Live Neurons. *ACS Chemical Neuroscience* **2015,** *6* (1), 189-198.

44. Fernández-Suárez, M.; Ting, A. Y., Fluorecent probes for super-resolution imaging in living cells. *Nature* **2008,** *9*, 929-946.

45. Tsien, R. Y., The green fluorescent protein. *Annual Review of Biochemistry* **1998,** *67*, 509-544.

46. Bredt, D. S.; Nicoll, R. A., AMPA receptor trafficking at excitatory synapses. *Neuron* **2003,** *40* (2), 361-379.

47. Keppler, A.; Gendreizig, S.; Gronemeyer, T.; Pick, H.; Vogel, H.; Johnsson, K., A general method for the covalent labeling of fusion proteins with small molecules *in vivi*. *Nature Biotechnology* **2003,** *21*, 86-90.

48. Gautier, A.; Juillerat, A.; Heinis, C.; Corrêa Jr., I. R.; Kindermann, M.; Beufils, F.; Johnsson, K., An engineered protein tag for multiprotein labeling in lving cells. *Chemistry & Biology* **2008** *15*, 128-136.

49. Ohana, R. F.; Encell, L. P.; Zhao, K.; Simpson, D.; Slater, M. R.; Urh., M.; Wood, K. V., HaloTag7: a genetically engineered tag that enhances bacterial expression of soluble proteins and improves protein purification. *Protein Expression and Purification* **2009,** *68* (1), 110-120.

50. Los, G. V.; Encell, L. P.; McDougall, M. G.; Hartzell, D. D.; Karassina, N.; Zimprich, C.; Wood, M. G.; Learish, R.; Ohana, R. F.; Ura, M.; Simpson, D.; Mendez, J.; Zimmerman, K.; Otto, P.; Vidugiris, G.; Zhu, J.; Darzins, A.; Klaubert, D. H.; Bulleit, R. F.; Wood, K. V., HaloTag:A novel protein labeling technology for cell imaging and protein analysis. *ACS Chemical Biology* **2008** *3*(6), 460-468.

51. (a) Mok, S.-A.; Lund, K.; LaPointe, P.; Campenot, R. B., A HaloTag method for assesing the retrograde axonl transport of the p75 neurotrophin receptor and other proteins in compartmental cultures of rat sympathetic neurons. *Journal of Neuroscience Methods* **2013,** *241*, 91-104; (b) Seki, T.; Yoshino, K.-i.; Tanaka, S.; Dohi, E.; Onji, T.; Yamamoto, K.; Hide, I.; Paulson, H. L.; Saito, N.; Sakai, N., Establishment of a novel fluorescence-based method to evaluate chaperone-mediated autophagy in a single neuron. *PlOs one* **2012,** *7* (2), e31232-e31243.

52. Los, G. V.; Darzins, A.; Karassina, N.; Zimprich, C.; Learish, R.; McDougall, M. G.; Encell, L. P.; Ohana, R. F.; Wood, M. G.; Vidugiris, G.; Zimmerman, K.; Otto, P.; Klaubert, D. H.; Wood, K. V., HaloTag interchangeable labeling technology for cell imaging and protein capture. *Promega Cell Notes* **2005,** (11), 2-6.

53. Liu, D. S.; Phipps, W. S.; Loh, K. H.; Howarth, M.; Ting, A. Y., Quantum Dot Targeting with Lipoic Acid Ligase and Halo Tag for Single-Molecule Imaging on Living Cells. *Acs Nano* **2012,** *6* (12), 11080-11087.

54.Adams, S. R.; Campbell, R. E.; Gross, L. A.; Martin, B. R.; Walkup, G. K.; Yao, Y.; Llopis, J.; Tsien, R. Y., New biarsenical ligands and tetracysteine motifs for protein labeling in vitro and in vivo: synthesis and biological application. *J. Am. Chem. Soc.* **2002,** *124*, 6063-6076.

55.Griffin, B. A.; Adams, S. R.; Jones, J.; Tsien, R. Y., Fluorescent labeling of recombinant proteins in living cells with FlAsH. *Methods Enzymol.* **2000,** *327*, 565-578.

56.Bhunia, A. J.; Miller, S. C., Labeling tetracysteine-tagged proteins with a SplAsH of color: a modular approach to bis-arsenical flurophores. *Chembiochem* **2007,** *8*, 1642-1625.

57.Marek, K. W.; Davis, G. W., Transgenic encoded protein photoinactivation (FlAsH-FALI): accute inactivation of synaptotagmin I. *Neuron* **2002,** *36*, 805-813.

58.Ju, W.; Morishita, W.; Tsui, J.; Gaietta, G.; Deerinck, T. J.; Adams, S. R.; Garner, C. C.; Tsien, R. Y.; Malenka, R. C., Activity-dependant regulation of dendritic synthesis and trafficking of AMPA recepotrs. *Nature Neuroscience* **2004,** *7* (3), 244-254.

59.Ban, N.; Escobar, C.; Garcia, R.; Hasel, K.; Day, J.; Greenwood, A.; McPherson, A., Crystal structure of an idiotype-anti-idiotype Fab complex. *Proc. Natl. Acad. Sci. U. S. A.* **1994,** *91*, 1604-1608.

60.Chan, J.; Dodani, S. C.; Chang, C. J., Reaction-based small-molecule fluorescent probes for chemoselective bioimagin. *Nature Chemistry* **2012,** *4*, 973-985.

61.Bruchez Jr., M.; Moronne, M.; Gin, P.; Weiss, S.; Alivisatos, A. P., Seminconducto nanocrystals as fluorescent biological labels. *Science* **1998,** *281* (5385), 2013-2016.

62.Rosenthal, S. J.; Tomlinson, I. D.; Adkins, E. A.; Schroeter, S.; Adams, S.; Swafford, L.; McBride, J.; Wang, Y.; DeFelice, L. J.; Blakely, R. D., Targeting cell surface receptors with ligand-conjugated nanocrystals. *J. Am. Chem. Soc.* **2002,** *124* (12), 4586-4594.

63.Tomlinson, I. D.; Gies, A. P.; Gresch, P. J.; Dillard, J.; Orndorff, R. L.; Sanders-Bush, E.; Hercules, D. M.; Rosenthal, S. J., Universal polyethylene gycol linkers for attaching receptor ligands to quantum dots. *Bioorganic & Medicinal Chemistry Letters* **2006,** *16* (24), 6262-6266.

64.Michalet, X.; Pinaud, F. F.; Bentolila, L. A.; Tsay, J. M.; Doose, S.; Li, J. J.; Sundaresan, G.; Wu, A. M.; Gambhir, S. S.; Weiss, S., Quantum dots for live cell, *in vivo* imagin, and diagnostics. *Science* **2005,** (307), 538-546

65.Dahan, M.; Lévi, S.; Luccardini, C.; Rostaing, P.; Riveau, B.; Triller, A., Diffusion dynamics of glycine receptors revealed by single-quantum dot tracking. *Science* **2003,** *302*, 442-445.

66.Groc, L.; Heine, M.; Cousins, S. L.; Stephenson, F. A.; Lounis, B.; Cognet, L.; Choquet, D., NMDA receptor surface mobilty depends on NR2A-2B subunits. *Proc. Natl. Acad. Sci. U. S. A.* **2006,** *103* (49), 18769-18774.
67.Heine, M.; Groc, L.; Frischknecht, R.; Béïque, J.-C.; Lounis, B.; Rumbaugh, G.; Hugnair, R. L.; Cognet, L.; Choquet, D., Surface mobilty of postsynaptic AMPARs tunes synaptic transmission. *Science* **2008,** *230*, 201-206.

68.a) Vytla, D.; Combs-Bachmann, R. E.; Hussey, A. M.; Hafez, I.; Chambers, J. J., Silent, fluorescent labeling of native neuronal receptors. *Organic & Biomolecular Chemistry* **2011,** *21*

(9), 7151-7161; (b) Combs-Bachmann, R. E.; Johnson, J. N.; Vytla, D.; Hussey, A. M.; Kilfoil, M. L.; Chambers, J. J., Ligand-directed delivery of fluorophores to track native calcium-permeable AMPA receptors in neuronal cultures. *J. Neurochem.* **2015,** *133* (3), 320-329.

69. (a) Eriksen, J.; Rasmussen, S. G. F.; Rasmussen, T. N.; Vaegter, C. B.; Cha, J. H.; Zou, M.-F.; Newman, A. H.; Gether, U., Visualization of dopamine transporter trafficking in live neurons by use of fluroescent cocain analogs. *The Journal of Neuroscience* **2009***, 29* (21), 6794-6808; (b) Zhang, P.; Jørgensen, T. N.; Loland, C. J.; Newman, A. H., A rhodamine-labeld citalopram analogue as a high-affinity fluorescent prove for the seratonin transporter. *Bioorganic & Medicinal Chemistry Letters* **2013,** *23*, 323-326; (c) Kumar, V.; Rahbek-Clemmensen, T.; Billesbolle, C. B.; Jorgensen, T. N.; Gether, U.; Newman, A. H., Novel and High Affinity Fluorescent Ligands for the Serotonin Transporter Based on (S)-Citalopram. *ACS Med. Chem. Lett.* **2014,** *5* (6), 696-699.

70. Nørager, N. G.; Jensen, C. B.; Rathje, M.; Andersen, J.; Madsen, K. L.; Kristensen, A. S.; Strømgaard, K., Development of a potent fluorescent polyamine toxins and applications in labeling ionotropic glutamate receptors in hippocampal neurons. *ACS Chemical Biology* **2013** *8*(9), 2033-2041.

71. Sainlos, M.; Tigaret, C.; Poujol, C.; Olivier, N. B.; Bard, L.; Breillat, C.; Thiolon, K.; Choquet, D.; Imperiali, B., Biomimetic divalent ligands for the acute disruption of synaptic AMPAR stabilization. *Nature Chemical Biology* **2011,** *7*, 81-92.

72. Bard, L.; Sainlos, M.; Bouchet, D.; Cousins, S. L.; Mikasova, L.; Breillat, C.; Stephenson, F. A.; Imperiali, B.; Choquet, D.; Groc, L., Dynamic and specific interaction between synaptic NR20NMDA receptor and PDZ proteins. *Proc. Natl. Acad. Sci. U. S. A.* **2010,** *107*, 19561-19566.

73. Sletten, E. M.; Bertozzi, C. R., Bioorthogonal Chemistry: Fishing for Selectivity in a Sea of Functionality. *Angewandte Chemie-International Edition* **2009,** *48* (38), 6974-6998.

74. (a) Saxon, E.; Bertozzi, C. R., Cell surface engineering by a modified Staudinger reaction. *Science* **2000,** *287* (5460), 2007-2010; (b) Staudinger, H.; Meyer, J., On new organic phosphorus bonding III Phosphine methylene derivatives and phosphinimine. *Helvetica Chimica Acta* **1919,** *2*, 635-646.

75. Lemieux, G. A.; de Graffenried, C. L.; Bertozzi, C. R., A fluorogenic dye activated by the Staudinger ligation. *J. Am. Chem. Soc.* **2003,** *125* (16), 4708-4709.

76. Hangauer, M. J.; Bertozzi, C. R., A FRET-based fluorogenic phosphine for live-cell Imaging with the Staudinger ligation. *Angewandte Chemie-International Edition* **2008,** *47* (13), 2394-2397.

77. (a) Cartwright, I. L.; Hutchinson, D. W.; Armstrong, V. W., Reaction between thiols and 8-azidoadenosine derivatives. *Nucleic Acids Research* **1976,** *3* (9), 2331-2339; (b) Staros, J. V.; Bayley, H.; Standring, D. N.; Knowles, J. R., Reduction of aryl azides by thiols - implications for use of photoaffinity reagents. *Biochemical and Biophysical Research Communications* **1978,** *80* (3), 568-572; (c) Reardon, J. E.; Crouch, R. C.; Stjohnwilliams, L., Reduction of 3'-azido-3'-deoxythymidine (AZT) and AZT nucelotides by thiols - kinetics and product identification. *Journal of Biological Chemistry* **1994,** *269* (23), 15999-16008.

78.Lin, F. L.; Hoyt, H. M.; van Halbeek, H.; Bergman, R. G.; Bertozzi, C. R., Mechanistic investigation of the Staudinger ligation. *J. Am. Chem. Soc.* **2005,** *127* (8), 2686-2695.

79.Rostovtsev, V. V.; Green, L. G.; Fokin, V. V.; Sharpless, K. B., A stepwise Huisgen cycloaddition process: Copper(I)-catalyzed regioselective "ligation" of azides and terminal alkynes. *Angewandte Chemie-International Edition* **2002,** *41* (14), 2596-+.

80.Huisgen, R., 1.3-Dipolare cycloadditione - ruckschau und ausblick. *Angewandte Chemie-International Edition* **1963,** *75* (13), 604-+.

81.Alder, K.; Stein, G., The polymerisation of cyclic hydrocarbon. IV. About the stereoisomer forms of perhydrate naphto and anthrachinone. *Justus Liebigs Annalen Der Chemie* **1933,** *501*, 247-294.

82.Wittig, G.; Krebs, A., *Chem. Ber.* **1961,** *94*, 3260.

83.Jewett, J. C.; Bertozzi, C. R., Cu-free click cycloaddition reactions in chemical biology. *Chemical Society Reviews* **2010,** *39* (4), 1272-1279.

84.(a) Dehnert, K. W.; Baskin, J. M.; Laughlin, S. T.; Beahm, B. J.; Naidu, N. N.; Amacher, S. L.; Bertozzi, C. R., Imaging the Sialome during Zebrafish Development with Copper-Free Click Chemistry. *Chembiochem* **2012,** *13* (3), 353-357; (b) Baskin, J. M.; Prescher, J. A.; Laughlin, S. T.; Agard, N. J.; Chang, P. V.; Miller, I. A.; Lo, A.; Codelli, J. A.; Bertozzi, C. R., Copper-free click chemistry for dynamic in vivo imaging. *Proc. Natl. Acad. Sci. U. S. A.* **2007,** *104* (43), 16793-16797; (c) Laughlin, S. T.; Baskin, J. M.; Amacher, S. L.; Bertozzi, C. R., In vivo imaging of membrane-associated glycans in developing zebrafish. *Science* **2008,** *320* (5876), 664-667.

85.Ostrowski, K.; Barnard, E. A., Application of isotopically-labelled specific inhibitors as a method in enzyme cytochemistry. *Experimental Cell Research* **1961,** *25* (2), 465-&.

86.(a) Speers, A. E.; Cravatt, B. F., Profiling enzyme activities in vivo using click chemistry methods. *Chemistry & Biology* **2004,** *11* (4), 535-546; (b) Speers, A. E.; Cravatt, B. F., A tandem orthogonal proteolysis strategy for high-content chemical proteomics. *J. Am. Chem. Soc.* **2005,** *127* (28), 10018-10019; (c) Tully, S. E.; Cravatt, B. F., Activity-Based Probes That Target Functional Subclasses of Phospholipases in Proteomes. *J. Am. Chem. Soc.* **2010,** *132* (10), 3264-+; (d) Niphakis, M. J.; Johnson, D. S.; Ballard, T. E.; Stiff, C.; Cravatt, B. F., O-hydroxyacetamide carbamates as highly potent and selective class of endocannabinoid hydrolase inhibitors. *ACS Chemical Neuroscience* **2012,** *3* (5), 418-426.

87.Willems, L. I.; Overkleeft, H. S.; van Kasteren, S. I., Current Developments in Activity-Based Protein Profiling. *Bioconjugate Chemistry* **2014,** *25* (7), 1181-1191.

CHAPTER 1

NANOPROBE 1 AS A NEW METHOD FOR VISUALIZATION OF GLUTAMATE RECEPTORS ON LIVE TARGETS

2.1 Introduction

AMPARs are the crucial glutamatergic neurotransmitters that are involved in memory formation. They are discussed in detail in Section 1.1.8. In brief, they are composed as tetrameric assemblies of GluA1-A4 subunits. AMPARs are calcium permeable if they either lack the GluA2 subunit or contain an unedited form of GluA2.[1] GluA2 undergoes a post-natal single RNA codon at what has been termed the Q/R site. Here, the encoded glutamine is changed to an arginine via action of the enzyme ADAR. (More about how this is exactly accomplished can be found in Section 1.1.9.) It is this key change that mediates calcium permeability in AMPARs. Calcium permeable AMPARs have very recently been shown to have a larger impact upon neuronal development and in certain neuropathological diseases, such as ischemic injury and ALS.[2] Though the importance of calcium permeable AMPARs has been demonstrated, methods to understand their exact abundance, expression patterns, and movements are lacking.

In live neurons, methods to track these receptors, and other proteins, have involved the delivery of a contrast agent to the receptor as either a small molecule fluorophore or as a proteinaceous fluorophore. Proteinaceous fluorophores involve the expression of either a fluorescent fusion protein or a small protein tag that is then targeted by a fluorescent antibody.[3] While these methods are exquisitely specific, they involve the genetic manipulation of the receptor of interest or the delivery of a large protein to the synaptic cleft. Genetic manipulation of iGluR subunits leads to formation of non-native

homotetramers, due to the overexpression of the fluorescently encoded subunit. These non-native homomers do not provide information about movement of the native system.[3b] The synaptic cleft, or the space between the presynaptic and postsynaptic side of the two neurons, is only about 20 nm in size.[4] The application of an antibody to the synaptic cleft targeted to the produced protein tag introduces a contrast agent that is similar in size to the synaptic cleft, thus, will again not provide much useful information about trafficking of the particular receptor of interest.[5]
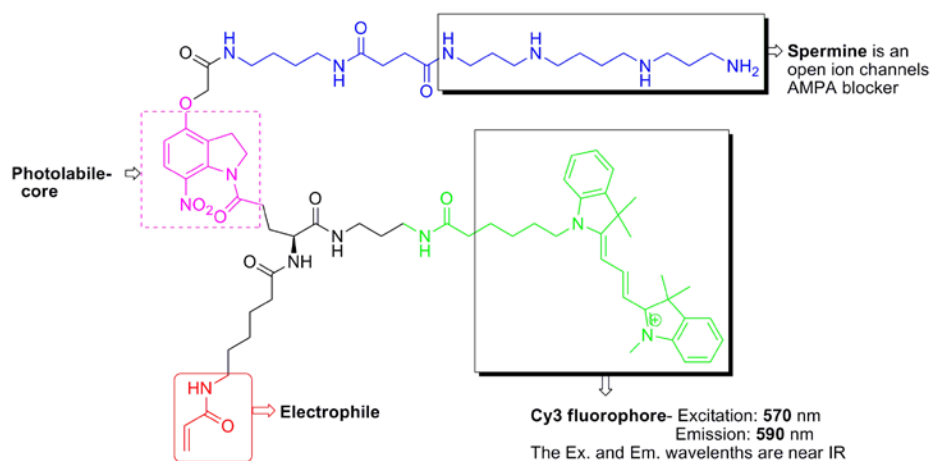
Figure 2.1: Structure of nanoprobe **1**. Nanoprobe **1** which contains spermine, an open ion channel blocker (blue) as the targeting ligand, a ANI core (pink) for photolysis, an acrylamide electrophile for bioconjugation to the surface of the protein (red), and a Cy-3 fluorophore (green) for visualization.

Taking the above into account, we decided to use the approach of delivering a small molecule probe to covalently tag our receptor of interest. In order to have an effective molecule for tagging native neuronal receptors, we must have a probe which is small, non-perturbing, and will provide a contrast agent (in this case a fluorophore) for visualization of the receptor. At its simplest, our probe design contains a photolabile core, a targeting ligand, an electrophile for bioconjugation, and a fluorophore for visualization. After probe application when we apply UV light to the system, the photolabile core is

cleaved, removing the targeting ligand, thus leaving behind our receptor tagged with our fluorophore for visualization via epifluorescence microscopy or confocal microscopy (Figure 2.2). The probe needs to add the electrophile in a non-perturbing manor, so that the receptor can function normally in order to fully understand how the receptor is trafficking in a condition which leads to memory formation, such as LTP. In our first version of this probe, termed nanoprobe **1**, we used alkoxynitroindoline (ANI) caged glutamate as our core, spermine as our targeting ligand, acrylamide as our electrophile, and Cy-3 as our fluorophore.(Figure 2.1) [6] We chose spermine as our targeting ligand for its known affinity for ionotropic glutamate receptors lacking GluA2 subunit, thus making a good candidate for the detection of calcium permeable AMPARs due to its well characterized use-dependency (discussed in Section 1.1.11).[7]
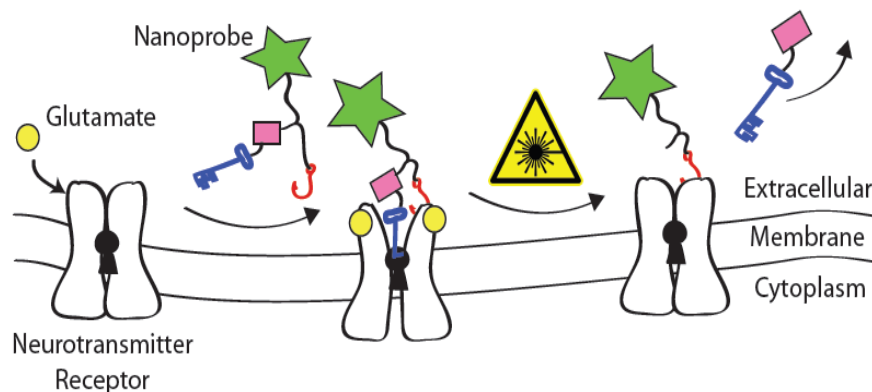
Figure 2.2: Cartoon of nanoprobe **1** mechanism. Glutamate (yellow dot) opens the ion channel and is targeted by our spermine ligand (blue key) which allows the acrylamide electrophile (red hook) to bind to nucleophile on the surface of the receptor. Photolysis with UV light breaks the ANI core (pink box) leaving the receptor tagged with the Cy-3 fluorophore (green star). Reproduced from Vytla, D. et al. *Org.Biomol. Chem.* **2011**, 9, pp. 7151-62 with permission from The Royal Society of Chemistry.

Tethered ligands have been used as a successful method of enhancing the local reactivity of an electrophile proximal to a good nucleophile. This is due to the effective local rise in concentration that comes after targeting ligand binds to its binding site, and

then places the electrophile in proximity with a nucleophile on the surface of the protein that is capable to undergo a Michael addition, such as a cysteine, serine, lysine, threonine, or tyrosine. The effective concentration of the nucleophile rises approximately 100-1000 fold locally in the small space where the electrophile is captive in.[6, 8]

2.2 Results

2.2.1 Patch-Clamp Electrophysiology Confirms Use-Dependence of the Probe
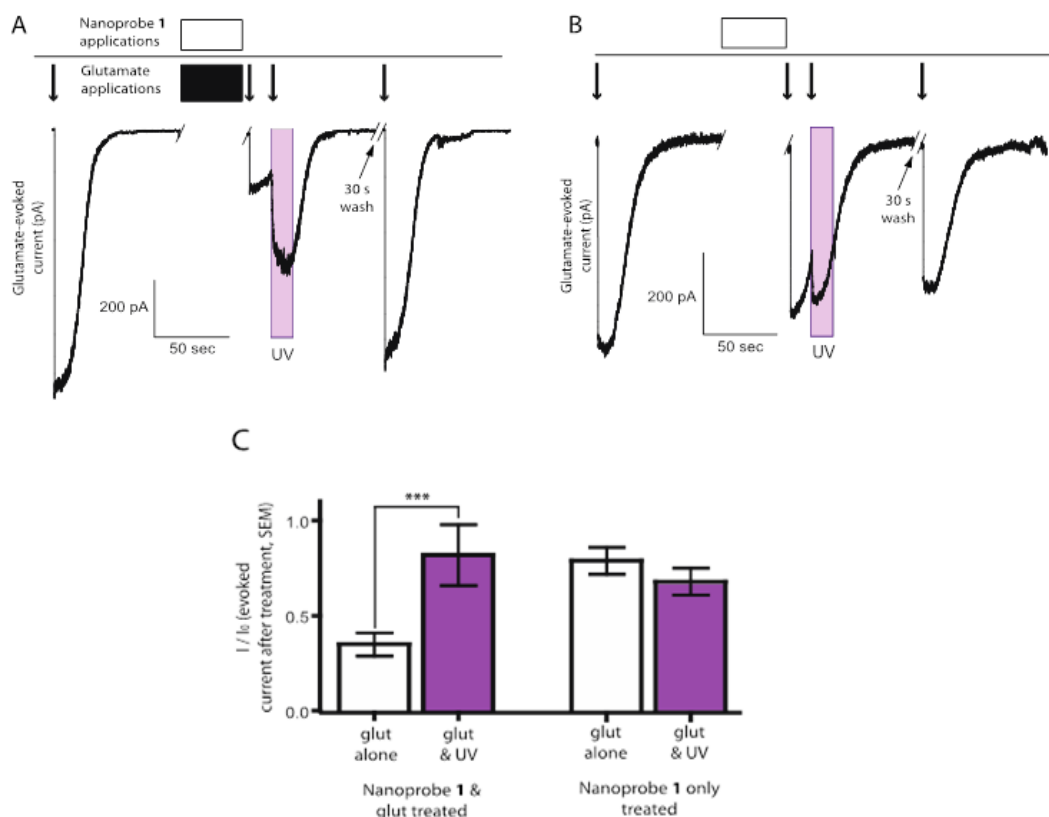
Figure 2.3: Patch-clamp electrophysiology results from nanoprobe **1. A)** Evoked glutamate currents in HEK 293T cells transfected with GluA1 (L497Y)-pIRES2-eGFP. The evoked current was taken first with 20 µM glutamate. Cells were incubated with 20 µM glutamate and 1 µM nanoprobe **1** for 1 min and then the evoked current was re-measured. UV light and glutamate were co-applied and the current was measured. A 60% blockage of current was observed. The cells were washed for 1 min and the evoked glutamate current was measured again, showing a return to the basal current. **B)** The same experiment was in A was performed without the co-incubation with 20 µM glutamate. A slight block in the evoked glutamate current was observed (~20%) without the co-incubation of glutamate and nanoprobe **1. C)** Quantification of the evoked glutamate current before and after UV photolysis of the ANI core with co-incubation of glutamate (n=10) and without the co-incubation of glutamate (n=6). Reproduced from Vytla, D. et al. *Org.Biomol. Chem.* **2011**, 9, pp. 7151-62 with permission from The Royal Society of Chemistry.

To confirm the use-dependence of the probe, we used patch-clamp electrophysiology to measure the block of current evoked by applied glutamate and adding in nanoprobe **1**. AMPARs display an inwardly rectifying current and this is lost upon biding of polyamines to the receptor. This loss of the current is also one of the key ways to determine if the receptor is calcium permeable or calcium impermeable, as calcium impermeable AMPARs are not sensitive to blocks by polyamine ligands; thus do not exhibit current loss.[9] We transiently transfected HEK-293T cells with GluA1 (L497Y)-pIRES2-eGFP homomultimers to create calcium permeable receptors in a heterologous system. We then co-applied 20 µM glutamate with nanoprobe **1** and measured the glutamate evoked current. The current decreased by approximately 60% to that of an initial pulse of glutamate. This is consistent with data that has been collected by others using other synthetic polyamines such as napthylacetylspermine (NAS).[10] We then applied UV light (380 nm) to the system to uncage the photolabile ANI core and applied constant pulses of glutamate and we found that the evoked current returned back to baseline glutamatergic signal. These experiments were repeated using 1µM nanoprobe **1** alone. What is found is there is only a slight blockage of the channel (~20%) and that there was no UV-dependence on release of the spermine ligand. The slight pore blockage may be due to the stochastic nature of AMPA receptors to open in the presentence of the applied voltage.[6, 10] This finding is graphically demonstrated in Figure 2.3.

2.2.2 Live Cell Imaging of Dissociated Cultures of Hippocampal Neurons with Nanoprobe 1 Using Epifluorescence Microscopy

Next, we investigated the targeting capability of nanoprobe **1** towards synaptically-active, polyamine-sensitive glutamate receptors in primary dissociated hippocampal cell culture. Dissociated cultures of rat hippocampal neurons were prepared and incubated to day *in vitro* (DIV) 20- 24. Neurons were first imaged using transmitted light in order to determine areas were synaptically active neurons should reside. They were then serially imaged using fluorescent light to acquire background data. Neurons were then bathed with either spermine ligand lacking nanoprobe (where a carboxylic acid is in place of the amide attached ligand) or nanoprobe **1** for 2 minutes in total darkness to prevent premature photolysis of the ANI core. UV light (380 nm) was then applied to the system and serial fluorescent imaging was then resumed. Extracellular buffer solution was constantly perfused across the system throughout the experiment, with the exception of the application of ligand lacking nanoprobe and nanoprobe **1**. The Cy-3 fluorescence that is observed is due to receptors being labeled in a use-dependent fashion with nanoprobe **1**. Fluorescence accumulation appears to be occurring in areas located at synaptic regions, which is where active glutamatergic receptors are known to reside. We can see from the bright-field image that these areas appear to contain synaptic spines, which is where any synaptic activity would occur. (Figure 2.4) [6]
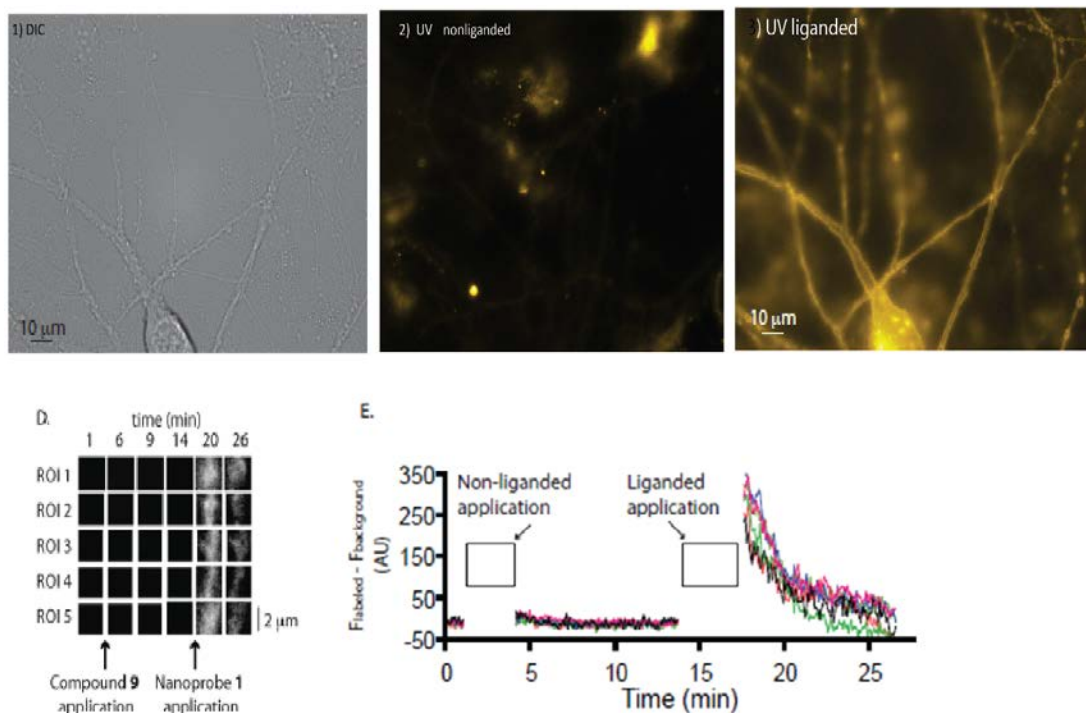
Figure 2.4: Representative images of neurons labeled with nanoprobe **1**. **A)** Transmitted light image of a neuron **B)** Fluorescence image of a neuron labeled with 750 nM of non-liganded nanoprobe **1 C)** Fluorescence image of a neuron labeled with 750 nM nanoprobe **1 D)** Time course of five ROIs (regions of interest) along a dendrite. The areas pointed out with the arrows are 1 min after non-liganded nanoprobe and nanoprobe **1** application .**E)** Fluorescence time course of the five ROIs (from **D**) during the course of the imaging experiment displaying the prolonged fluorescence after the liganded application of the probe. Reproduced from Vytla, D. et al. *Org.Biomol. Chem.* **2011**, 9, pp. 7151-62 with permission from The Royal Society of Chemistry.

When the ligand lacking probe is applied to the system, there is a slight increase in fluorescence. This fluorescence is not persistent as it is quickly washed away when perfusion is resumed. However, when nanoprobe **1** is applied to the same system, there is persistence to the fluorescence accumulation that remains through the imaging event. These results taken together suggest that nanoprobe **1** is acting in a ligand-dependent manner and that we are achieving covalent attachment of the probe through a Michael addition of the acrylamide to the biological nucleophile on the receptor surface.[6]

2.2.3 Live Cell of Dissociated Cultures of Hippocampal Neurons with Nanoprobe 1 Using Confocal Microscopy

We then wanted to further investigate the efficacy of our probe on neurons. We first examined the dose dependency of our probe to find the optimal, minimal concentration that can be used. Dissociated cultures of rat hippocampal neurons were grown to DIV 14-17, as this is reported to be when cultured neurons are found to be expressing synaptically active AMPARs.[11] We explored a concentration range from 100 nM, 300 nM, 1 µM, and 3 µM of nanoprobe **1** to determine the lowest concentration that would give us the best fluorescence accumulation. Imaging took place similar to that of the epifluorescence imaging, with the major difference being the lack of constant perfusion of fresh extracellular recording buffer being flowed across the neurons due to technical limitations of the confocal microscope. Coverslips of neurons were removed from their home media and washed three times with extracellular recording solution. They were then imaged to collect the background fluorescence and then incubated with 20 µM glutamate along with the various concentrations of nanoprobe **1** in extracellular buffer for 5 minutes in total darkness to prevent premature photolysis of the ANI core. UV light was then applied to the system, and the coverslip was washed three times with extracellular buffer. Neurons were then imaged to determine the fluorescence accumulation on the cells. The same coverslip of neurons were used for each concentration range to best determine the dose dependence of nanoprobe **1**.[11b]
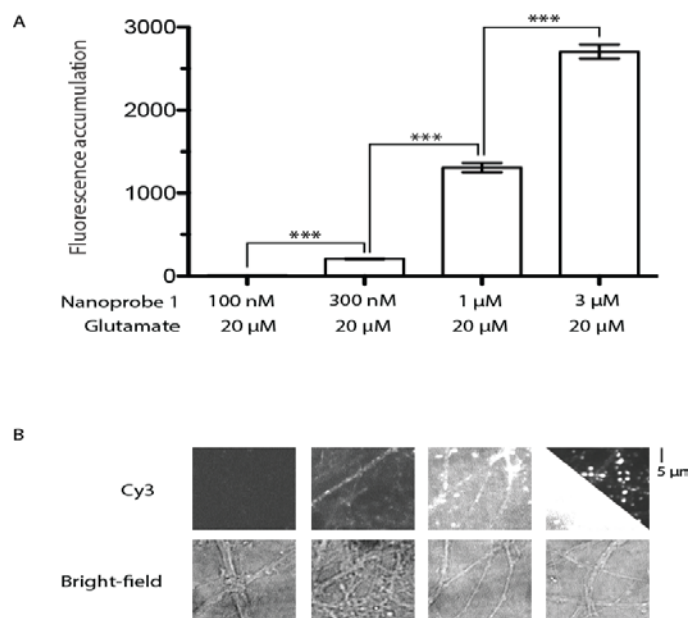
Figure 2.5: Fluorescence accumulation with increasing amounts of nanoprobe **1**. Nanoprobe **1** was incubated with DIV 14-17 neurons along with 20µM glutamate. Nanoprobe**1** was used at 100 nM, 300 nM, 1µM, and 3µM to determine the lowest working concentration to be used on cells with minimal background. The bar graph quantifies fluorescence accumulation. Representative images are shown underneath. Reproduced from Combs-Bachmann, R.E., et al. *J. Neurochem.* **2015** 133(3), pp.320-29with permission from John Wiley and Sons.

We found that our lowest concentration, 100 nM, did not provide significant fluorescence over the background. However, the next highest concentration, 300 nM, resulted in a marked increase of fluorescence over background and in areas that we had seen in our epifluorescence imaging experiments. The brightest areas appeared to be on that of synaptic spines, which was confirmed by examining the bright-field morphology. (Figure 2.5) When the concentrations were increased to 1 µM and 3µM, the fluorescence density at the areas described above was increased, but also increased amounts of non-specific labeling of other structures. We determined that for all further imaging experiments incubations of 20µM glutamate with 300 nM nanoprobe **1** would give us the best fluorescence density with the lowest background.[11b]

2.2.4 Competition Experiments of Nanoprobe 1 with Napthylacetylspermine and DNQX

We next wanted to determine the specificity of nanoprobe **1** against known

AMPAR antagonists. We chose napthylacetylspermine (NAS) and 6,7-

dinitroquinoxaline-2,3-dione (DNQX) as our antagonists. Nanoprobe **1** was designed to

act like NAS, so NAS was chosen to determine if the fluorescence we are seeing is due to

off-target reactions of nanoprobe **1** or if it is targeting the same channels as NAS. As

mentioned in the Section 1.1.9, NAS is used as a specific targeting moiety of calcium

permeable AMPARs and KARs over NMDARs.[10] DNQX was chosen due it is known

activity to block the glutamate binding site on AMPARs and KARs, preventing the ion

channel from opening.
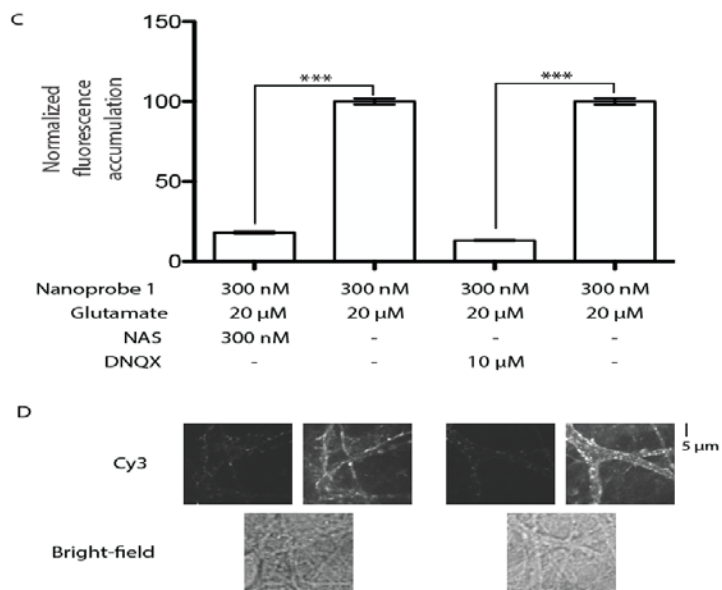
Figure 2.6: Dose-dependent labeling of nanoprobe **1** in competition with NAS and DNQX. Nanoprobe **1** (300 nM) was dosed in competition with NAS (300 nM) or DNQX (10μM). Fluorescence activity (shown in bar graphs) was decreased in the presence of the antagonist and regained after subsequent dosing with nanoprobe **1**. Fluorescence was normalized to maximal accumulation. Representative images are shown beneath bar graph. Reproduced from Combs-Bachmann, R.E., et al. *J. Neurochem.* **2015** 133(3), pp.320-29with permission from John Wiley and Sons.

For our NAS experiments, dissociated cultures of rat hippocampal neurons were grown to DIV 14-18. Cells were washed three times with extracellular buffer and were then imaged to collect background fluorescence. They were then co-incubated with 300 nM NAS and 300 nM nanoprobe **1** in the presence of 20 µM glutamate for 5 minutes. Cells were then washed three times with extracellular recording buffer and had UV light applied to them for photolysis of the ANI cage. Fluorescent images were then collected. The same set of cells were then washed and bathed in 300 nM nanoprobe **1** with 20 µM glutamate for 5 minutes. Cells were washed three times in extracellular solution and then fluorescent images were collected. Co-incubation of the neurons with NAS and nanoprobe **1** lead to a slight increase in fluorescence over the background, however, application of nanoprobe **1** alone lead to a large amount of fluorescence. This suggests that NAS and nanoprobe **1** are in competition for the same binding site. (Figure 2.6)

For our DNQX experiments, co-applications of 10 µM DNQX and 300 nM nanoprobe 1 and all imaging were carried out the same as for the NAS experiments. We found that co-application of DNQX and nanoprobe **1** once again has a slight increase in fluorescence compared to that of the background. The application of 300 nM nanoprobe **1** alone caused a large increase in fluorescence, suggesting that nanoprobe **1** is targeting neurons that are sensitive to DNQX. Taken together, the NAS and DNQX co-application data suggests that nanoprobe **1** is labeling neurons that may indeed be calcium permeable AMPARs.[11b]

2.2.5 Fluorescence Gel with Nanoprobe 1

We wanted to confirm that we were indeed labeling calcium permeable AMPARs with nanoprobe **1**. To do so, we turned to SDS-PAGE analysis of nanoprobe **1** labeled neurons. Each AMPAR is composed of heterotetramers of GluA1-GluA4 subunits; the weight of each is ~ 100 kDa. Also, the density of AMPARs is varied across

brain regions and neuronal subtypes. Knowing this, we chose to label the cortex, the

midbrain, and the cerebellum with two different concentrations of nanoprobe **1** in order to

pulldown subunits that would suggest calcium permeable AMPARs are being labeled.

Dissociated cultures of rat cortex, midbrain, and cerebellum were grown to DIV 18 in T-

flasks. T-flasks were washed three times with extracellular buffer and then 300 nM or

3µM nanoprobe **1** along with 20 µM glutamate were applied for 5 minutes. Cells were

then washed three times with extracellular solution and lysed with a probe sonicator. The

cell lysates were then spun down and the cell pellet was re-suspended in PBS. The cell

lysates were separated on a 10% SDS-PAGE gel and fluorescence was measured using a

Typhoon gel scanner. Western blots were first run against a pan-AMPA antibody to

confirm that ionotropic glutamate subunits were present, then against GluA1 and GluA2

antibodies.
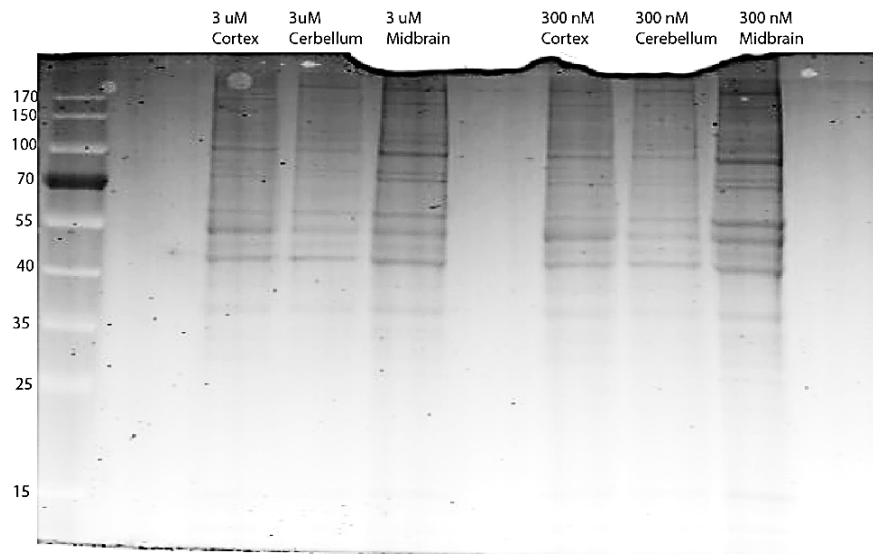
Figure 2.7: Fluorescence gel of nanoprobe **1** labeled neuronal proteins.
Cortex, mid-brain, and cerebellar neurons were grown to they were
synaptically active. Neurons were labeled with either 300 nM or 3
µM nanoprobe **1**, lysed, and the proteins were separated on a 10%
SDS-PAGE gel. Fluorescence bands were measured using a
Typhoon 9210 flatbed imager. Fluorescence bands were measured at
the desired 100 kDa band, as well as 180, 85, 80, 60, 50, and 45 kDa.

Our gel results show that we are indeed labeling a band that is around 100 kDa, as well as many other bands (Figure 2.7).We are also labeling targets which are at 180, 85, 80, 60, 50, and 45 kDa. Nanoprobe **1** is based upon a class of polyamine toxins that have been shown to display antagonism towards AMPARs, but there are other polyamine sensitive targets, specifically acetylcholine receptors and KARs, that are be present in primary culture. We cannot say if these are specific targets of the probe, or are just targets which are reactive to the acrylamide electrophile on nanoprobe **1**.

2.3 Discussion

Using a heterologous system of HEK 293T cells transfected with GluA1 L497Y homomers and patch-clamp electrophysiology, we were able to determine that our probe was indeed acting in a use-dependent fashion. Polyamine toxins have been used to target towards active calcium permeable AMPARs as they will block the glutamate evoked current that travels through the ion pore. This has been found with natural polyamine toxins, such as Joro spider toxin and argiotoxin,[9b, 12] as well as synthetic polyamines, such as NAS.[10] The IC_{50} of NAS is 0.33μM and blockage of calcium permeable AMPARs is around 70%.[10] This places our probe on par with NAS, however the IC_{50} of nanoprobe **1** would be extremely challenging, if not impossible, to determine as nanoprobe **1** does not have a detectable off-rate.

In our initial imaging experiments, we targeted our probe to areas of known pathology where synaptically-active, polyamine-sensitive glutamatergic neurons are known to reside in dissociated cultures of rat hippocampal neurons. The distribution of these receptors is heterologous between cultures and contains many other neuronal receptor subtypes, specifically acetylcholine receptors. Our cultures also contain a very large number of biological nucleophiles that could be potentially targeted by nanoprobe **1**. Thus it is not impossible to imagine that we should have a large amount of

background reactivity of the probe towards these nucleophiles. However, nanoprobe **1** is not just the acrylamide electrophile, rather a molecule that contains acrylamide as part of its structure. Labeling of the targeted protein is only occurring once the effective concentration of the probe and the acrylamide is achieved. This is clearly seen when neurons are labeled with spermine lacking nanoprobe. We do not observe a large accumulation of fluorescence anywhere, which would be expected if acrylamide was having a large amount of off-target labeling.[6]

Our cultures also do not only contain active AMPARs, rather active glutamate receptors. This means that we have both NMDARs and KARs present in culture. It is possible that we are labeling both of these receptor subtypes as we are using a high concentration of probe in our initial imaging experiments. Spermine can have activity against NMDARs,[13] however, much like how our probe is not simply acrylamide, our probe is not simply spermine. Nanoprobe **1** was designed to resemble NAS, and NAS has been used as a specific target towards calcium permeable AMPARs over NMDARs.[10] We can say that nanoprobe **1** is sensitive to non-NMDAR polyamine-sensitive glutamatergic receptors.

Confocal imaging data of neurons labeled with nanoprobe **1** furthered our understanding of where nanoprobe **1** is targeting. We first determined the lowest concentration that we could use in imaging experiments in order to limit off-target effects. The IC_{50} of polyamine toxins varies, but ranges from ~ 10 nM to 15 µM depending on its intended target.[14] Our probe falls into this scale, as 300 nM gave us the best contrast. Once determined, our next goal was to determine the specificity of nanoprobe **1**. By using known AMPAR antagonists NAS and DNQX, we examined the competition of nanoprobe **1** against them. What we found is that co-incubation with NAS or DNQX prevents nanoprobe **1** binding, which is regained when nanoprobe **1** is

49

reapplied alone. This suggests that nanoprobe **1** is indeed targeting towards receptors that would appear to be calcium permeable AMPARs.

We then wanted to determine which receptors we were truly targeting. This was done via SDS-PAGE analysis of three different regions of neurons labeled with nanoprobe **1**. What we found is that there is labeling something that could be an AMPAR subunit, along with a variety of other unintended targets. This is certainly due to our polyamine targeting ligand on nanoprobe **1**, spermine, directing towards other polyamine sensitive receptors, chiefly acetylcholine receptors. Our cultures come from a primary rat source and contain a wide variety of receptor subtypes. These subtypes vary not only in where they are located in the brain, but also from culture to culture. However, not all of these receptors will be blocked by both NAS and DNQX as our imaging experiments clearly show. Literature widely reports that both NAS and DNQX are antagonists towards calcium permeable AMPARs, but they could not be as selective as reported. Most of the early work in the literature is done in heterologous cultures in which AMPAR subunits are present in high concentrations. There could very well be other targets in neuronal culture that are polyamine sensitive that are yet to be identified. In conclusion, nanoprobe **1** is a useful tool for the detection of active glutamate receptors in dissociated culture of rat neurons, but questions about subtype inclusion in these tagged receptors still need to be addressed.

2.4 Methods

2.4.1 HEK 293T Cell Culture

Cells were grown to they were 70 % confluent on cover glass (12mm, 1.0 size) in DMEM media containing 10% FBS. Cells were grown at 6 % CO_2 at 37°C. Cells were transfected using LipoD293 (SignaGen Laboratories, Gaithersburg, MD, USA) with

bicistronic vector GluA1 (L497Y)-pIRES2-eGFP [15] 1-3 days before electrophysiological experiments.

2.4.2 Dissociated Hippocampal Cell Culture

Primary dissociated hippocampal cell cultures were prepared from embryonic day E18-20 Sprague-Dawley rat embryos and were cultured on polylysine-coated coverglass (25.5 mm, 1.0 size for epifluorescence microscopy; 12mm 1.0 size for confocal microscopy) in serum containing media identical to previous reports.[16] Cells were grown in 5% CO_2 and at 37°C. All animal care and experimental protocols were approved by the Animal Care and Use Committee at University of Massachusetts, Amherst, Amherst, MA, USA.

2.4.3 Dissociated Cortex, Midbrain, and Cerebellar Cell Culture

Primary dissociated cortex, midbrain, and cerebellar cell cultures were prepared from embryonic day E18-20 Sprague-Dawley rat embryos and were cultured on 25 cm^2 T-Flasks coated in poly-lysine in serum containing media identical to previous reports.[16] Cerebellar culture media was supplemented with 1M potassium chloride (1mL in 50 mL).[17] Cells were grown in 5% CO_2 and at 37°C. All animal care and experimental protocols were approved by the Animal Care and Use Committee at University of Massachusetts, Amherst, Amherst, MA, USA.

2.4.4 Live Cell Imaging with Nanoprobe 1 Using Epifluorescence Microscopy

Hippocampal neurons were imaged by excitation with a light from a Sutter Lambda-LS illuminator (Sutter Instruments, Novato, CA,USA). A Nikon Eclipse Ti series microscope (Nikon Corps, Tokyo, Japan) with a CFI Plan Apo VC 60X 1.4 NA oil objective lens (Nikon) was employed for all imaging epifluorescence experiments. The Cy-3 filter cue contained a 540/30 excitation filter, a 570 DRLP dichroic mirror, and 575

ALP emission filter (all from Omega Optical Corp., Brattleboro, VT, USA). Images were acquired using a Hamamatsu ORCA ER camera (Hamamatsu, Hamamatsu City, Japan) and NIS Elements BR 3.1 software (Nikon Corps, Melville, NY, USA).

Cells were mounted in a 25 mm perfusion apparatus (ALA M-525, ALA Scientific, Farmingdale, NY, USA) and bathed in extracellular buffer solution containing 138 mM NaCl, 1.5 mM KCl, 1.2 mM $MgCl_2$, 5 mM HEPES, 2.5 mM $CaCl_2$, and 14 mM glucose at pH 7.4. Fresh recording buffer was constantly perfused over hippocampal cultures using a perfusion device (ALA-UM8, ALA Scientific) at all times except for nanoprobe **1** or ligand lacking nanoprobe were incubated. Fluorescence images were acquired at 20 frames per second using the Cy-3 filter set to capture background and post-labeled stopped leaving minimal buffer on cells. Next, 200 µL of 750 nM ligand lacking nanoprobe was added to the bath and incubated for 2 minutes. Perfusion was restarted and imaging was carried out for 10 minutes at which point the background fluorescence was re-established and measured again for 1 minute. Perfusion was again stopped, leaving minimal buffer on the cells. Finally, 200 µL of 750 nM nanoprobe **1** was added to the bath and incubated for 2 minutes. Perfusion was reinstated and imaging was carried out for 10 minutes.

2.4.5 Image Analysis of Epifluorescence Imaging Data

Images were analyzed using ImageJ (U.S. National Institutes of Health, Bethesda, MD, USA). Fluorescence was quantified using ROI (region of interest) analysis of multiple regions placed over putative synaptic sites and areas of background. The mean fluorescence intensity was background subtracted and normalized to the measured fluorescence at 1 minute before the application of ligand lacking nanoprobe and time courses were plotted using GraphPad Prism (La Jolla, CA, USA). Seven image

series were analyzed and the data combined for a total of 131 ROIs analyzed. GraphPad Prism was used to plot the data.

2.4.6 Live Cell Imaging with Nanoprobe 1 Using Confocal Microscopy

Hippocampal neurons were imaged using a Nikon TiE microscope fitted with a CSU-x1 Yokogawa spinning disk confocal scan head (PerkinElmer, Waltham, MA, USA) and an Andor iXon+ electron-multiplying CCD camera (Andor, Belfast, Northern Ireland). All confocal settings were kept the same for the labeling experiments. The microscope and lasers were controlled by MetaMorph software (Molecular Devices, Sunnyvale, CA, USA). A 100x 1.4 NA objective (Nikon) was used for imaging. 250 ms exposures of a 561 nm laser were used to image all fluorescence images, keeping everything below pixel saturation. Pixel size is a 140 x 140 nm square.

Coverslips containing neurons were removed from their home media and mounted into a 12 mm perfusion apparatus (Warner Instruments, P-3, RC-25, Warner Instruments LLC, Hamden, CT, USA) and were bathed in extracellular recording buffer. Coverslips were then washed three times and placed in a static bath of extracellular solution. They were then imaged for 2 minutes to establish background fluorescence levels. Testing solutions were then applied, either 20 µM glutamate with the ranging nanoprobe **1** concentration, or the co-application of nanoprobe **1** with 10µM DNQX (Tocris Bioscience, Bristol, United Kingdom) or 300 nM NAS (Sigma Aldrich St. Louis, MO, USA), for 5 minutes in total darkness. Coverslips were irradiated with 405 nm light for 15 seconds for photolysis of the ANI core. Coverslips were then washed three times with extracellular solution and returned to a static bath. Imaging was then resumed.

2.4.7 Image Analysis of Confocal Imaging Data

All images were analyzed using ImageJ. To quantify fluorescence accumulation of nanoprobe 1, areas of the field of view in which there was fluorescence activity after

53

application of glutamate and nanoprobe 1 were identified by using the Triangle threshold, in which the maximum of the histogram along a data linear data range is used as the maximum threshold value.[18] These threshold values were then used to generate a massive ROI list of all labeled regions in the field. ROIs were then used at all previous time points for quantification during the dosage and competition experiments. Fluorescence intensities were quantified using the mean grey value of regions labeled with nanoprobe 1 and then background subtracted from the average of three ROIs drawn in areas where no cells were present in the corresponding brightfield image. All brightness and contrast was set equal in groups of comparative images for analysis. Group mean values at each dosage or competition experiment were compared to the respective control values using a one-way nonparameteric Kruskal-Wallis test. Significance values were assigned using a Dunn's multiple comparison test. In all cases, significance was determined to be $p < 0.05$ and p values are reported in all cases. Asterisks signify statically significance.

2.4.8 Fluorescent SDS-PAGE gel of nanoprobe 1 labeled neurons

25 cm^2 T-Flasks were washed three times with extracellular buffer. 7 mL of 300 nM or 3 µM solutions of nanoprobe **1** in extracellular buffer with 20 µM glutamate were added into the flasks and allowed to sit for 5 minutes at room temperature. Flasks were then washed again three times with extracellular buffer. 2 mL of lysis solution, 1x PIC in 1x PBS buffer, were added to each flask and cells were then scraped into a 2 ml Eppendorf tube. The cell lysates were then sonicated with a probe sonicator at 30% power for 1 minute. A bicinchoninic acid (BCA) assay was run to ensure that same amount of protein was added to each lane. Samples were run on a 10% SDS-PAGE gel and sat for 16 hours in 10% acetic acid solution. The gel was imaged using a Typhoon 9210 flatbed imager using 532 laser line set using a 588 bandpass filter.

2.4.9 Western Blots of Nanoprobe 1 Labeled Neurons

Using the same samples as the fluorescence gels and a BCA assay was run prior to each blot. Protein lysate samples were run on 10% SDS-PAGE gels and transferred to a nitrocellulose membrane using CAPS buffer for 16 hours at 4°C. Blots were first probed with 1:200 Pan-AMPA (GluR-1/2/3/4) rabbit polyclonal antibody (Santa Cruz Biotechnology Inc. Dallas, TX, USA). Subsequent blots were probed for GluA1 (Millipore, Billerica, MA, USA) and GluA2 (Millipore).

2.5 References

1.Isaac, J. T. R.; Ashby, M.; McBain, C. J., The role of the GluR2 subunit in AMPA receptor function and synaptic plasticity. *Neuron* **2007,** *54* (6), 859-871.

2.(a) Tateno, M.; Sadakata, H.; Tanaka, M.; Itohara, S.; Shin, R. M.; Miura, M.; Masuda, M.; Aosaki, T.; Urushitani, M.; Misawa, H.; Takahashi, R., Calcium-permeable AMPA receptors promote misfolding of mutant SOD1 protein and development of amyotrophic lateral sclerosis in a transgenic mouse model. *Hum. Mol. Genet.* **2004,** *13* (19), 2183-2196; (b) Kwak, S.; Hideyama, T.; Yamashita, T.; Aizawa, H., AMPA receptor-mediated neuronal death in sporadic ALS. *Neuropathology* **2010,** *30* (2), 182-188; (c) Talos, D. M.; Fishman, R. E.; Park, H.; Rebecca, D. F.; Follett, P. L.; Volpe, J. J.; Jensen, F. E., Developmental regulation of alpha-amino-3-hydroxy-5-methyl-4-isoxazole-propionic acid receptor subunit expression in forebrain and relationship to regional susceptibility to hypoxic/ischemic injury. I. Rodent cerebral white matter and cortex. *Journal of Comparative Neurology* **2006,** *497* (1), 42-60; (d) Weiss, J. H., Ca^{2+} permeable AMPA channels in disease of the nervous system. *Frontiers in Molecular Neuroscience* **2011,** *4* (42), 1-7.

3.(a) Ju, W.; Morishita, W.; Tsui, J.; Gaietta, G.; Deerinck, T. J.; Adams, S. R.; Garner, C. C.; Tsien, R. Y.; Malenka, R. C., Activity-dependant regulation of dendritic synthesis and trafficking of AMPA recepotrs. *Nature Neuroscience* **2004,** *7* (3), 244-254; (b) Bredt, D. S.; Nicoll, R. A., AMPA receptor trafficking at excitatory synapses. *Neuron* **2003,** *40* (2), 361-379; (c) Madani, F.; Lind, J.; Damberg, P.; Adams, S. R.; Tsien, R. Y.; Gräslund, A. O., Hairpin structure of biarsenical-tetracysteine motif determined by NMR spectroscopy. *J. Am. Chem. Soc.* **2009,** *131*, 4613-4615.

4.Zuber, B.; Nikonenko, I.; Klauser, P.; Muller, D.; Dubochet, J., The mammalian central nervous synaptic cleft contains a high density of periodically organized complexes. *Proc. Natl. Acad. Sci. U. S. A.* **2005,** *102* (52), 19192-19197.

5.(a) Hussey, A. M.; Chambers, J. J., Methods To Locate and Track Ion Channels and Receptors Expressed in Live Neurons. *ACS Chemical Neuroscience* **2015,** *6* (1), 189-198; (b) Sobolevsky, A. I.; Rosconi, M. P.; Gouaux, E., X-ray structure, symmetry and mechanism of an AMPA-subtype glutamate receptor. *Nature* **2009,** *462* (7274), 745-U66.

6.Vytla, D.; Combs-Bachmann, R. E.; Hussey, A. M.; Hafez, I.; Chambers, J. J., Silent, fluorescent labeling of native neuronal receptors. *Organic & Biomolecular Chemistry* **2011,** *21* (9), 7151-7161.

7.Bowie, D.; Mayer, M. L., Inward rectification of both AMPA and kainate subtype glutamate receptors generated by polyamine-mediated ion-channel block *Neuron* **1995,** *15* (2), 453-462.

8.(a) Levitsky, K.; Boersma, M. D.; Ciolli, C. J.; Belshaw, P. J., Exo-mechanism proximity-accelerated alkylations: Investigations of linkers, electrophiles and surface mutations in engineered cyclophilin-cyclosporin systems. *Chembiochem* **2005,** *6* (5), 890-899; (b) Gallagher, S. S.; Jing, C.; Peterka, D. S.; Konate, M.; Wombacher, R.; Kaufman, L. J.; Yuste, R.; Cornish, V. W., A Trimethoprim-Based Chemical Tag for Live Cell Two-Photon Imaging. *Chembiochem* **2010,** *11* (6), 782-784.

9.(a) Stromgaard, K.; Mellor, I., AMPA receptor ligands: Synthetic and pharmacological studies of polyamines and polyamine toxins. *Medicinal Research Reviews* **2004,** *24* (5), 589-620; (b) Herlitze, S.; Raditsch, M.; Ruppersberg, J. P.; Jahn, W.; Monyer, H.; Schoepfer, R.; Witzemann, V., Argiotoxin detects molecular differences in AMPA receptor channels. *Neuron* **1993,** *10* (6), 1131-1140.

10.Koike, M.; Iino, M.; Ozawa, S., Blocking effect of 1-naphthyl acetyl spermine on Ca^{2+} - permeable AMPA receptors in cultured rat hippocampal neurons. *Neuroscience Research* **1997,** *29*, 27-36.

11.(a) Bats, C.; Farrant, M.; Cull-Candy, S. G., A role of TARPs in the expression and plasticity of calcium-permeable AMPARs: Evidence from cerebellar neurons and glia. *Neuropharmacology* **2013,** *74*, 76-85; (b) Combs-Bachmann, R. E.; Johnson, J. N.; Vytla, D.; Hussey, A. M.; Kilfoil, M. L.; Chambers, J. J., Ligand-directed delivery of fluorophores to track native calcium-permeable AMPA receptors in neuronal cultures. *J. Neurochem.* **2015,** *133* (3), 320-329.

12.Blaschke, M.; Keller, B. U.; Rivosecchi, R.; Hollmann, M.; Heinemann, S.; Konnerth, A., A single amino-acid determines the subunit-specific spider toxin block of alpha-amino-3-hydroxy-5-methylisoxazole-4-propionate kainate receptor channels. *Proc. Natl. Acad. Sci. U. S. A.* **1993,** *90* (14), 6528-6532.

13.Mony, L.; Kew, J. N. C.; Gunthorpe, M. J.; Paoletti, P., Allosteric modulators of NR2B-containing NMDA receptors: molecular mechanisms and therapeutic potential. *British Journal of Pharmacology* **2009,** *157* (8), 1301-1317.

14.Mellor, I. R.; Usherwood, P. N. R., Targeting ionotropic receptors with polyamine-containing toxins. *Toxicon* **2004,** *43* (5), 493-508.

15.Nagarajan, N.; Quast, C.; Boxall, A. R.; Shahid, M.; Rosenmund, C., Mechanism and impact of allosteric AMPA receptor modulation by the Ampakine (TM) CX546. *Neuropharmacology* **2001,** *41* (6), 650-663.

16.Chambers, J. J.; Kramer, R. H., Light-Activated Ion Channels for Remote Control of Neural Activity. In *Methods in Nano Cell Biology*, Jena, B. P., Ed. 2008; Vol. 90, pp 217-+.

17.Bilimoria, P. M.; Bonni, A., Cultures of cerebellar granule neurons. *CSH protocols* **2008,** *2008*, pdb.prot5107-pdb.prot5107.

18.Zach, G. W.; Rogers, W. E.; Latt, S. A., Automatic measurements of sister chromatid exchange frequencies. *J. Histochem. Cytochem.* **1977,** *25* (7), 741-53.

CHAPTER 2

PHILANTHOTOXIN BASED PROBE FOR THE DETECTION OF CALCIUM PERMEABLE AMPA RECEPTORS

3.1 Introduction

From our prior studies with nanoprobe **1**, it is clear that we need to develop a probe that could identify the proteins we were targeting. We also wanted to develop a probe that could be easily synthesized and be used with a wide number of applications for probing our receptors of interest. There are a wide number of polyamine toxins (Figure 1.7) that are used and modified to be used study calcium permeable AMPARs. Looking at each of the polyamine toxins, the two main moeites of each are the aromatic head group and the polyamine tail. We selected philanthotoxin-433 to move forward with as a potential new probe for the detection of calcium permeable AMPARs for a number of reasons, including its selectivity towards calcium permeable AMPARs and the ease of modification.

Philanthotoxin-433 is the toxin in the venom of the parasitic wasp, *Philanthus triangulum*, or the Egyptian digger wasp (also known as the European bee wolf). This solitary wasp is generally an herbivore, but the pregnant wasp uses its venom to paralyze its prey, honeybees, to leave for the larvae to eat.[1] The venom of *P. triangulum* was show by Piek and colleagues to be an antagonist of glutamatergic synapses in the motor neurons of both locus leg muscle and honeybee muscle junctions.[2] In 1988, philanthotoxin was isolated from the venom via HPLC, its structure was determined, and then pure toxin was synthesized. This molecule was named phlianthotoxin-433, with the numbering referring to the number of methylene units contained in the polyamine tail.[1] Derivatives of phlianthotoxin have since been synthesized, aiming to increase the efficacy over the first isolated compound.[3]

Nanoprobe **2** modifies philanthotoxin so that we can use it as a probe for the detection of calcium permeable AMPARs. To do so, we added an electrophile for bioconjugation onto the surface of the protein. We also installed an alkyne handle so that our probe can be targeted and visualized with azido functionalized reporter tags that can be attached using a 1,3-dipolar cycloaddition, or a click reaction.

We redesigned our nanoprobe to allow us to determine which receptors our probe was targeting. One of the key reasons that we installed an alkyne handle onto nanoprobe **2**, was to use our new probe in activity-based protein profiling experiments. Chemical activity based protein profiling (described in Section 1.3.3 (chem ABPP)) was refined by Benjamin Cravatt's group, and involves a small molecule probe, equipped with an alkyne, being directed towards a target of interest. Once the probe is covalently attached, the protein can then be visualized using an azide functionalized reporter tag, usually a fluorophore or biotin.[4] The output can be visualized via SDS-PAGE analysis. Any bands that are marked by the reporter tag can then be further analyzed by mass spectrometry. [4b]

3.2 Results

3.2.1 Design of Nanoprobe 2

Nanoprobe **2** was designed to retain the key features of phlianthotoxin as much as possible; unlike nanoprobe **1**which was based on a synthetic analogue. To do so, we eliminated the photoreactive core in nanoprobe **1** from the probe design of nanoprobe **2**. This was done for two main reasons. One was for the ease of synthesis of nanoprobe **2**. Nanoprobe **1** was completed in 26 steps, with the synthesis of the nitroindole core being a portion of them. The second was to make a probe that was more representative of the polyamine toxin class. We wanted to produce a probe that more closely resembled the natural toxin, so that some of the off-target effects we were observing with nanoprobe **1** could be eliminated. We also wanted a probe that was a bit easier to use in the chemical

ABPP experiments. Removal of the photolabile core also eliminates the photolysis step, which simplifies its use. To the core structure of philanthotoxin-433, we amended the butyl chain so it contains an electrophile, acrylamide, for bioconjugation to the surface of the receptor. Much like nanoprobe **1**, we are relying on proximity accelerated reactivity to facilitate the Michael addition of the acrylamide to a nucleophile on the surface of the protein. We also amended the phenolic hydroxide so that it contains an alkyne handle than can be used for conjugation with an azide functionalized reporter tag.

Synthesis of nanoprobe **2** commenced with tyrosine. We then protected the primary amine with Boc and the carboxylic acid with a methyl ester to install the alkyne handle. Subsequent Boc deprotection allowed for the installation of n-acrylaminohexanoic acid for the addition of the electrophile. We then deprotected the carboxylic acid for peptide coupling with triBoc spermine. Boc deprotection afforded nanoprobe **2**, which contains spermine as our targeting ligand, much like nanoprobe **1.** (Scheme 3.1)
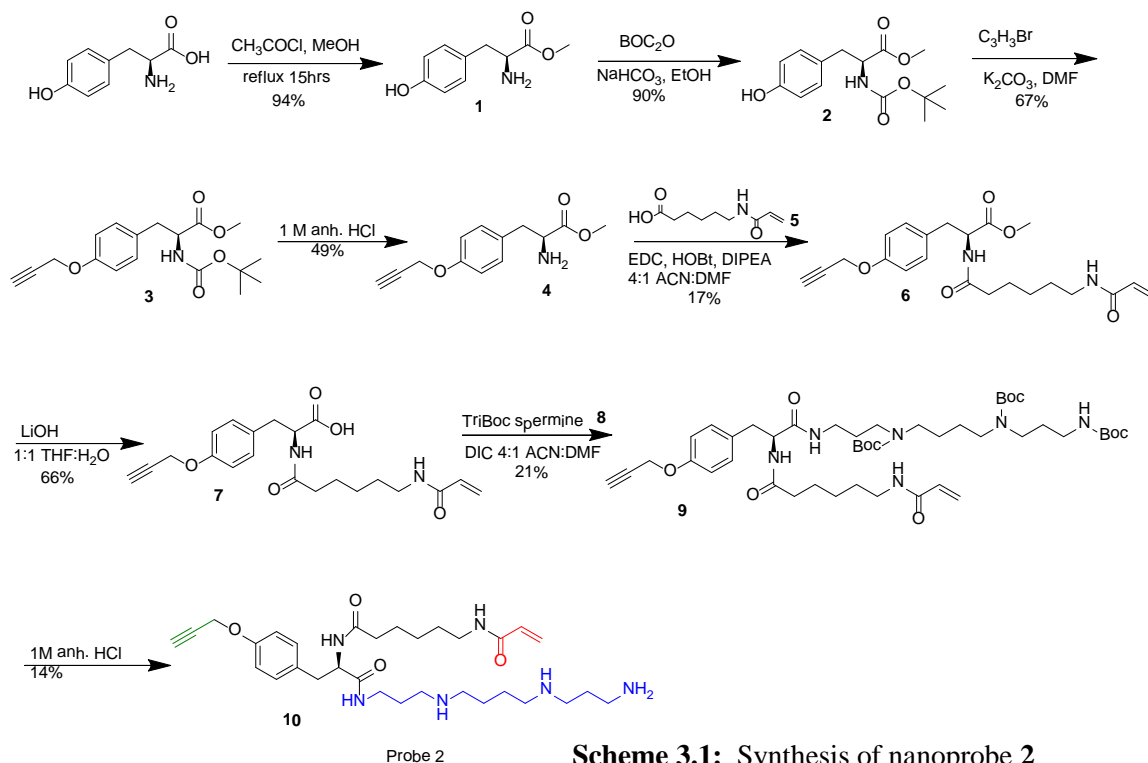
Scheme 3.1: Synthesis of nanoprobe **2**

3.2.2 Confocal Imaging of Cerebellar Neurons with Nanoprobe 2

We wanted to investigate if nanoprobe **2** was behaving similar to nanoprobe **1** in dissociated cultures of neurons. We chose to use dissociated cultures of rat cerebellar neurons in this case due to a reported higher concentration of calcium permeable AMPARs.[5] We first needed to make nanoprobe **2** amendable for visualization in live cell imaging. To do this, we clicked on a fluorescent reporter tag, fluorescein (FAM-5) azide, to nanoprobe **2**. Since this click reaction is done through copper catalyzed methods, it needed to be done prior to application to live cells to prevent the toxic effects of copper on the neurons. Neuronal cultures were grown to DIV 18-20, washed three times with extracellular recording solution, and mounted into a perfusion apparatus. They were then covered in extracellular solution and imaged to collect background fluorescence data. Nanoprobe **2** (10 µM) in extracellular solution was added to the neurons for 5 minutes at room temperature. Neurons were then washed three times and imaged to collect fluorescence.

Similar to what we observed with nanoprobe **1**, nanoprobe **2** had fluorescence accumulation that occurred in areas around synaptic regions that were seen in the brightfield image. This suggests that nanoprobe **2** is targeting areas similar to nanoprobe **1**. The fluorescence accumulation in these areas is greater than that of the background. This is seen in Figure 3.2
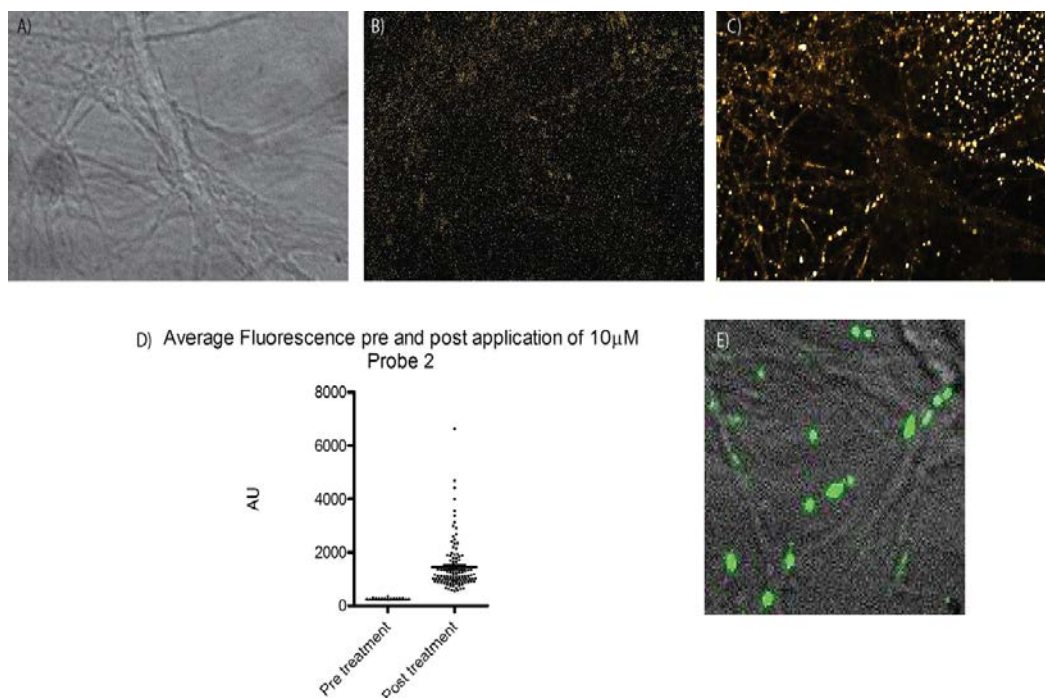
Figure 3.1: Confocal imaging of cerebellar neurons with nanoprobe **2**. **A)** Transmitted light image of cerebellar neurons **B)** Pre-probe application fluorescence image **C)** Post-probe application fluorescence image **D)** Graph of fluorescence accumulation in synaptic regions. Fluorescence is higher than the pre-probe application. **E)** Overlay of post-probe fluorescence image with white light image showing that fluorescence accumulation is in areas that are synaptically active.

3.2.3 Chemical Activity Based Protein Profiling on Dissociated Cultures of Rat Cortex, Mid-Brain, and Cerebellar Neurons

We then planned to investigate which ionotropic glutamate receptor subtypes we are targeting with nanoprobe **2**. To do so, 25 cm^2 T-flasks of cortex, mid-brain, and cerebellar neurons were grown to synaptically active (DIV 14-18). Flasks were washed three times with extracellular recording buffer and then 0, 1, 3, or 10 µM of nanoprobe **2** dissolved in 7 mL of extracellular solution with 20 µM glutamate was applied for 5 minutes at room temperature. Control solutions containing equal concentration of nanoprobe **2** and NAS were also made for additional flasks. Flasks were then washed

three more times with extracellular solution. Next, 1 mL of lysis solution (1 x PIC, 1x PBS) was added to each flask and cells were scrapped to remove from sides of the T-flask. Cells were lysed, and the membrane portions were spun down. The membrane pellet was lysed again and the lysates were subjected to chemical activity based protein profiling, chem ABPP. In chem ABPP, the azide functionalized reporter tag is added to the lysate to undergo copper mediated click chemistry. The treated lysates were then separated on a 10% SDS-PAGE gel.
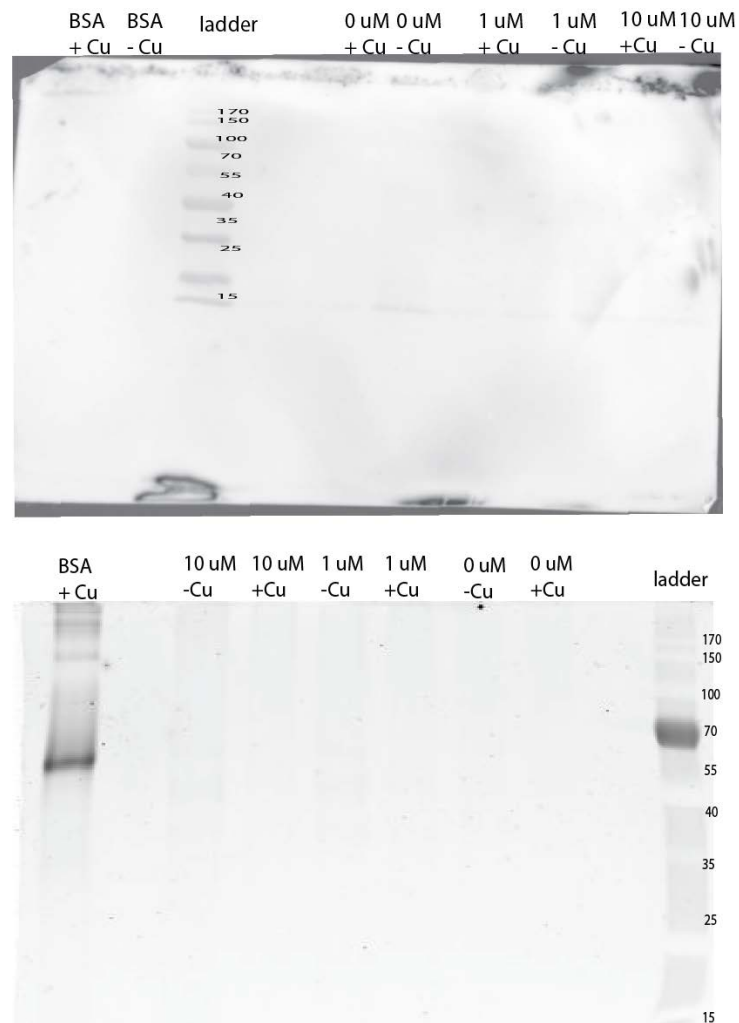
Figure 3.2: In-gel fluorescence and Western blot of rat midbrain samples labeled with nanoprobe **2**. Top: Western blot of nanoprobe **2** labeled midbrain samples conjugated with biotin azide. Samples were separated on a 10 % SDS-PAGE gel, transferred to a nitrocellulose membrane, and probed using streptavidin-HRP. Bottom: In-gel fluorescence of nanoprobe **2** labeled midbrain samples conjugated with rhodamine azide. Samples were separated on 10% SDS-PAGE gel. In both cases, no signal was detected in probed neuronal samples.

We used either rhodamine azide for fluorescence visualization or biotin azide for Western blot analysis with streptavidin-HRP. The dual mode of visualization allows for different levels of detection due to different sensitivities of each technique. The amount of protein we are targeting amounts to only a very small portion of the total brain lysate. After running both of these gels multiple times, we do not observe any signal in lanes which contain brain lysate. (Figure 3.3)

3.2.4 Chemical Activity Based Protein Profiling with Cortex and Cerebellum Samples from Female C57BL/6 Mice

After multiple trials with pre-natal dissociated culture, we then went to try nanoprobe **2** in adult mouse brain samples because we were concerned that there was a low concentration of our desired protein in our dissociated culture samples. Brain samples were kindly provided by Jesse Mager's lab in Veterinary and Animal Sciences at UMass, Amherst. Brains were removed, segmented, and placed into extracellular solution containing 20 µM glutamate and 0, 1, or 3 µM nanoprobe **2** or solutions containing 20 µM glutamate with equimolar mixtures of nanoprobe **2** and NAS at the same concentration as above. Brain samples were allowed to incubate in these solutions for 15 minutes at room temperature and were then washed three times with extracellular solution. Samples were then lysed using a probe sonicator and the lysates underwent chem ABPP with biotin azide. Lysates were separated on a 10% SDS-PAGE gel, transferred to a nitrocellulose membrane, and then probed using streptavidin-HRP. The bands in this case were inconclusive (Figure 3.4), as biotin staining was present in control samples which did not have any probe present. The cerebellum has a large amount of endogenous biotin present in the mouse brain, the quantity is large enough that it can be identified with streptavidin conjugated reporter tags.[6]
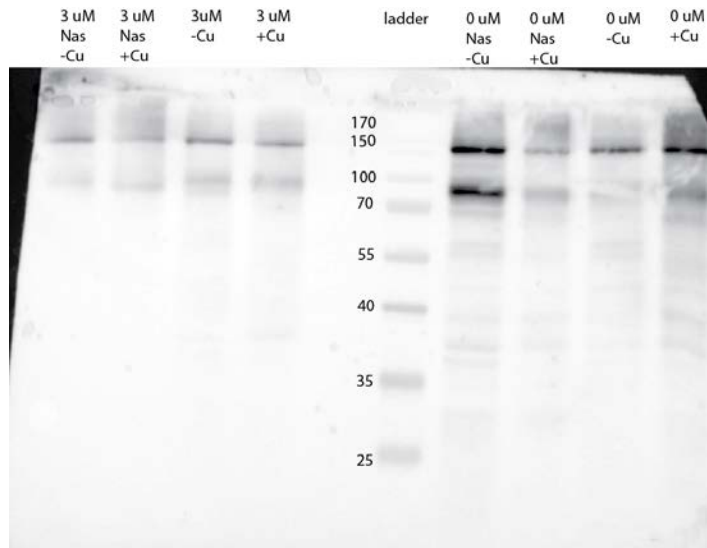
Figure 3.3: Western Blot on C57BL/6 Cerebellum Samples. Cerebellum samples were separated on a 10% SDS-PAGE gel, transferred to nitrocellulose, and probed using StrepHRP (1:10000). There is strong biotin staining in the 0 µM control lanes.

With this new information, we aliquoted 100µL of cell lysate to pre-clear with streptavidin beads and run the supernate through the chem ABBP process. The supernate was loaded onto a 10 % SDS-PAGE gel and a Western blot was done with streptavidin-HRP. Again, there was strong labeling for biotin in the control lanes. (Figure 3.5) This may be due to the amount of biotin present being higher than the capacity of the NeutrAvidin beads.
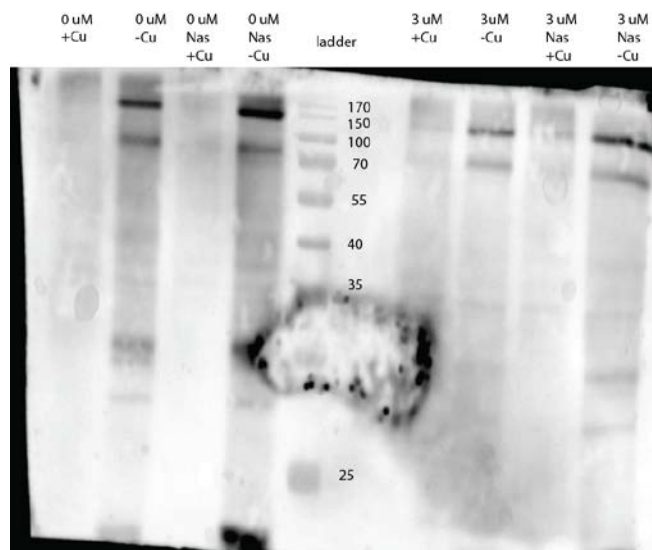
Figure 3.4: Western Blot on C57BL/6 Cerebellum Samples after NeutrAvidin pre-clearing. Cerebellum samples were first incubated using NeutrAvidin beads. The supernatant was then separated on a 10% SDS-PAGE gel, transferred to nitrocellulose, and probed using StrepHRP (1:10000). There is still strong biotin staining in the 0 µM control lanes.

3.2.5 Chemical Activity Based Protein Profiling with Neurons from *Protophormia terraenovae*

We decided to try a different approach in the testing of nanoprobe 2. Since nanoprobe 2 is based on an AMPA receptor antagonist that has known activity in insects, we decided to try to see if we could pull down targeted receptors in *Protophormia terraenovae,* or the northern blowfly, (also known as the blue-bottle fly). (Gift from Dr. John G. Stoffolano Jr., UMass, Amherst Plant, Soil, and Insect Science.) Flies were anesthetized with chloroform and injected with 10 µL of 30µM nanoprobe **2**. This concentration is similar to that used in the locus and honeybee experiments performed by Piek.[2] Flies appeared to be paralyzed after injection with nanoprobe **2.** They were then were beheaded and the heads were placed in fly saline. The heads were then lysed using a probe sonicator and the lysate was centrifuged to pellet exoskeleton. The supernatant was removed and 75 µL was used for chem ABPP with rhodamine azide. Clicked lysate

was run on a 12.5 % SDS-PAGE gel. Again, the gel did not show any fluorescence

bands. (Figure 3.6)
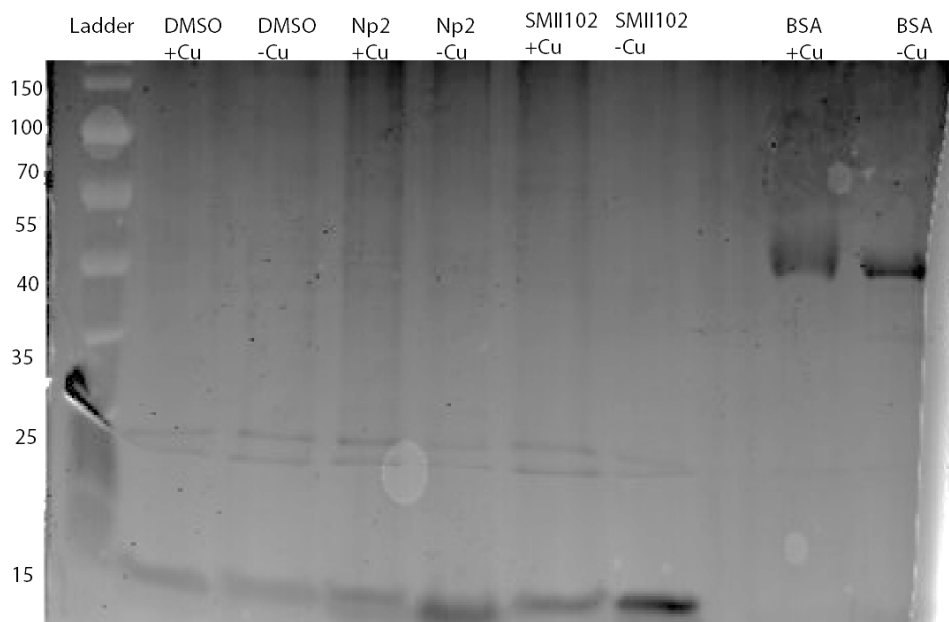
Figure 3.5: In-gel fluorescence of *Protophormia terraenovae* samples labeled with nanoprobe **2**. *Protophormia terraenovae* samples were labeled with DMSO, nanoprobe **2**, and SMII103. BSA was run a control. No signal was seen in probe containing samples.

3.3 Discussion

Nanoprobe **2** was designed to be a probe which could target calcium permeable AMPARs and provide information about which subunits we were targeting, thus identifying the subunit composition of this phenotype of receptors. Nanoprobe **2** was designed from a philanthotoxin scaffold and an acrylamide electrophile was added for bioconjugation to the surface of the targeted protein and an alkyne handle for "click" conjugation to an azide functionalized reporter tag.

The synthesis of nanoprobe **2** that we designed was straightforward, however the key peptide coupling step of triBoc spermine to compound **7** ((S)-2-(6-acrylamidohexanamido)-3-(4-(prop-2-yn-1-yloxy) phenyl) propanoic acid) proved to be more difficult than expected. The synthesis of triBoc spermine involves the protection of

one of the primary amines with a trifluroacetatyl group, then the protection of the

remaining primary amine with Boc, then the deprotection of the ethyl trifluroacetate

group, and finally a column clean up step. (Scheme 3.2) The column clean-up is run with

ammonia containing running solution and detection of the molecule is done by ninhydrin

staining, as there are no easily detectable UV active moieties on the molecule.[7] The

highest yield reported for this sequence of synthetic steps is 50%, [7-8] thus there is a large

amount of heterogeneity from batch to batch of triBoc spermine due to the difficult

purification that is required. This heterogeneity could be leading to some of the issues

that come in the peptide coupling experiment. Also, the peptide coupling reaction

between the carboxylic acid on compound **7** and the primary amine on triBoc spermine

proceeds slowly and to only 55% completion. Attempts were made to speed up the

reaction by making an activated ester of the carboxylic acid, but these efforts were futile

as it only seemed to impair the reaction even further. Multiple peptide coupling

conditions were attempted before choosing diisopropylcarbodiimide as our peptide

coupling reagent.
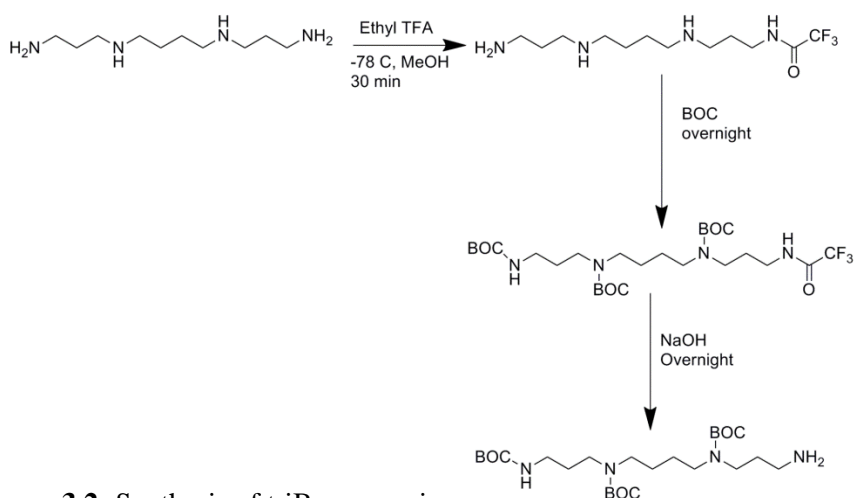
Scheme 3.2: Synthesis of triBoc spermine

In imaging experiments with dissociated cultures of rat cerebellar neurons,

nanoprobe **2** appears to be behaving similar to that of nanoprobe **1**. Fluorescence

accumulation was observed in areas where synaptic regions are present in the bright field image. This indicates that nanoprobe **2** is binding to similar areas to that of nanoprobe **1**. Nanoprobe **2** was designed to be a probe to be better targeted towards calcium permeable AMPARs, so it was encouraging that the fluorescence activity is similar to that of nanoprobe **1**. Also, it is encouraging that the modifications that were made to the philanthotoxin structure did not disrupt the binding of the probe. As stated in Section 1.1.11, polyamine toxins target the open ion pore with the polyamine tail biding inside the ion channel and having the aromatic head act as a steric mass that prevents full passage though the ion conduction pore. The main modifications to the philanthotoxin structure were made to regions on the aromatic head (see Scheme 3.1), so binding into the pore should not be disrupted. Further study with AMPAR antagonists would conclusively determine if we are indeed targeting receptors that may be calcium permeable AMPARs.

We then assayed whole brain lysates for ionotropic glutamate receptor identification with chem ABPP in three variant species, dissociated cultures of embryonic rat neurons, sectioned brain samples of adult female mice, and neurons from *Protophormia terraenovae*. All of these have known populations of receptors that are sensitive to polyamine toxins. We applied nanoprobe **2** to these samples, lysed the protein, and then separated the lysate on SDS-PAGE gels. With the dissociated culture of embryonic rat neurons, we did not find any bands on the gel using either in-gel fluorescence or Western blot analysis. This analysis was performed on cultured cortex, midbrain, and cerebellar neurons. We hypothesized this may be due to the overall low expression of calcium permeable AMPARs. Since the protein samples are from a primary source, there are myriad other proteins in the samples. Also, the amount of receptors is variable from culture to culture. So with a low amount of native protein

available, it is plausible that we could be labeling something but simply not able to detect the signal.

We then decided to use mature brain samples from C57BL/6 female mice. Samples of the cortex and the cerebellum were removed, treated with nanoprobe **2**, and lysed with a probe sonicator. The first set of gels was probed against streptavidin-HRP. Unfortunately, our first set of experiments resulted in positively labeled bands in the non-labeled (0 µM probe) lanes in the areas where we would expect to see ionotropic glutamate receptors. The cerebellum has a large amount of endogenous biotin present.[6] Biotin is present in many tissues as it is a required cofactor in oxidative metabolism for carboxylases; thus is heterogeneously distributed throughout tissues in the body. In neurons, here is expression of biotinidase (a biotin recycling enzyme), and there is also the presence of active carrier-mediated biotin transport mechanisms. All of these add to the endogenous amount of biotin that is present in the brain.[6] We tried adding NeutrAvidin beads into the lysate prior to the click reaction with azido biotin in an attempt to pre-clear any biotinylated proteins. This was only marginally successful as subsequent gels still contained positive biotin bands in the control lanes, albeit less than that of the original.

```
Mouse     ETQSSESTNEFGIFNSLWFSLGAFMQQGCDISPRSLSGRIVGGVWWFFTL 631
Rat       ETQSSESTNEFGIFNSLWFSLGAFMQQGCDISPRSLSGRIVGGVWWFFTL 631
Human     ETQSSESTNEFGIFNSLWFSLGAFMQQGCDISPRSLSGRIVGGVWWFFTL 631
Fly       EMERQ---NIWHLSNALWLVLGSMLNQGCDLLPRGLPMRLLTAFWWIFAL 638
          * : .    * : : *:**: **:::****: **.*. *:: ..**:*:
```

Figure 3.6: ClustalW alignment of GluA2 isoforms. ClustalW alignment of the M2 transmembrane domain of mouse, rat, human, and drosophila. The Q/R site is highlighted in blue and is conserved through species.

We decided to take a step back from the complex networks of the mammalian brain and see if nanoprobe **2** would work as an antagonist in insects as the glutamate receptor is reported in insects (Figure 3.6). We obtained *Protophormia terraenovae,* a

70

large fly species, for these experiments. We first injected nanoprobe **2** into the abdomen of the flies and observed the behavior of the fly. Flies showed lethargic effects including paralysis of wings, staggered walking, and slowed reaction to noise stimulus. This was not present in flies injected with a DMSO control. Flies were then beheaded to analyze their main neurons. The lysates underwent click chemistry with FAM-5 azide and SDS-PAGE gels were run. Again, these results were inconclusive as the fluorescence gels showed no bands, however coomassie staining showed the presence of protein. This suggested to us that nanoprobe **2** is not covalently binding to the receptor of interest.

These results from all of the gel experiments taken together suggest that nanoprobe **2** is not covalently modifying the target protein (or other proteins). We made major changes to the structure of nanoprobe **1** in the design of nanoprobe **2**, the largest being the removal of the photolabile core to a phenolic one. This changed the position of the points of attachment for the ligands on nanoprobe **2** over nanoprobe **1**. Likely the most important difference between the two molecules is the distance between the polyamine ligand and the targeting electrophile. In nanoprobe **2** this distance is much shorter, thus the electrophile is not exploring the same protein space as nanoprobe **1**. Attachment to the receptor of interest involves the Michael addition of our acrylamide electrophile to a biological nucleophile on the surface of the receptor. If there is not a suitable partner, then the covalent attachment will not occur. The binding pocket of the AMPA receptor is quite greasy, composed of proline, isoleucine, and threonine,[9] so it is quite possible that there are simply no competent nucleophiles present in the area of our electrophile. Without this covalent attachment, the receptor is not tagged, thus any subsequent experiments into identification would lead to the non-result that we have observed.

71

3.4 Methods

3.4.1 General Information

All reagents were purchased through Fisher Scientific (Fair Lawn, NJ, USA) unless otherwise noted. FAM-5 azide was purchased from Lumiprobe (Hallendale Beach, FL, USA). All moisture sensitive reactions were done under an argon atmosphere using a syringe-septum cap technique. Dry dimethylformamide (DMF) and acetonitrile (MeCN) were purchased from Sigma Aldrich (St. Louis, MO, USA). Analytical thin layer chromatography (TLC) was carried out on Merck Silica gel 60 F254 glass plates and visualized using UV light (254 nm), ninhydrin, or bromocrestol green staining. Sorbent Technologies (Atlanta, GA, USA) silica gel (230-450 mesh) was used for flash chromatography. ^{1}H NMR and ^{13}C NMR spectra were collected on a 400 MHz Bruker NMR spectrometer using the residual proton or carbon resonance of the solvent as the standard. Chemical shifts are reported in parts per million (ppm). The following abbreviations are used for peak multiplicities: s, singlet; d, doublet; dd, doublet of doublets; t, triplet; m, multiplet. Mass spectra were measured using either a Waters ZQ for LCMS, or at the UMass Mass Spec facility for HRMS, UMass Amherst.

3.4.2 Synthesis of Nanoprobe 2
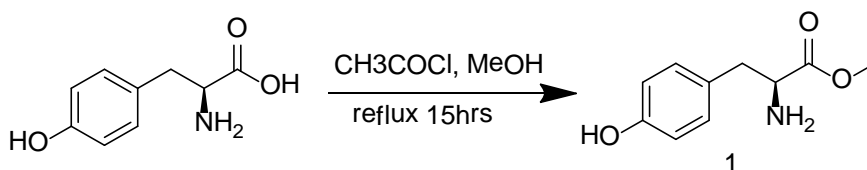
Methyl Ester Protection of Tyrosine (1)

Acetyl chloride (15 mL, 210.9 mmol) was added slowly to methanol (110 mL) while stirring vigorously. Tyrosine (5.59g, 30.6 mmol) was added and the solution was heated to reflux for 18 hours. The solution was cooled to room temperature and the

solvent was removed *in vacuo*. (5.04 g, 94 % yield). The product matched literature

spectra and was used without further purification.[10]
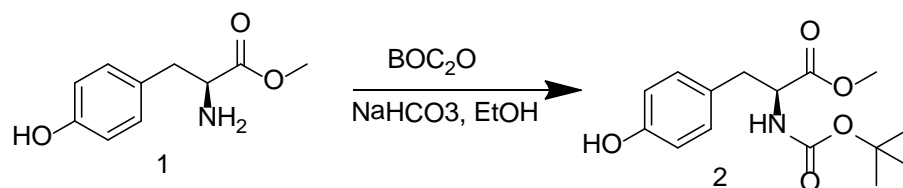
Boc Protection of Tyrosine Methyl Ester (2)

Compound **1** (5.04 g, 25.8 mmol) was dissolved in absolute ethanol (110 mL).

Sodium bicarbonate (22.52 g, 268.1 mmol) and di-*tert*-butyl dicarbonate (8.42 g, 38.6

mmol) were added and the reaction was stirred at room temperature for 24 hours. The

reaction was passed through a fritted funnel to remove sodium bicarbonate and the

solvent was removed *in vacuo*. The resulting white solid was spectroscopically identical

to literature and was used without further purification. (6.53 g, 90%.) [10]
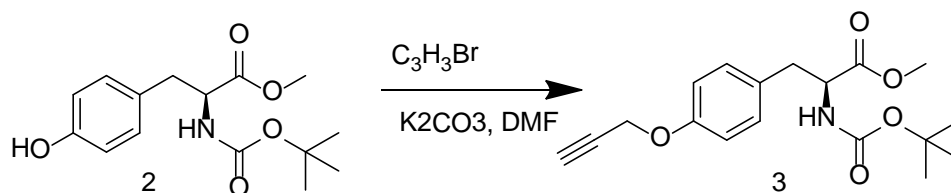
Methyl 2-((tert-butoxycarbonyl) amino)-3-(4-(prop-2-yn-1-yloxy)
phenyl)propanoate (3)

Compound **2** (5.00 g, 16.9 mmol) was dissolved in dry DMF (100 mL).

Anhydrous potassium carbonate (7.05 g, 51.0 mmol) was added and the reaction mixture

stirred for 30 min at 0°C. Propargyl bromide (80% solution in toluene, 3.02 g, 25.4

mmol) of was added dropwise and the reaction mixture was allowed to warm to room

temperature with stirring for 18 hours. The reaction was then quenched with deionized

water (100 mL) and extracted using ethyl acetate (3x 20 mL). The solvent was removed

in vacuo. The resulting yellow oil was spectroscopically identical to literature and was

used without further purification. (4.43g, 67% yield) [11]
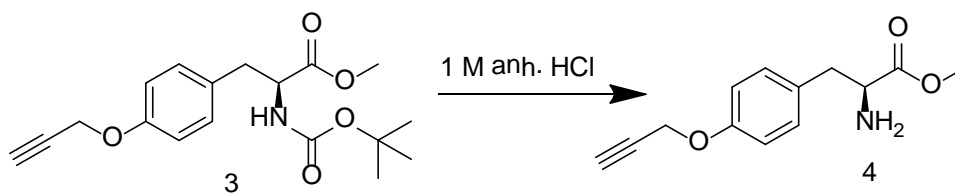
(S)-Methyl 2 amino-3-(4-(prop-2-yn-1-yloxy)phenyl)propanoate(4)

        Compound 3 (2.83 g) was deprotected using 1M anhydrous hydrochloric acid (50

mL). The reaction mixture was stirred for 4 hours and hexanes (10 mL) was added to

precipitate the HCl salt of the desired product. A solid white precipitate was filtered,

dried, and was used without further purification as it was spectroscopically identical to

literature. (1.28 g, 49%)[11]
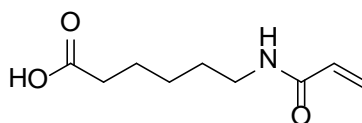
6-Acrylamidohexanoic acid (5)

        Hexanoic acid (5.17 g, 39.4 mmol) was combined with calcium hydroxide (5.34

g, 44.5 mmol) in deionized water (70 mL). A catalytic amount of hydroquione (1 mg, 9

mmol) was added and the reaction stirred at 0°C for 20 min. Acryolyl chloride (3.6 ml,

44.51 mmol) was added dropwise and the reaction mixture was stirred at 0°C for an

additional 15 minutes on ice. Conc. hydrochloric acid (6 mL) was added drop wise until

the product precipitated out. The resulting pale brown solid was spectroscopically

identical to literature and was used without further purification. (2.76 g, 67% yield) [12]
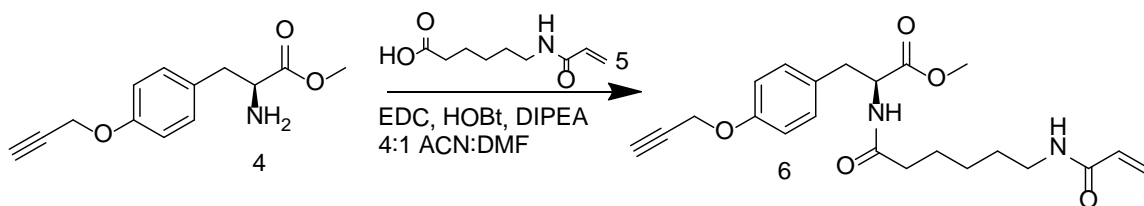
(S)-Methyl 2-(6-acrylamidohexanamido)-3-(4-(prop-2-yn-1-
    yloxy)phenyl)proanoate (6)

        Compound **5** (1.52 g, 8.24 mmol) was combined with 1-ethyl-3-(3-

dimethylaminopropyl)carbodiimide (1.39 g ,7.24mmol) and hydroxybenzyltriazole (1.11

g ,7.18 mmol) in 4:1 acetonitrile:DMF (15 mL). This solution was stirred for 10 minutes,

then *N,N*-diisopropylethylamine (9.55 mL, 54.9 mmol) was added. The reaction mixture

was stirred for an additional 30 minutes, and then compound **4** (1.28 g, 5.84 mmol) was

added and stirred overnight at room temperature. The reaction underwent an extraction

with 3x10 mL of 1 M hydrochloric acid and 3x10 ml of 1M sodium chloride into

dichloromethane and was dried over sodium sulfate to leave a white solid. (334 mg, 17%)

^{1}H NMR (400MHz , CDCl$_3$) δ = 7.02 (d, *J* = 8.3 Hz, 2 H), 6.88 (d, *J* = 8.6 Hz, 2 H), 6.23

(s, 1 H), 6.27 (s, 1 H), 6.16 - 6.05 (m, 2 H), 5.58 (d, *J* = 10.1 Hz, 1 H), 4.80 (q, *J* = 6.3

Hz, 1 H), 4.64 (s, 2 H), 3.70 (s, 3 H), 3.37 - 3.22 (m, 2 H), 3.07 (dd, *J* = 5.6, 14.1 Hz, 1

H), 2.99 (dd, *J* = 6.3, 13.9 Hz, 1 H), 2.56 - 2.50 (m, 1 H), 2.16 (t, *J* = 7.2 Hz, 2 H), 1.64 -

1.44 (m, 5 H), 1.37 - 1.21 (m, 3 H), 1.21 - 1.04 (m, 1 H). ^{13}C NMR (101MHz , CDCl$_3$) δ

= 172.2, 171.9, 165.3, 156.3, 130.7, 129.8, 128.5, 125.7, 114.6, 78.1, 76.7, 76.4, 75.2,

55.4, 52.7, 51.9, 38.7, 36.5, 35.6, 28.5, 25.8, 24.4 LCMS (M/Z = 401.1), HRMS

$C_{22}H_{28}N_2O_5$; calculated (M +Na)$^+$= 423.1890; observed (M + Na 423. 1892)$^+$
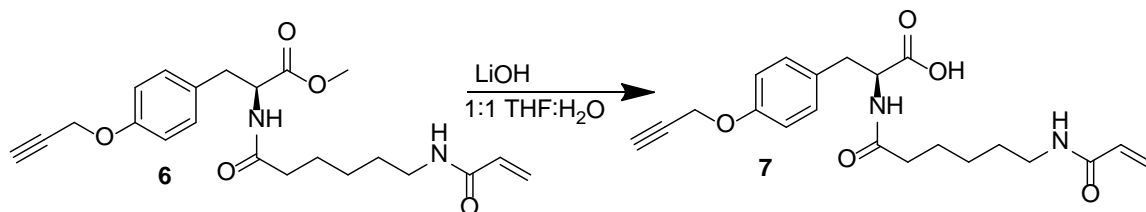
2-(6-acrylamidohexanamido)-3-(4-(prop-2-yn-1-yloxy)phenyl)propanoic acid(7)
          Compound **6** (334.4 mg, 0.835 mmol) was dissolved in 1:1 THF: water (4 mL)

and stirred at 0°C for 20 minutes. Lithium hydroxide (214.6 mg, 5.11 mmol) was added

and the reaction mixture was stirred for 3 hours. The reaction was quenched with 3M

hydrochloric acid until pH equal to 1 on pH paper. The resulting solution was extracted

with ethyl acetate and dried over magnesium sulfate. The solvent was evaporated *in*

vacuo. (214 mg, 66 %). ^{1}H NMR (400MHz ,Methanol-D$_4$) δ = 7.20 - 7.14 (m, *J* = 8.6 Hz,

2 H), 6.96 - 6.86 (m, *J* = 8.6 Hz, 2 H), 6.31 - 6.15 (m, 2 H), 5.65 (dd, *J* = 3.7, 8.2 Hz, 1

H), 4.70 (d, *J* = 2.3 Hz, 2 H), 4.65 (dd, *J* = 4.9, 9.5 Hz, 1 H), 3.26 - 3.19 (m, 2 H), 3.16

(d, J = 4.8 Hz, 1 H), 2.96 - 2.85 (m, 2 H), 2.19 (t, J = 7.3 Hz, 2 H), 1.60 - 1.44 (m, 4 H),

1.32 - 1.17 (m, 2 H) ^{13}C NMR (101MHz ,Methanol-D$_4$) δ = 174.5, 173.5, 166.7, 156.8,

130.8, 129.8, 125.0, 114.6, 78.5, 75.3, 55.2, 53.8, 47.6, 38.8, 36.2, 35.2. LCMS

(M+H=384.4); HRMS C$_{21}$H$_{26}$N$_2$O$_5$ calculated (M + Na)$^+$=409.1734; observed (M+ Na)$^+$

= 410.1781)
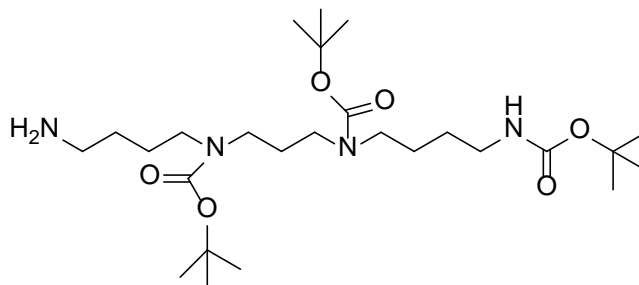
Tert-butyl (4-((3-aminopropyl)(tert-butoxycarbonyl)amino)butyl)(2-(((tert-butoxycarbonyl)amino)ethyl)carbamate (8)

        Spermine (1.61g, 7.95 mmol) was dissolved in methanol (40 mL) and cooled to -

78°C using an acetone/dry ice bath for 20 minutes. Ethyltrifluoroacetate (1.35 mL,

1.12g) was added dropwise and reaction stirred at -78°C for 1 hour. The reaction was

then warmed to 0°C for one hour before addition of di-*tert*-butyl dicarbonate (6.85 g,

31.3g). The reaction mixture was warmed to room temperature and stirred overnight.

Conc. ammonia was added dropwise until the pH equaled 11 on pH paper, and the

reaction was stirred an additional 18 hours. The solvent was then evaporated *in vaccuo*

and a flash column was run using 70:10:1 CH$_2$Cl$_2$:CH$_3$OH:ammonia to 50:10:1

CH$_2$Cl$_2$:CH$_3$OH:ammonia gradient as the mobile phase. The resulting pale yellow oil was

spectroscopically identical to literature. (543 mg, 13.5 %) [7]
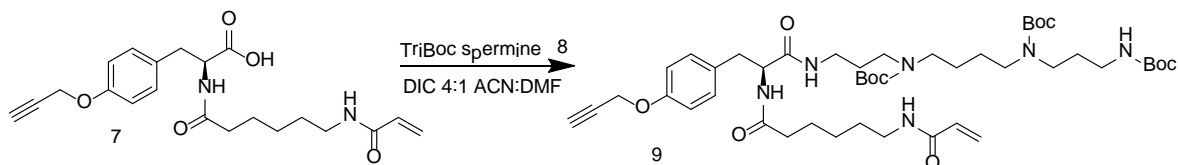
(S)-tert-butyl (3-(2-(6-acrylamidohexanamido)-3-(4-(prop-2-yn-yloxy)phenyl)propanamido)propyl) (4-((tert-butoxycarbonyl)(3-((tert-butoxycarbonyl)amino)propyl)amino)butyl)carbamate (9)

Compound **7** (149.8 mg, 0.3876 mmol) was dissolved in 4:1 acetonitrile:DMF (2 mL) and then added N,N-diisoproylcarbodiimide (127.2 mg, 157.9 uL, 1.00 mmol) and diisopropylethylamine (cat.). The reaction mixture was stirred for 20 minutes, and then compound **8** (676.2 mg, 1.34 mmol.) dissolved in DMF (2 mL) was added. The reaction mixture was stirred overnight and then extracted into ether (40 mL); the reaction mixture was washed with 1 N HCl (3x20 mL) and 1 N NaOH (3x 20 mL) and dried over magnesium sulfate. The solvent was removed *in vacuo*. and the resulting residue was purified via preparative HPLC (minutes 1-5 75% water, 25% acetonitrile; minute 5-35 5% water, 95% acetonitrile) (70 mg, 21%)) ^{1}H NMR (400MHz ,CDCl$_3$) d = 7.19 - 7.12 (m, J = 8.6 Hz, 2 H), 6.96 - 6.87 (m, J = 8.3 Hz, 2 H), 6.30 (dd, J = 1.5, 16.9 Hz, 1 H), 6.13 (dd, J = 10.4, 16.9 Hz, 1 H), 5.64 (dd, J = 1.4, 10.2 Hz, 1 H), 4.68 (d, J = 2.3 Hz, 2 H), 3.33 (d, J = 6.1 Hz, 4 H), 3.33 (d, J = 19.7 Hz, 2 H), 3.23 - 3.01 (m, 9 H), 2.54 (t, J = 2.3 Hz, 1 H), 2.22 (d, J = 6.8 Hz, 2 H), 1.73 (br. s., 2 H), 1.66 - 1.60 (m, 4 H), 1.54 (br. s., 2 H), 1.48 (s, 13 H), 1.44 (s, 9 H), 1.36 - 1.27 (m, 2 H). LCMS (M+H) = 871.11
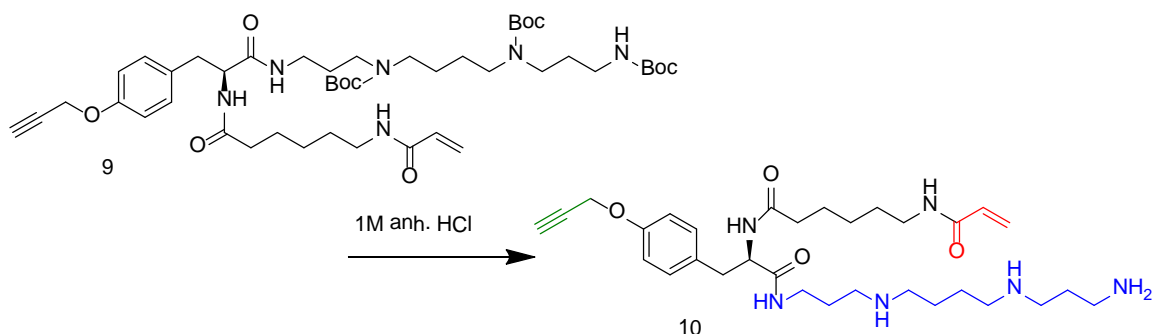
(S)-6-acrylamido-N-(1-((3-((4-((3-aminopropyl)amino)butyl)amino)propyl)amino)-1-oxo-3-(4-(prop-2-yn-1-yloxy)phenyl-2-yl)hexanamide (10)

Compound **9** (70 mg, 0.12 mmol) was deprotected using 3M anhydrous hydrochloric acid (2 mL) in ethanol. The reaction stirred for 18 hours and was precipitated as the HCl salt using hexanes (1 mL). (9.8 mg, 14%) LCMS (M+H=571.6)
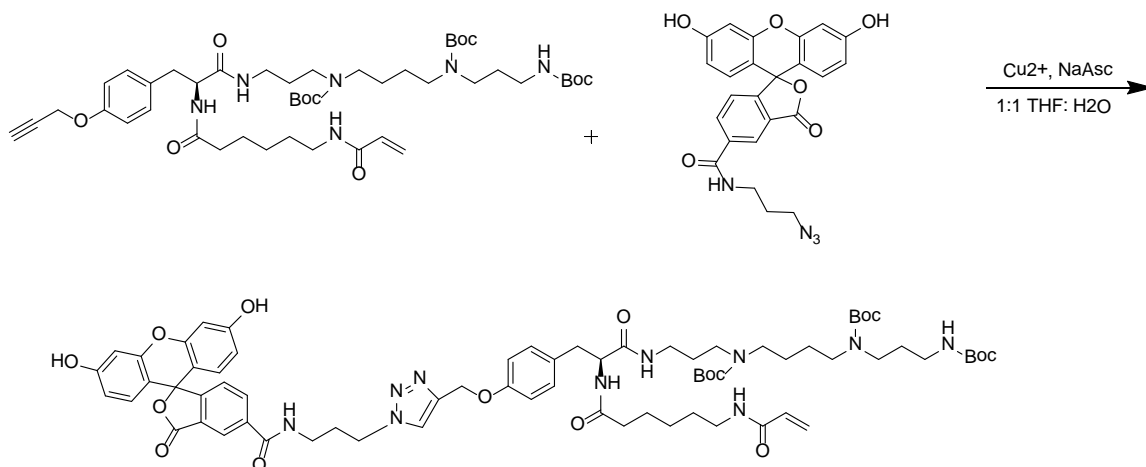
(S)-Tert-butyl (3-(2-(6-acrylamidohexanamido)-3-(4-((4-(2-(3',6'-dihydroxy-3-oxo-3H-spiro[isobenzofuran-1,9'-xanthen]-6-ylcarboxamido)ethyl)-1H-1,2,3-triazol-1-yl)methoxy)phenyl)propanamido)propyl)(4-((tert-butoxycarbonyl)(3-((tert-butoxycarbonyl)amino)propyl)amino)butyl)carbamate(11)

Compound **9**(27 mg, 0.031 mmol) was combined with 10uL of 10 mM stock

FAM-5 azide in DMSO, 5% copper sulfate pentahydrate (0.032 mmol) dissolved in

water, and 10% sodium ascorbate (0.0313 mmol) dissolved in water and was stirred for

48 hours. The resulting solution was extracted into CH_2Cl_2 and the solvent was removed

in vacuo. (9.7 mg, 1%) LCMS= 1329.19.
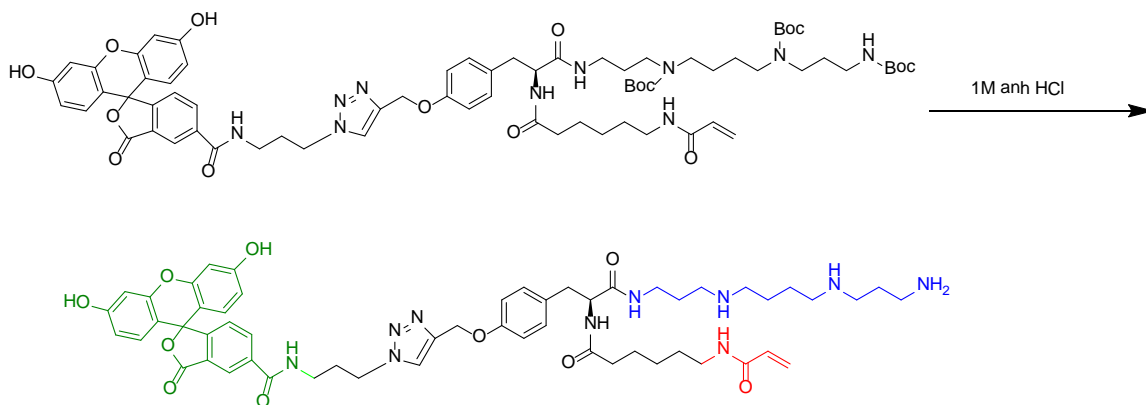
(S)-N-(2-(1-((4-(2-(6-acrylamidohexanamido)-3-((3-((4-((3-aminopropyl)amino)butyl)amino)propyl)amino)-3-oxopropyl)phenoxy)methyl)-1H-1,2,3-triazol-4-yl)ethyl)-3',6'-dihydroxy-3-oxo-3H-spiro[isobenzofuran-1,9'-xanthene]-6-carboxamide (12):

Compound **11** (9.7 mg, 0.001 mmol) was deprotected using 3M anhydrous hydrochloric acid (2 mL) in ethanol. The reaction stirred for 18 hours and was precipitated as the HCl salt using hexanes (1 mL). (3.1 mg, 5%) LCMS= 1028.19

3.4.3 Dissociated Cerebellar Cell Culture

Primary dissociated cerebellar cell cultures were prepared from embryonic day E18-19 Sprague-Dawley rat embryos and were cultured on polylysine-coated coverglass (12mm, 1.0 size) in serum-containing media identical to previous reports.[13] Cells were grown in 5% CO_2 at 37°C. All animal care and experimental protocols were approved by the Animal Care and Use Committee at the University of Massachusetts Amherst, Amherst, MA, USA.

3.4.4 Dissociated Cortex, Midbrain, and Cerebellar Cell Culture

Primary dissociated cortex, midbrain, and cerebellar cell cultures were prepared from embryonic day E18-20 Sprague-Dawley rat embryos and were cultured on 25 cm^2 T-Flasks coated in poly-lysine in serum containing media identical to previous reports.[14] Cerebellar culture media was supplemented with 1M potassium chloride (1 mL in 50 mL of total media)[13] Cells were grown in 5% CO_2 and at 37°C. All animal care and experimental protocols were approved by the Animal Care and Use Committee at University of Massachusetts, Amherst, Amherst, MA, USA.

3.4.5 Live Cell Imaging with Nanoprobe 2

Cells were imaged using a 488 nm laser line on a Yokogawa Spinning Disc Confocal (Tokyo, Japan) on a Nikon Eclipse Ti series microscope (Nikon Corps Tokyo, Japan) with a CFI Plan Apo VC 100x 1.4 NA oil objective lens (Nikon) was used for imaging experiments. Images were acquired using an Andor cooled EMCCD camera

(Andor Technology Belfast, UK) and MetaMorph software (Molecular Devices Sunnyvale, CA USA).

Cells were removed from their home media and washed three times in extracellular buffer solution (138 mM NaCl, 1.5 mM KCl, 1.2 mM $MgCl_2$, 5 mM HEPES, 2.5 mM $CaCl_2$, and 14 mM glucose at pH 7.4). They were then placed into a static bath of extracellular solution and imaged for a minute to collect the background fluorescence. 2 µM nanoprobe **2** was added to the bath for 5 minutes at room temperature and cells were washed three more times with extracellular solution. Cells were then imaged for 5 minutes to collect fluorescent data.

3.4.6 Image Analysis of Confocal Imaging Data

Images were analyzed using ImageJ (U.S. National Institutes of Health, Bethesda, MD, USA). Fluorescence was quantified using ROI (region of interest) analysis of multiple regions placed over putative synaptic sites and areas of background. The mean fluorescence intensity was background subtracted and fluorescence intensities were plotted using GraphPad Prism (La Jolla, CA, USA). Two image series were analyzed and the data combined for a total of 118 ROIs analyzed.

3.4.7 Chemical Activity Based Protein Profiling on Dissociated Cultures of Rat Cortex, Midbrain, and Cortex Neurons

25 cm^2 T-flasks of cortex, mid-brain, and cerebellar neurons were grown to they were synaptically active (DIV 14-18). Flasks were washed three times with extracellular recording buffer. 0, 1, 3, or 10 µM of nanoprobe **2** dissolved in 7 mL of extracellular solution with 20 µM glutamate was applied for 5 minutes at room temperature. Control solutions containing equimolar concentrations of nanoprobe **2** and NAS were also made for additional flasks. Flasks were then washed three more times with extracellular solution. 1 ml of lysis solution (1 x PIC, 1x PBS) was added to each flask and cells were

scrapped to remove from sides of the T-flask. Cells were lysed with a probe sonicator 30% power for 1 minute, and the membrane portions were spun down. The membrane pellet was lysed again using the same conditions and a BCA assay was run to quantitate protein concentrations. Master mixes for click solutions were prepared with 1 mM CuSO$_4$*5H$_2$O (50 mM stock), 100 µM THPTA (1.7 mM stock), and freshly prepared 1 mM TCEP (50 mM stock). These incubated for 10 minutes and 10 µM of either rhodamine azide or biotin azide were then added. A separate control master mix was prepared by substituting deionized water in for the CuSO$_4$*5H$_2$O. 50 µL of cell lysate were removed and the appropriate master mix was added to the tube with the reaction going for one hour. Samples were then separated on a 10% SDS-PAGE gel. For in-gel fluorescence experiments, gels were placed into 10% acetic acid for a minimum of 10 mintures and imaged using a Typhoon imager. For Western blot experiments, proteins were transferred to a nitrocellulose membrane and probed against streptavidin HRP (1:10,000) (Thermo Scientific, Waltham, MA, USA). HRP was activated using Super Substrate West Pico Chemiluminescent substrate (Thermo Scientific). Chemiluminescence was measured using a PxSys imaging system.

3.4.8 Chemical Activity Based Protein Profiling of Cortex and Cerebellum Samples from C57BL/6 Female Mice

Brain samples were kindly provided by Jesse Mager's lab in Veterinary and Animal Sciences at UMass, Amherst. Brain samples were removed after cervical dislocation of the mice and placed into extracellular solution containing 20 µM glutamate and 0, 1, or 3 µM nanoprobe **2** or solutions containing 20 µM glutamate with equimolar mixtures of nanoprobe **2** and NAS at the same concentration as above. Brain samples were allowed to incubate in these solutions for 15 minutes and were then washed three times with extracellular solution. Samples were then lysed using a probe sonicator and

underwent chem ABPP with biotin azide similar to Section 3.4.7. Lysates were separated

on a 10% SDS-PAGE gel and then probed using streptavidin-HRP.

100µL of cell lysate to pre-clear with streptavidin beads (NeutrAvidin agrose

resin, Thermo Scientific) and run the supernate through the chem ABPP process. The

supernate was loaded onto a 10 % SDS-PAGE gel, separated, and transferred to a

nitrocellulose membrane. Western blots were done against streptavidin-HRP. HRP was

detected using SuperSignal West Pico Chemiluminescent subtrate, and imaged using the

PxSys imaging system.

3.4.9 Chemical Activity Based Protein Profiling on Neurons from *Protophormia terraenovae*

Protophormia terraenovae were a gift from Dr. John G. Stoffolano Jr., UMass,

Amherst Plant, Soil, and Insect Science. *P. terraenovae* were obtained at their young

adult stage and kept in a cage with sugar water. Flies were removed from their

confinement with a 50 mL Falcon tube, anesthetized with chloroform, and injected with

10 µL of 30µM nanoprobe **2** or DMSO with a 27.5 G needle into the thorax. Flies were

beheaded and the heads were placed in fly saline (140 mM NaCl, 5.0 mM KCl, 7.0 mM

$CaCl_2*2H_2O$, 1.0 mM $MgCl_2*6H_2O$, 5.0 mM TES, 4.0 mM $NaHCO_3$, 5.5 mM trehalose,

and 9.4 mM sucrose, pH= 6.9). The heads were then lysed using a probe sonicator and

the lysate was centrifuged to pellet exoskeleton. The supernatant was removed and 75

µL was used for chem ABPP with FAM-5 azide. Tagged lysate was separated on a 12.5

% SDS-PAGE gel. In-gel fluorescence was measured using a Typhoon 9210 imager.

3.5 References

1.Eldefrawi, A. T.; Eldefrawi, M. E.; Konno, K.; Mansour, N. A.; Nakanishi, K.; Oltz, E.; Usherwood, P. N. R., Structure and synthesis of a potent glutamate receptor antagonist in wasp venom. *Proc. Natl. Acad. Sci. U. S. A.* **1988,** *85* (13), 4910-4913.

2.(a) Piek, T.; Mantel, P.; Engels, E., Neuromuscular block in insects caused by the venom of the digger wasp philanthus-triangulum. *Comparative and General Pharmacology* **1971,** *2* (7), 317-

331; (b) Piek, T.; Njio, K. D., Neuromuscular block in honeybees by venom of bee wolf wasp (philanthus-triangulum-f). *Toxicon* **1975,** *13* (3), 199-&.

3.(a) Poulsen, M. H.; Lucas, S.; Stromgaard, K.; Kristensen, A. S., Evaluation of PhTX-74 as Subtype-Selective Inhibitor of GluA2-Containing AMPA Receptors. *Molecular Pharmacology* **2014,** *85* (2), 261-268; (b) Stromgaard, K.; Jensen, L. S.; Vogensen, S. B., Polyamine toxins: development of selective ligands for ionotropic receptors. *Toxicon* **2005,** *45* (3), 249-254; (c) Stromgaard, K.; Mellor, I., AMPA receptor ligands: Synthetic and pharmacological studies of polyamines and polyamine toxins. *Medicinal Research Reviews* **2004,** *24* (5), 589-620.

4.(a) Speers, A. E.; Cravatt, B. F., Profiling enzyme activities in vivo using click chemistry methods. *Chemistry & Biology* **2004,** *11* (4), 535-546; (b) Speers, A. E.; Cravatt, B. F., A tandem orthogonal proteolysis strategy for high-content chemical proteomics. *J. Am. Chem. Soc.* **2005,** *127* (28), 10018-10019; (c) Niphakis, M. J.; Johnson, D. S.; Ballard, T. E.; Stiff, C.; Cravatt, B. F., O-hydroxyacetamide carbamates as highly potent and selective class of endocannabinoid hydrolase inhibitors. *ACS Chemical Neuroscience* **2012,** *3* (5), 418-426.

5.Bats, C.; Farrant, M.; Cull-Candy, S. G., A role of TARPs in the expression and plasticity of calcium-permeable AMPARs: Evidence from cerebellar neurons and glia. *Neuropharmacology* **2013,** *74*, 76-85.

6.McKay, B. E.; Molineux, M. L.; Turner, R. W., Endogenous Biotin in Rat Brain. 2007; Vol. 418, pp 111-128.

7.Blagbrough, I. S.; Geall, A. J., Practical synthesis of unsymmetrical polyamine amides. *Tetrahedron Letters* **1998,** *39* (5-6), 439-442.
8.Kostiainen, M. A.; Hardy, J. G.; Smith, D. K., High-affinity multivalent DNA binding by using low-molecular-weight dendrons. *Angewandte Chemie-International Edition* **2005,** *44* (17), 2556-2559.

9.Armstrong, N.; Gouaux, E., Mechanisms for activation and antagonism of an AMPA-Sensitive glutamate receptor: Crystal structures of the GluR2 ligand binding core. *Neuron* **2000,** *28* (1), 165-181.

10.Richter, J. M.; Whitefield, B. W.; Maimone, T. J.; Lin, D. W.; Castroviejo, M. P.; Baran, P. S., Scope and mechanism of direct indole and pyrrole couplings adjacent to carbonyl compounds: Total synthesis of acremoauxin A and oxazinin 3. *J. Am. Chem. Soc.* **2007,** *129* (42), 12857-12869.

11.Nonaka, H.; Tsukiji, S.; Ojida, A.; Hamachi, I., Non-enzymatic covalent protein labeling using a reactive tag. *J. Am. Chem. Soc.* **2007,** *129*, 15777-15779.

12.Auernheimer, J.; Dahmen, C.; Hersel, U.; Bausch, A.; Kessler, H., Photoswitched cell adhesion on surfaces with RGD peptides. *J. Am. Chem. Soc.* **2005,** *127* (46), 16107-16110.

13.Bilimoria, P. M.; Bonni, A., Cultures of cerebellar granule neurons. *CSH protocols* **2008,** *2008*, pdb.prot5107-pdb.prot5107.

14.Chambers, J. J.; Kramer, R. H., Light-Activated Ion Channels for Remote Control of Neural Activity. In *Methods in Nano Cell Biology*, Jena, B. P., Ed. 2008; Vol. 90, pp 217-+.

CHAPTER 3

PHOTOCHEMCIAL PHLIANTHOTOXIN BASED PROBE FOR THE DETECTION OF CALCIUM PERMEABLE AMPA RECEPTORS

4.1 Introduction

From experiments with nanoprobe **2** (see Chapter 3 for full details), it became clear that our electrophile was not attaching to the surface of the receptor, even though imaging studies suggested that we were targeting that same receptors as nanoprobe **1**. We had assumed the acrylamide moiety on nanoprobe **2** would conjugate to the receptor of interest through proximity accelerated reactivity. In the absence of a suitable nucleophile for bioconjugation, the nanoprobe **2** will simply be removed during the multiple wash steps that occur during each activity based protein profiling experiment that was performed to determine the receptor subtype we were targeting. Philanthotoxin, and other polyamine toxins, are use-dependent meaning that only the open channels are blocked. Use-dependency in polyamines has been well characterized [1] and there is a voltage dependency which is also associated with them. Typically, intracellular polyamines block AMPARs internally and result in an inward rectification of the evoked current. Our polyamines are applied externally and prevent current influx. To remove our polyamines, we must depolarize the membrane, which releases the block.[1] Since our acrylamide electrophile was not tagging, we can hypothesize that either it was being excised from the channel before the Michael addition could occur, or there was not a competent nucleophilic partner for crosslinking.

Keeping the current probe design in mind, we decided that we needed to change our electrophile to one that would be less discriminating for covalent attachment to our protein of interest. We decided to use an aryl azide, which adds to a protein of interest via UV-induced photolysis, thus making nanoprobe **3** a photoaffinity probe. Once photolysed, the probe has a highly reactive intermediate which can react with the closest

neighboring partner, thus labeling the protein with the probe.[2] A good photoaffinity probe must be inert when added, only reacting when photolysed with UV-light; thus UV-activation of the photophore must not destroy the biomolecule of interest, and lifetime of the activated photophore must be short, shorter than that of the ligand receptor interaction.[3] Once the activated photophore binds, the binding is covalent, and in an ideal probe should not disrupt the natural dynamics of the receptors that it labels. The use of photoaffinity labels also allows for identification of the amino acids that are involved in binding to the probe, thus making an affinity label a good system for the detection of calcium permeable AMPARs.

Previous photolabile philanthotoxin based probes have been synthesized. [4] Nakanishi and co-workers developed a photolabile probe targeted towards nicotinic acetylcholine receptors (nAChRs), which are also targets of polyamine toxins. Much like AMPARs, nAChRs are also ligand-gated, ion channels, but are sensitive to acetylcholine and nicotine. They are comprised of five transmembrane subunits and are located in the synaptic cleft. In their probe, the scaffold was based off of philanthotoxin 434 rather than the philanthotoxin 433 that nanoprobe **2** and **3** are based on. The numbering system that is used for these polyamines is to count the methylene units contained in the polyamine tail.[1a, 4b]This, and the addition of ^{125}I, makes their photolabile probe have higher affinity for nAChRs over AMPARs. Also, the ^{125}I addition allowed for radiolabeling experiments to study labeled receptors. [4b] Our probe lacks the radiolabel, but has an orthogonal handle which allows for affinity purification of the labeled lysate.

4.2 Results

4.2.1 Nanoprobe 3 Design

We kept the major features of nanoprobe **2** in mind when designing nanoprobe **3**. Much like before, we designed nanoprobe **3** from a philanthotoxin scaffold. This was done to create a probe that kept the features of philanthotoxin, yet could provide information about the receptors we are targeting. For nanoprobe **3**, we changed the phenolic hydroxide to an azide for photoreactivity and bioconjugation to the surface of the receptor. We then changed the butyl chain so it contains a Poc group for attachment of an azide functionalized reporter tag. (Scheme 4.1)
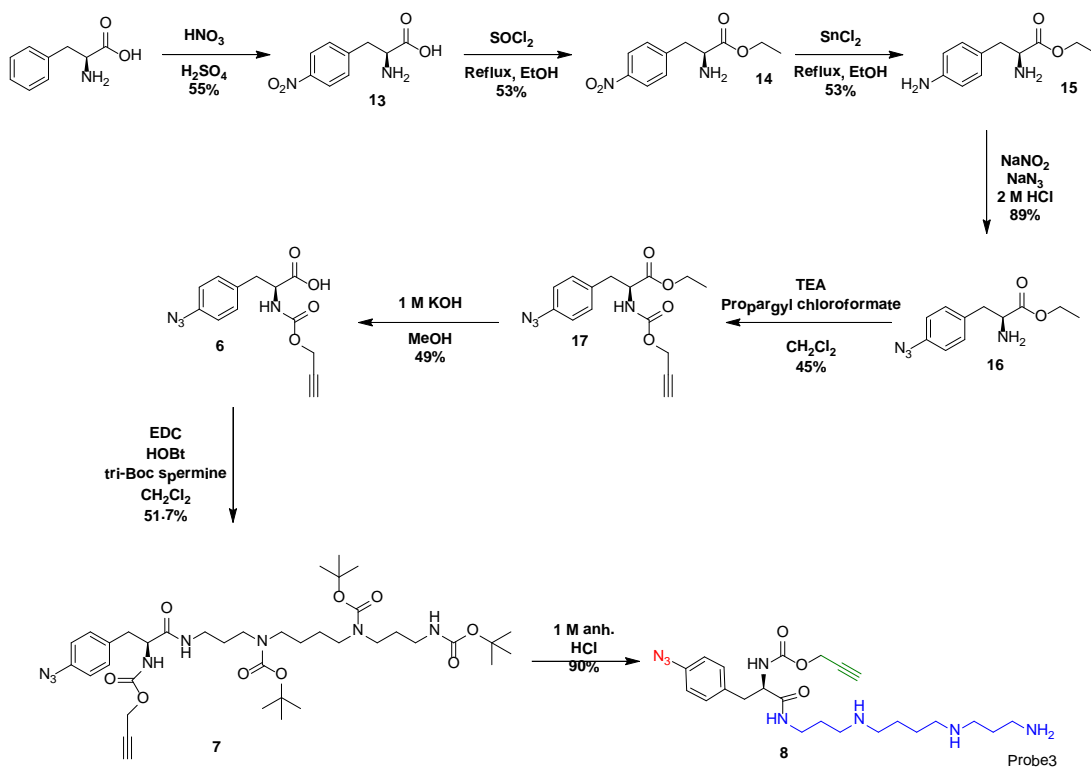
Scheme 4.1: Synthesis of nanoprobe **3**

4.2.2 Initial Photolysis Testing With Nanoprobe 3

To confirm that nanoprobe **3** would undergo photolysis in times that would be biologically relevant the molecule was irradiated under UV light (365 nm) for 1-10

minutes to determine the minimum amount of time it takes for generation of the UV

byproduct. Formation of the nitrene product was monitored via LCMS analysis. We

determined that four minutes of irradiation by UV light is sufficient for biological studies.

(Figure 4.1) This is important because we did not want our protein to be degraded due to

the UV-light.
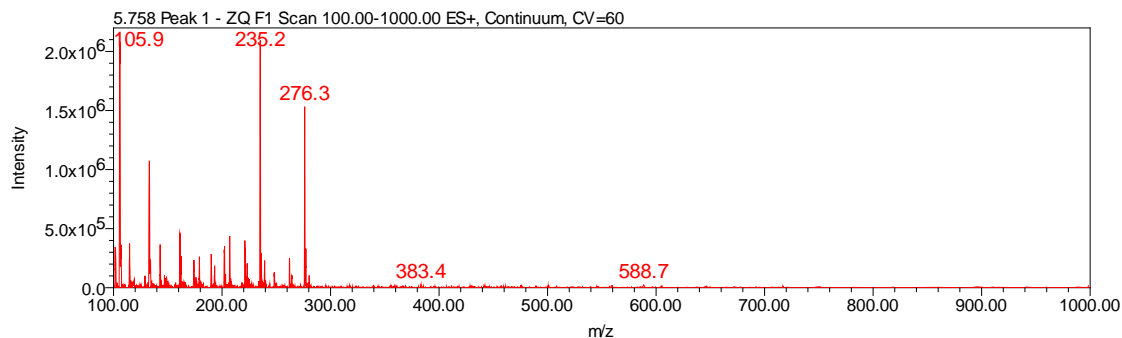
Figure 4.1: Mass spectrum of nanoprobe **3** precursor after 4 minute UV
irradiation. Compound **17** (mw=276) was irradiated for 4 minutes with
365 nm light. Formation of the nitrene (mw=235) was observed.

Next, we wanted to confirm that nanoprobe **3** could label proteins. We

performed *in vitro* studies using nanoprobe **3** to test the photolysis reaction using bovine

serum albumin (BSA) and lysozyme. BSA and lysozyme were irradiated for 4 minutes

using UV light with nanoprobe **3** and then the proteins were subjected to chem ABPP as

described in Section 3.2.3 with rhodamine azide. Proteins were then separated on a 10%

SDS-PAGE gel and fluorescence was visualized using a Typhoon 9210 gel scanner.

(Figure 4.2) The results demonstrated that nanoprobe **3** is able to covalently label proteins

in vitro.
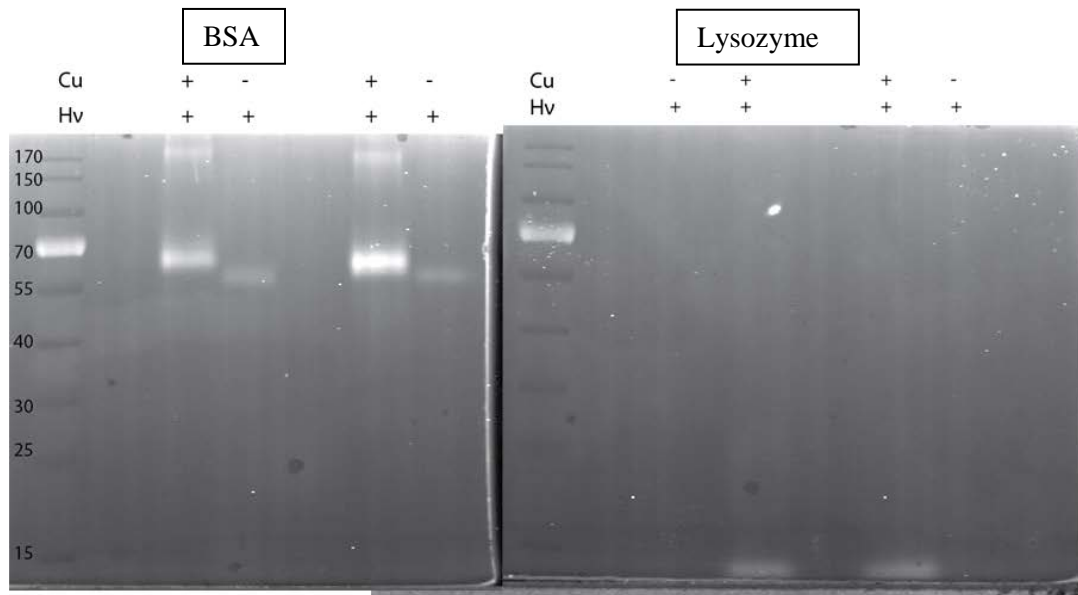
Figure 4.2: In-gel fluorescence of BSA and lysozyme labeled with nanoprobe **3**. BSA (70 kDa) and lysozyme (20 kDa) were labeled and irradiated with nanoprobe **3** and separated using 10% SDS-PAGE gels. Labeling with nanoprobe **3** was seen in when both light and copper were present.

4.2.3 Chemical Activity Based Protein Profiling of Cortex, Midbrain, and Cerebellum Neurons with Nanoprobe 3

With the information that nanoprobe **3** was able to label proteins using *in vitro* conditions, we next moved into labeling neurons to determine which receptors we were targeting. Nanoprobe **3** is designed to targets calcium permeable AMPA receptors much like nanoprobe **1** and **2**, so by performing chem ABPP we should be able to determine which receptor subtypes we are targeting. To 25 cm^2 T-Flasks, 10 µM of nanoprobe **3** was applied for 5 minutes at room temperature and then the flasks were irradiated for 4 minutes with UV-light. Equimolar NAS to nanoprobe **3** controls were also done at the same time. Cells were lysed using a probe sonicator, and the membranes were pelleted. The membrane pellet was then lysed and the lysate underwent chem ABPP with either azido rhodamine or azido biotin. Labeled lysates were separated on a 10% SDS-PAGE gel. For rhodamine labeled protein gels, fluorescence was measured using a Typhoon 9210 scanner. For biotin labeled protein, 10 % SDS-PAGE gels were used to separate protein, transferred to a nitrocellulose membrane, biotin was probed for using

streptavidin-HRP, and imaged on a BioRad Protein Box. (Figure 4.3) Gels did not show

any labeled fluorescent bands. This may be due to the electrophile not being able to bind

to our protein of interest.
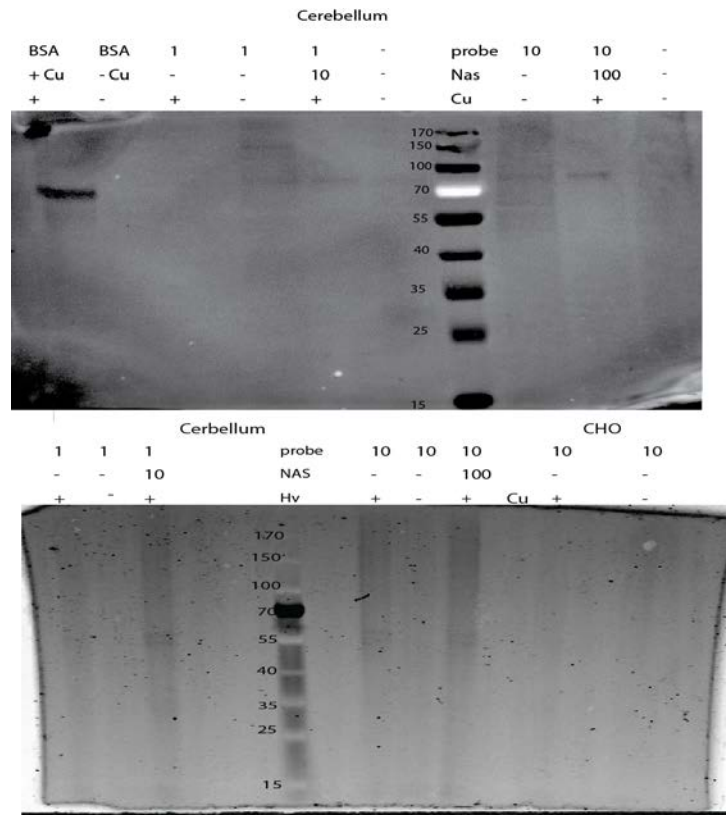
Figure 4.3: Cerebellum samples probed with nanoprobe **3.** (Left) Cerebellum samples run on a Western blot, probed with Strep-HRP (1:10000) (Right) In-gel fluorescence of cerebellum samples with rhodamine azide. No signal was seen in probe labeled neuronal protein lanes.

4.2.4 Fixed Cell Imaging of Hippocampal and Cerebellar Neurons with Nanoprobe 3

Since the gel experiments appeared to lack any covalent labeling of the natively

expressed AMPARs, we took a step back and went back to imaging experiments with

neurons. Nanoprobe **3** contains an alkyne group for conjugation to the reporter tag, so it

is necessary to fix the neurons before the copper catalyzed click reaction of the reporter

tag. This is due to the toxic effects of copper on proteins. Neurons were labeled with

nanoprobe **3** for 5 minutes at room temperature and then irradiated with UV-light for 4

minutes. Equimolar NAS to nanoprobe **3** controls were also prepared. Neurons were then

fixed in 4% paraformaldehyde for 10 minutes. They immediately underwent chem ABPP

with rhodamine azide and were washed ten times with 1x PBS. Coverslips containing

cells were then mounted on a glass slide with ProLong Gold Antifade. Coverslips were

imaged using epifluorescence microscopy; however fluorescent images were taken of all

samples. (Figure 4.4) Fluorescence accumulation was seen in samples targeted by

nanoprobe **3** and that had also been irradiated with UV-light. However, fluorescence

accumulation was also seen in the dark samples, and the equimolar NAS and nanoprobe **3**

samples. We also saw fluorescence accumulation in samples which contained only

rhodamine azide. This suggests that the fixation process may have permeabilized the

membrane allowing for rhodamine azide to cross.
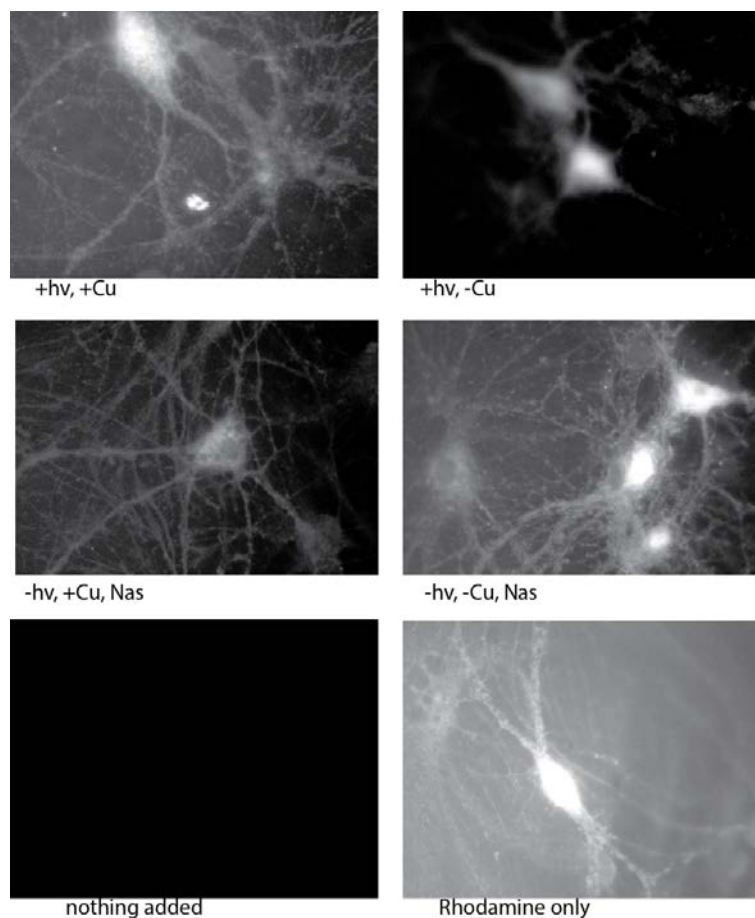
Figure 4.4: Fixed neuronal imaging with nanoprobe **3.** DIV 18hippocampal neurons
were labeled with nanoprobe **3**, irradiated, and fixed in 4% paraformaldehyde.
They were then labeled with rhodamine azide with and without copper for click
chemistry. Controls were done in the presence of NAS, with just rhodamine,
and with nothing at all. Fluorescence signal was averaged over the positive
controls (n=8) and was set for all of the images. Fluorescence accumulation is
seen in all cases where rhodamine azide is present.

4.2.5 Fixed Cell Imaging of CHO Cells with Nanoprobe 3

Since we received confusing results from our imaging experiments with

nanoprobe **3**, we decided to move into a simpler heterologous system of CHO cells

transfected with GluA1 (L497Y)-pIRES2-eGFP. Nanoprobe **3** was applied to the cells for

5 minutes and then irradiated for 4 minutes with UV light. Equimolar NAS to nanoprobe

3 controls were also prepared. Cells were then fixed using 4% paraformaldehyde and then

conjugated with rhodamine azide. Coverslips containing cells were then mounted onto

coverglass with ProLong Gold Antifade. Coverslips were imaged using epifluorescence microscopy. Again, fluorescence was seen in all cases, both probed containing samples and the controls. (Figure 4.5)
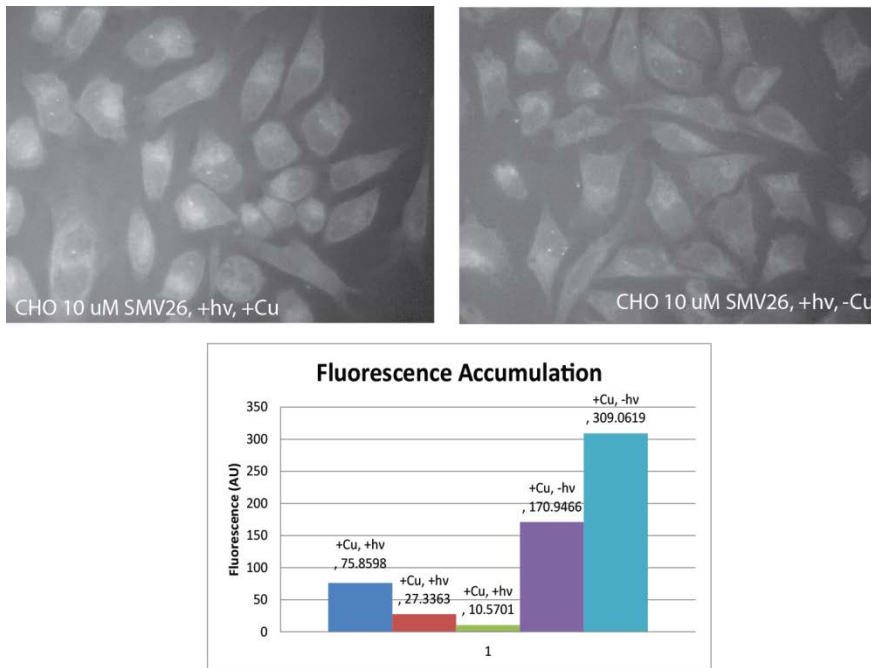
Figure 4.5: GluA1 CHO cells labeled with nanoprobe **3**. GluA1 CHO cells were labeled with nanoprobe **3**, irradiated, and fixed with 4% paraformaldehyde. Fluorescence accumulation was averaged for with and without copper. The samples containing no copper had a higher fluorescence accumulation.

We thought that the increase in fluorescence in all samples may be due to the probe not being fully washed away. Multiple washes were performed ranging from 3-24 washes with 1x ECS prior to being fixed with 4% paraformaldehyde. Cells were then orthogonally targeted with rhodamine azide and imaged via epifluorescence microscopy. Again, fluorescence was seen in all cases. (Figure 4.6)
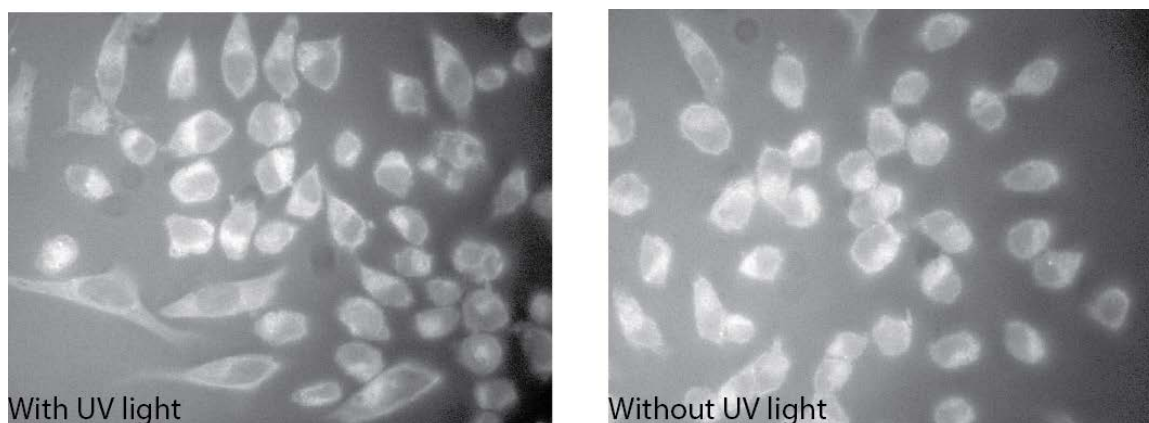
Figure 4.6: Nanoprobe **3** labeled GluA1 CHO cells after multiple ECS washes. GluA1 CHO cells were labeled with nanoprobe **3**, irradiated, washed 24 x 1mL with 1x ECS, and then fixed with 4% paraformaldehyde. Fluorescence was set for the with UV light samples. Fluorescence accumulation is similar in both cases.

We then hypothesized that the polyamine portion of nanoprobe **3** might not able to leave the ion channel. To facilitate this, we depolarized the membrane using a high KCl solution (1M). We placed this solution on the cells 1-4 times, washing three times in between with 1x ECS. Cells were then fixed with 4% paraformaldehyde and labeled with rhodamine azide. Cells were then imaged using epifluorescence microscopy. Again, there were large amounts of fluorescence in all cases. (Figure 4.7)
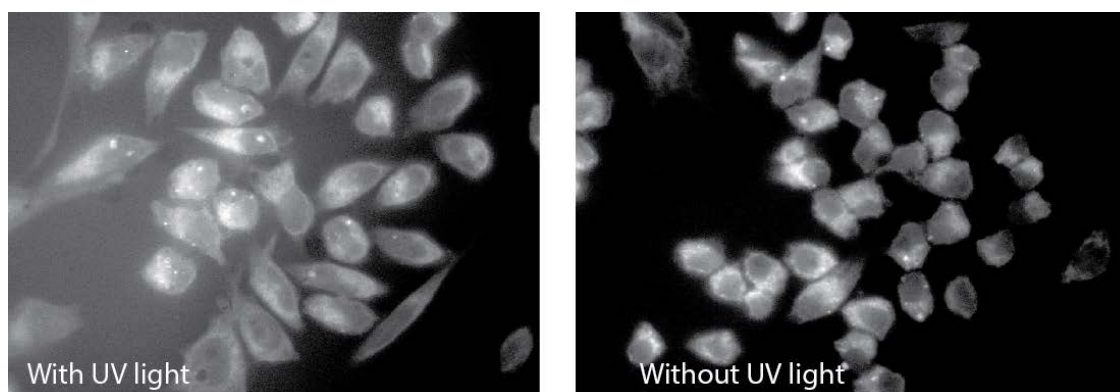
Figure 4.7: Nanoprobe **3** labeled GluA1 CHO cells after KCl washes**.** GluA1 CHO cells were labeled with nanoprobe **3**, irradiated, washed 4 x 1mL with 1M KCl, and then fixed with 4% paraformaldehyde. Fluorescence was set for the with UV light samples. Fluorescence accumulation is similar in both cases.

4.2.6 Chemical Activity Based Protein Profiling with GluA1 CHO Cells

To confirm that it is just the polyamine that is binding into the channel and that our aryl azide electrophile is not tagging, chem ABPP was run on GluA1 CHO cells. To 60 mm^2 petri dishes, solutions containing 10 µM nanoprobe **3** were placed on for 5 minutes at room temperature. Dishes were then irradiated for 10 minutes under UV-light (no irradiation was used as a control) and cells were lysed using a probe sonicator. The membranes were then pelleted and the membrane pellet was then lysed. The lysate was then conjugated with biotin azide and separated on 10% SDS-PAGE gels. Biotin was probed for by streptavidin-HRP and imaged using a BioRad imaging system. (Figure 4.8)
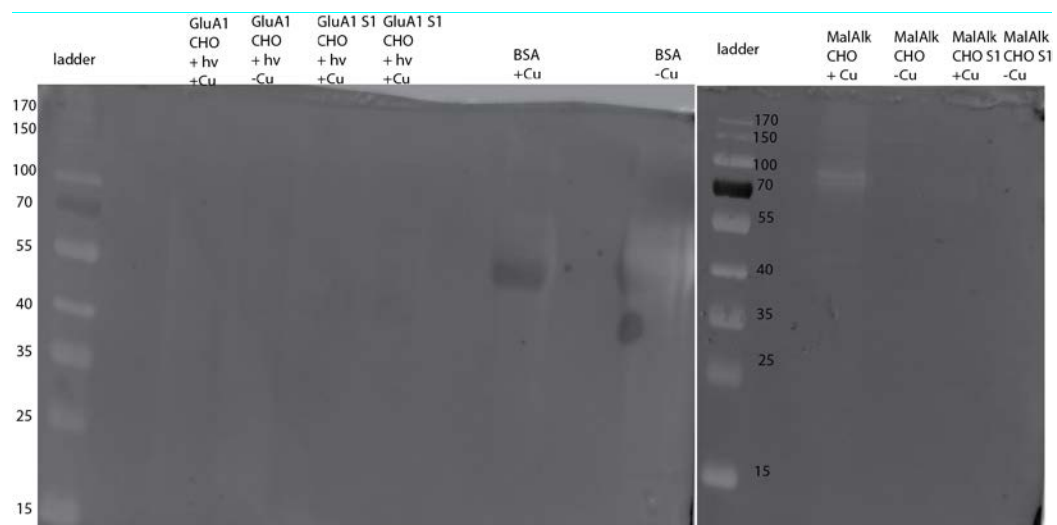
Figure 4.8: Western blot of GluA1 CHO cells labeled with nanoprobe **3.** GluA1 CHO cells were labeled with nanoprobe **3** and irradiated. Controls were performed with CHO cells labeled with malemide alkyne and BSA. All samples were lysed, separated on 10% SDS-PAGE gels, transferred to a nitrocellulose membrane, and probed using streptavidin-HRP. Signal was only seen in the positive controls, not in samples labeled with nanoprobe **3.**

4.3 Discussion

Nanoprobe **3** was designed from a scaffold of philanthotoxin-433. Much like nanoprobe **2**, the rationale for designing this probe was to allow us to determine which subunits comprise calcium permeable AMPARs. To do so, we designed the probe so that it contained an aryl azide for photocrosslinking bioconjugation to the surface of the receptor. Mass spec experiments were conducted to determine the minimum amount of time that is need to fully photolyse the probe, which was determined to be four minutes. Initial testing of the probe was conducted *in vitro* using BSA and lysozyme and demonstrated that we were able to label both proteins.

We then began testing nanoprobe **3** in neurons. Initial testing took place in dissociated cultures of rat cortex, midbrain, and cerebellar neurons. We probed using azido labeled rhodamine, fluorescein, and biotin for the detection of labeled subunits. The in-gel fluorescence and Western blot data showed that nanoprobe **3** is not covalently binding to the receptors of interest, or for that matter, any receptors in the neuronal samples. However, coomassie staining showed that there was indeed protein present on the gels and our control samples of BSA that were irradiated with the same probe work. A subsequent silver stain was done on other gels to again show the presence of protein, and to determine if there is any difference in labeling. (Figure 4.9) We were not able to visualize any fluorescent bands using either the fluorophore azide or the biotin azide, suggesting that the probe was not covalently attaching to the surface of the protein.

	Cerbellum						Cortex					
probe	1	1	5	5	10	10	1	1	5	5	10	10
NAS	-	-	-	-	-	-	-	-	-	-	-	-
Cu	+	-	+	-	+	-	+	-	+	-	+	-
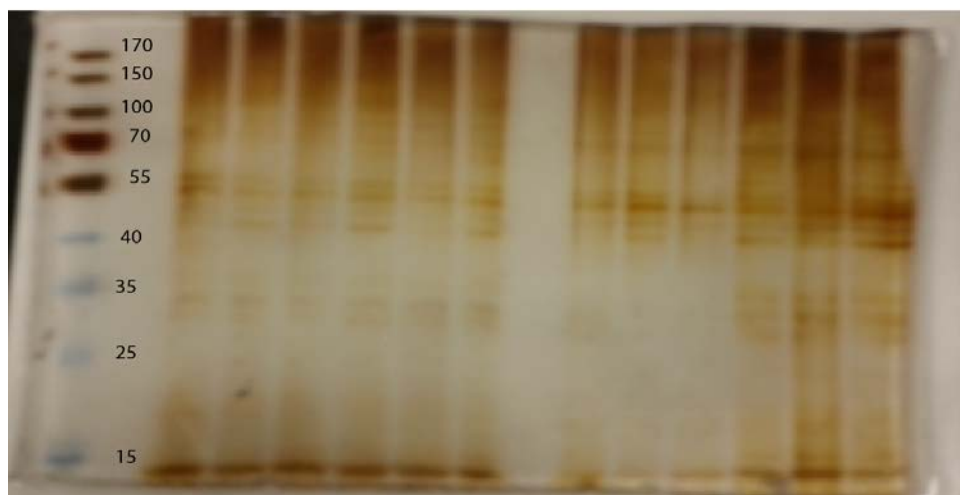
Figure 4.9: Silver stain of SDS-PAGE gel of nanoprobe **3** labeled cerebellum
samples. Protein is present when the gel is silver stained, however, we
do not see any protein bands in the fluorescence gels or the Western
Blots.

We then wanted to see if we are targeting the same receptor sites that nanoprobe

1 and nanoprobe **2** targeted. In this case, we were not able to do live cell imaging as we

did before, as we need to use copper to attach our reporter tag to the probe. Copper can be

very toxic when introduced to biological systems at the amounts needed to catalyze click

reactions. Unlike nanoprobe **2**, the addition of the reporter prior to cell imaging would be

difficult as nanoprobe **3** contains both an azide, albeit an arylazide, and alkyne on the

same molecule. We wanted to limit these toxic effects, so we fixed the neurons prior to

applying azido-rhodamine for visualization. Here, we received very confusing results as

some coverslips behaved as we expected and others did not. Our control coverslips, those

that were non-irradiated and/or contained NAS, had fluorescence accumulation equal to

or higher than that of the fully irradiated probe samples. This could be due to nanoprobe

3 being internalized in vesicles prior to fixation with 4% paraformaldehyde. [5] Here, we

could not be able to tell if nanoprobe **3** was attached to the surface of the receptor, on that

it was present when the cells were fixed. Also, the rhodamine dye might be an issue as well. (Figure 4.4) In control samples in which only rhodamine azide was present, there was a large amount of somal staining, as well as dendritic staining. This suggests that the rhodamine azide is non-specifically targeting the membranes even after fifteen wash steps with 1x PBS. We cannot use a green fluorophore, as neurons autofluorescence at the 488 nm excitation for FITC and, as a result, use of another red fluorophore would give us better information.

We then moved into a heterologous system of CHO cells stably transfected with GluA1. This represents a model calcium permeable AMPA receptor. GluA1 CHO cells were subjected to the same treatment as the neurons and probed using azido rhodamine. As with the neurons, we observed prodigious staining of the cell body which appeared to be non-specific. We wanted to then test if we could possibly remove nanoprobe **3** from the ion channel through either multiple wash steps or through depolarization of the membrane. Polyamine toxins block the ion current that goes through glutamatergic receptors and in neurons would be removed when the electrochemical gradient in the membrane shifts and depolarizes the membrane.[6] This can also be done through chemical methods by using a high KCl solution. GluA1 CHO cells were washed up to 24 times with 1x PBS to try to remove the probe from the ion channel. GluA1 CHO cells were also washed with 1M KCl up to four times to depolarize the membrane, again to try to remove nanoprobe **3** from the ion channel before fixation. Again, there was no significant difference in cells that were either washed or depolarized compared to the control.
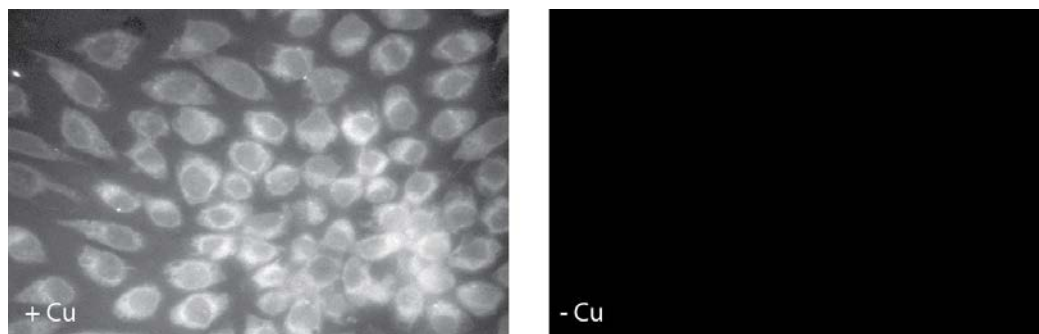
Figure 4.10: CHO cells labeled with malemide alkyne with and without copper

We then tried chem ABPP on GluA1 CHO cells this time affixing biotin azide to the probe. Controls were done using non-transfected cells labeled with malemide alkyne (Figure 4.10). Cells were irradiated for 10 minutes in this case to ensure that nanoprobe **3** was labeling. Probing with streptavidin-HRP showed that nothing was labeled in the probe lanes, but the control lanes were labeled. This means that our click conditions are working just fine, but nanoprobe **3** is not. One potential reason is that the nitrene that is formed is reacting with water in the binding pocket.[7] When the activate photophore is formed, it is indiscriminate in its binding partner and will react with to the closest neighboring molecule. In this case, it could be the OH of water and not the CH of the nearest amino acid in the binding pocket. All of these results, taken together, suggest that nanoprobe **3** does not function as a suitable probe for the detection of calcium permeable AMPARs.

A better probe should take into account some of the design details that were incorporated into nanoprobe **1**. The main difference between nanoprobe **1** and nanoprobes **2** and **3** is the placement of the electrophile to the targeting polyamine. It might be fruitful to move the position of the electrophile so that it can explore the same target space as nanoprobe **1**. A better design for these nanoprobes will be described in chapter 6.

4.4 Methods

4.4.1 General Methods

All reagents were purchased through Fisher Scientific (Fair Lawn, NJ, USA) unless otherwise noted. FAM-5 azide was purchased from Lumiprobe (Hallendale Beach, FL, USA). All moisture sensitive reactions were done under an argon atmosphere using a syringe-septum cap technique. Dry dimethylformamide (DMF) and acetonitrile (MeCN) were purchased from Sigma Aldrich (St. Louis, MO, USA). Analytical thin layer chromatography (TLC) was carried out on Merck Silica gel 60 F254 glass plates and visualized using UV light (254 nm), ninhydrin or bromocrestol green stain. Sorbent Technologies (Atlanta, GA, USA) silica gel (230-450 mesh) was used for flash chromatography. ^{1}H NMR and ^{13}C NMR spectra were collected on a 400 MHz Bruker NMR spectrometer using the residual proton or carbon resonance of the solvent as the standard. Chemical shifts are reported in parts per million (ppm). The following abbreviations are used for peak multiplicities: s, singlet; d, doublet; dd, doublet of doublets; t, triplet; m, multiplet. Mass spectra were measured using either a Waters ZQ for LCMS, or at the UMass Mass Spec facility for HRMS, UMass Amherst.

4.4.2 Synthesis of nanoprobe 3
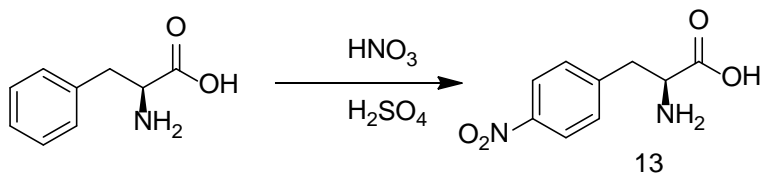
(S)-2-amino-3-(4-nitrophenyl)propanoic acid(13)

L-phenylalanine (15.0 g, 90.8 mmol) was dissolved in H_2SO_4 (45 mL) and a mixture of HNO_3 (4.50 mL, 108.9 mmol) in H_2SO_4 was added dropwise at 0°C. The solution was warmed to room temperature and stirred for 4 hours and then poured onto

ice (50 g) and neutralized with solid NaOH until pH equaled 7 using pH paper. A solid white precipitate was filtered, dried, and was used without further purification as it was spectroscopically identical to literature (10.41 g, 55 % yield).[8]
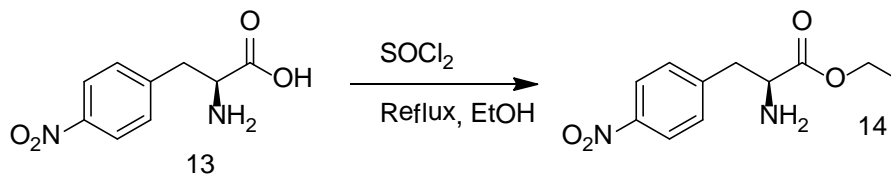
(S)-Ethyl 2-amino-3-(4-nitrophenyl)propanoate (14)

To a stirred suspension of compound **13** (5.0 g, 23 mmol) in ethanol (40 mL), SOCl$_2$ (2.07 mL, 28.5 mmol) was added dropwise and the reaction was heated to reflux overnight. The solvent was removed *in vacuo* and the product was purified via column chromatography using 10:1 CH$_2$Cl$_2$:CH$_3$OH as the mobile phase. A solid white precipitate was filtered, dried, and was used without further purification as it was spectroscopically identical to literature (2.97 g, 53% yield) [9]
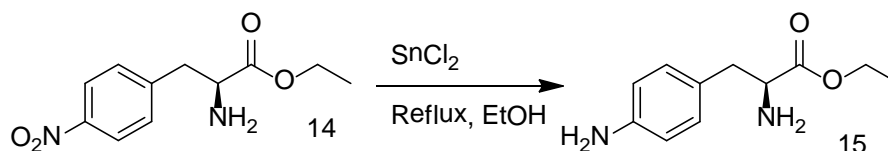
(S)-Ethyl 2-amino-3-(4-nitrophenyl)propanoate(15)

Compound **14** (2.95 g, 338.8 mmol) was dissolved in ethanol (50 mL) and was treated with Sn (II)Cl$_2$ (5.92 g, 26.3 mmol) at reflux for 18 h. The solution was then cooled to room temperature, poured on ice (50 g), and made basic (pH equaled to 9) using sat. NaHCO$_3$. The solution was then filtered through Celite and washed with CH$_2$Cl$_2$. It was then extracted with brine, dried over MgSO$_4$ (anhyd.), and the solvent was removed *in vacuo*. The product was recovered as a white solid. (2.97 g, 53% yield) [ ]

[1H] NMR (400 MHz, CDCl$_3$) d ppm 6.98 (d, *J*=8.34 Hz, 2 H) 6.63 (d, *J*=8.34 Hz, 2 H) 4.17 (q,*J*=7.16 Hz, 11 H) 3.65 (dd, *J*=7.45, 5.43 Hz, 5 H) 2.98 (dd, *J*=13.64, 5.31 Hz, 6 H) 2.77 (dd, *J*=13.77, 7.71 Hz, 7 H) 1.26 (t, *J*=7.20 Hz, 17 H).
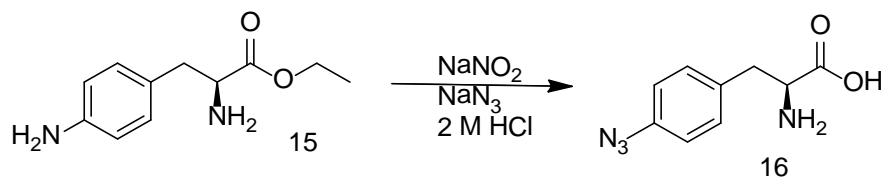
(S)-Ethyl 2-amino-3-(4-azidophenyl)propanoate (16)

Compound **15** (1.40 g, 4.5 mmol) was dissolved in aqueous 2 N HCl and cooled

to 0°C. To that, NaNO$_2$ (319 mg, 4.6 mmol) dissolved in water (3.6 mL) was slowly

added. The reaction was stirred for 15 minutes and NaN$_3$ (301 mg, 4.6 mmol) dissolved in

water (7.2 mL) was added dropwise. The reaction mixture was then warmed to room

temperature and then stirred for an additional 30 minutes. The reaction mixture was then

poured into deionized water (50 mL) and made basic with saturated NaHCO$_3$. The

solution was extracted into ethyl acetate (3 x 20 mL), dried over anhydrous sodium

sulfate, and filtered. The solvent was removed *in vacuo*. The product was recovered as a

white solid. (1.40g, 89% yield) ^{1}H NMR (400 MHz, CDCl$_3$) ppm 7.18 (d, *J*=8.34 Hz, 2

H) 6.91 - 6.97 (m, 2 H) 4.15 (q, *J*=7.07 Hz, 13 H) 3.03 (dd, *J*=13.64, 5.31 Hz, 6 H) 2.84

(dd, *J*=13.64, 7.58 Hz, 6 H) 1.20 - 1.27 (m, 21 H).
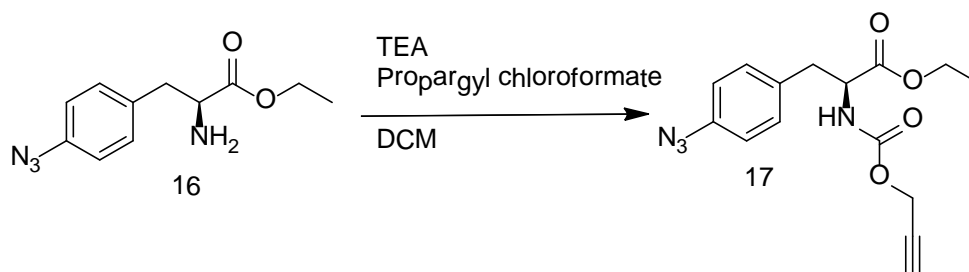
(S)-Ethyl 3-(4-azidophenyl)-2-(((prop-2-yn-1-yloxy) carbonyl) amino)propanoate
(17)

Compound **16** (1.32 g, 5.63 mmol) and triethylamine (942 µL, 6.76 mmol) were

dissolved in CH$_2$Cl$_2$ (5 mL) and cooled to 0°C. Propargyl chloroformate (550 µL, 5.63

mmol) was dissolved in CH$_2$Cl$_2$ (30 mL) and was added slowly to the reaction mixture.

The reaction was warmed to room temperature and stirred overnight. The reaction

mixture was diluted with CH$_2$Cl$_2$ and underwent a water work-up (3 x 20 mL). The

extract was dried over anhydrous sodium sulfate, filtered, and then evaporated *in vacuo*.

The residue was purified using column chromatography using 10:1 CH_2Cl_2:CH_3OH as

the mobile phase. The product was recovered as an yellow oil. (0.759 g, 44.8% yield) [1]H

NMR (400 MHz, CDCl$_3$) ppm 7.13 (d, *J*=8.34 Hz, 2 H) 6.94 - 6.99 (m, 2 H) 5.32 (s, 3

H) 4.63 - 4.71 (m, 2 H) 4.19 (dd, *J*=7.07, 1.77 Hz, 2 H) 3.11 (dd, *J*=15.66, 5.81 Hz, 2 H)

2.50 (t, *J*=2.53 Hz, 1 H) 1.27 (t, *J*=7.20 Hz, 3 H).
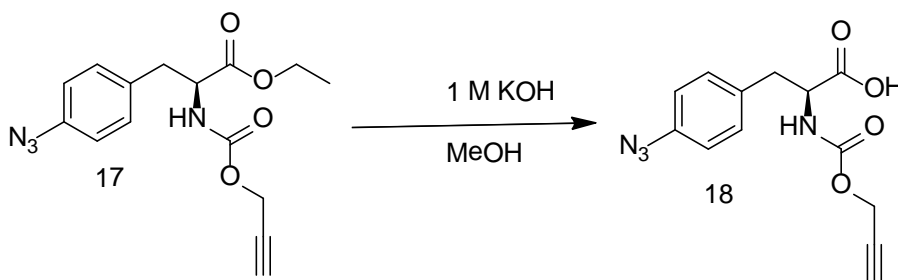
(S)-3-(4-azidophenyl)-2-(((prop-2-yn-1-yloxy)carbonyl)amino)propanoic acid (18)
Compound **17** (730 mg, 2.31 mmol) was dissolved in methanol (15 mL) and

treated with aqueous 1M KOH (3.46 mL, 3.46 mmol) overnight. The solution was

neutralized with 1M citric acid (5 mL) and concentrated. The residue was diluted with

water (10 mL) and acidified to pH equal to 2 with 1M citric acid monitored using pH

paper. The resulting mixture was extracted into CH_2Cl_2 and the solvent was removed *in*

vacuo. The product was recovered as an yellow oil. (0.3985 g, 49 % yield) ^{1}H NMR (400

MHz, CDCl$_3$) ppm 7.14 - 7.21 (m, 2 H) 6.99 (d, *J*=8.34 Hz, 2 H) 5.27 - 5.34 (m, 8 H)

4.65 - 4.71 (m, 2 H) 3.22 (dd, *J*=14.02, 5.43 Hz, 8 H) 3.05 - 3.15 (m, 6 H) 2.51 (t, *J*=2.40

Hz, 6 H) 1.41 - 1.50 (m, 14 H).
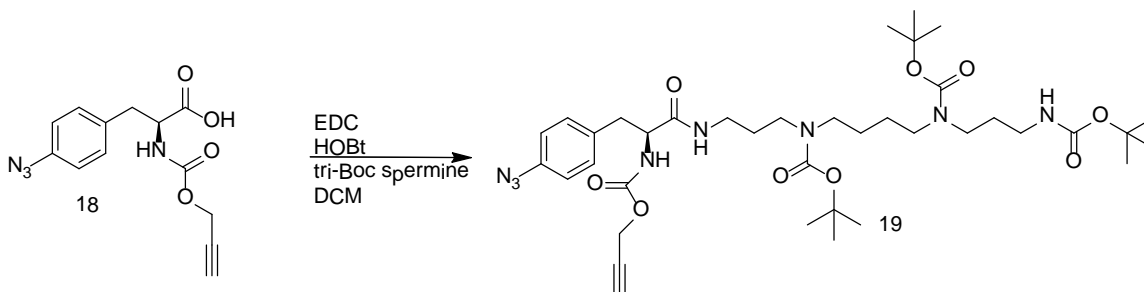
(S)-Tert-butyl (3-(3-(4-azidophenyl)-2-(((prop-2-yn-1-yloxy)carbonyl)amino)propanamido)propyl)(4-((tert-butoxycarbonyl)(3-((tert-butoxycarbonyl)amino)propyl)amino)butyl)carbamate (19)

Compound **18** (31 mg, 0.108 mmol) was dissolved in CH_2Cl_2 (5 mL) along with

EDC (27 mg, 0.140 mmol) and HOBt (21 g, 0.140 mmol) for 15 minutes, then triBoc

spermine (54 mg, 0.108 mmol) was added. The reaction mixture was placed under argon

and stirred overnight at room temperature. The solvent was evaporated and the crude

mixture was taken up in ethyl acetate (10 mL) and underwent an acid/base extraction

with 1 N HCl (2x 10 mL) and 1 N NaOH (2x10 mL). The organic fraction was dried over

anhydrous sodium sulfate, filtered, and the solvent was removed *in vacuo*. The product

was recovered as a white solid. (43 mg, 51.7% yield) LCMS=772.9
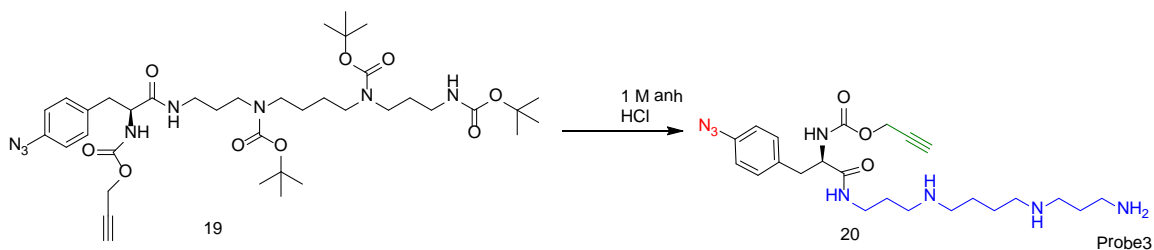
(S)-(3-(3-(4-azidophenyl)-2-(((prop-2-yn-1-yloxy) carbonyl) amino)propanamido)propyl) (4-(carboxy(3-(carboxyamino) propyl)amino)butyl) carbamic acid (20)

Compound **19** (43 mg, 0.0557 mmol) was taken up in 200 proof ethanol (3 mL)

and acetyl chloride (0.75 mL) was added in dropwise to produce a 1M anhydrous HCl

solution. The reaction was stirred overnight, hexanes (1 mL) was added to precipitate the

product, and solvent was removed *in vacuo*. The product was recovered as an yellow oil.

(36.7 mg, 90 % yield) LCMS= 472.8

4.4.3 Chemical Activity Based Protein Profiling on Bovine Serum Albumin and Lysozyme

5 µL of 2.0 mg/mL BSA or lysozyme was placed in 50 µL of 1x PBS and 1 mM

of nanoprobe **3**. Samples were irradiated for 4 minutes with 365 nm light. Control non-

irradiated samples were also prepared. Samples were then subjected to chemical ABPP.

Master mixes for click solutions were set up with 1 mM $CuSO_4*5H_2O$ (50 mM stock),

100 µM THPTA (1.7 mM stock), and freshly prepared 1 mM TCEP (50 mM stock). These incubated for 10 minutes and 10 µM of rhodamine azide. A separate control master mix was prepared by substituting deionized water in for the $CuSO_4*5H_2O$. Samples were then separated on a 10% SDS-PAGE gel and fluorescence was measured using a Typhoon 9210 imager.

4.4.4 Dissociated Culture of Rat Cortex, Midbrain, and Cerebellar Neurons

Primary dissociated cortex, midbrain, and cerebellar cell cultures were prepared from embryonic day E18-20 Sprague-Dawley rat embryos and were cultured on 25 cm^2 T-Flasks or 60 mm^2 petri dishes coated in poly-lysine in serum containing media identical to previous reports.[10] Cerebellar culture media was supplemented with 1M potassium chloride (1 mL in 50 mL).[11] Cells were grown in 5% CO_2 at 37°C. All animal care and experimental protocols were approved by the Animal Care and Use Committee at University of Massachusetts, Amherst, Amherst, MA, USA.

4.4.5 Chemical Activity Based Protein Profiling on Rat Cortex, Midbrain, and Cerebellar Neurons

Cultures of neurons from of cortex, mid-brain, and cerebellum were grown on 25 cm^2 T-flasks (or 60 mm^2 petri dishes) were grown to a point where they were synaptically active (DIV 14-18). Flasks were washed three times with extracellular recording buffer. 5 mL of 10 µM of nanoprobe **3** in extracellular solution with 20 µM glutamate was applied for 5 minutes at room temperature. Cells were then irradiated with 365 nm light for 4 minutes. Control samples were prepared either by non-irradiation with UV light or as equimolar mixtures of NAS and nanoprobe **3** with and without UV light. Flasks were then washed three more times with extracellular solution. To this, 1 mL of lysis solution (1x PIC, 1x PBS) was added to each flask and cells were scrapped to remove from sides of the T-flask. Cells were lysed with a probe sonicator 30% power for 1 minute, and the

membrane portions were pelleted. The membrane pellet was lysed again using the same

conditions and a BCA assay was run to quantitate protein concentrations. Master mixes

for click solutions were prepared with 1 mM CuSO$_4$*5H$_2$O (50 mM stock), 100 µM

THPTA (1.7 mM stock), and freshly prepared 1 mM TCEP (50 mM stock). These

lysates were incubated for 10 minutes and 10 µM of either rhodamine azide or biotin

azide were then added. A separate control master mix was prepared by substituting

deionized water in for the CuSO$_4$*5H$_2$O. To an Eppendorf tube, 50 µL of cell lysate and

the appropriate master mix were added to the tube with the reaction going for one hour.

Samples were then separated on a 10% SDS-PAGE gel. For in-gel fluorescence

experiments, gels were placed into 10% acetic acid and imaged using a Typhoon 9210

imager. For Western blot experiments, proteins were transferred to a nitrocellulose

membrane and probed against streptavidin HRP. HRP was activated using SuperSignal

West Pico Chemiluminescence Substrate. Chemiluminescence was measured using a

BioRad imaging system.

4.4.6 Dissociated Culture of Rat Hippocampal and Cerebellar Neurons

Primary dissociated cerebellar cell cultures were prepared from embryonic day

E18-19 Sprague-Dawley rat embryos and were cultured on polylysine-coated coverglass

(12mm, 1.0 size) in serum-containing media identical to previous reports. [11] Cells were

grown in 5% CO$_2$ at 37°C. All animal care and experimental protocols were approved by

the Animal Care and Use Committee at the University of Massachusetts Amherst,

Amherst, MA, USA.

4.4.7 Fixed Cell Imaging of Rat Hippocampal and Cerebellar Neurons

Coverslips containing neurons were grown until they were synaptically active

(DIV 14-18). Three imaging solutions were prepared: a sham solution containing 4 mL

of 1x ECS and 20µM l-glutamate, 8 mL of 10 µM of nanoprobe **3** in 1x ECS with 20 µM

l-glutamate, and 8 mL of equimolar 10 µM nanoprobe **3** and NAS in 1x ECS with 20 µM l-glutamate. Coverslips were washed three times with 1x ECS and probe solutions were applied for 5 minutes at room temperature. Appropriate coverslips were irradiated with UV (365nm) light for 4 minutes, and dark controls were left in the dark for the same amount of time. Coverslips were then washed three times with 1x ECS. All coverslips were fixed in 4% paraformaldehyde for 8 minutes and were then washed three times with 1x PBS. Click solutions (1 mM $CuSO_4*5H_2O$ (50 mM stock), 100 µM THPTA (1.7 mM stock), freshly prepared 1 mM TCEP (50 mM stock), and 10 µM rhodamine azide (10 mM stock)) were placed onto the coverslips. Control solutions were also prepared using deionized water in place of $CuSO_4*5H_2O$. Coverslips were then washed six times with 1x PBS and mounted onto coverglass using ProLong Gold Antifade. Coverslips cured overnight and were sealed using clear nail polish.

Hippocampal and cerebellar neurons were imaged by excitation with a light from a Sutter Lambda-LS illuminator (Sutter Instruments, Novato, CA,USA). A Nikon Eclipse Ti series microscope (Nikon Corps, Tokyo, Japan) with a CFI Plan Apo VC 60X 1.4 NA oil objective lens (Nikon) was employed for all imaging epifluorescence experiments. The Cy-3 filter cue contained a 540/30 excitation filter, a 570 DRLP dichroic mirror, and 575 ALP emission filter (all from Omega Optical Corp., Brattleboro, VT, USA). Images were acquired using a Hamamatsu ORCA ER camera (Hamamatsu, Hamamatsu City, Japan) and NIS Elements BR 3.1 software (Nikon Corps, Melville, NY, USA).

Images were analyzed using ImageJ (U.S. National Institutes of Health, Bethesda, MD, USA). The mean of the minimum and maximum overall fluorescence values were set for all images collected from each of the 16 coverslips (32 in all). Images were not further analyzed as analysis by eye could tell there were differences between the nanoprobe **3** and control images.

4.4.8 Cell Culture of GluA1 CHO Cells

A stable cell line was prepared by Nate Johnson in the lab. Cells were grown to they were 70% confluent on cover glass (12mm, 1.0 size) in Hams-F12 media containing 10% FBS. Cells were grown at 5 % CO_2 at 37°C.

4.4.9 Fixed Cell Imaging of GluA1 CHO Cells

Coverslips containing CHO cells were grown until they were 70-85% confluent. Two imaging solutions were prepared: 8 mL of 10 µM of nanoprobe **3** in 1x ECS with 20 µM l-glutamate, and 8 mL of equimolar 10 µM nanoprobe **3** and NAS in 1x ECS with 20 µM l-glutamate. Coverslips were washed three times with 1x ECS and probe solutions were applied for 5 minutes at room temperature. Appropriate coverslips were irradiated with UV (365nm) light for 4 minutes, and dark controls were left in the dark for the same amount of time. Coverslips were then washed three to twenty four times with 1x PBS for washing experiments. For depolarization experiments, cells were washed one to four times with 1M KCl, washing three times with 1x PBS in between each addition.

All coverslips were fixed in 4% paraformaldehyde for 10 minutes and were then washed three times with 1x PBS. Click solutions (1 mM $CuSO_4*5H_2O$ (50 mM stock), 100 µM THPTA (1.7 mM stock), freshly prepared 1 mM TCEP (50 mM stock), and 10 µM rhodamine azide (10 mM stock)) were placed onto the coverslips. Control solutions were also prepared using deionized water in place of $CuSO_4*5H_2O$. Coverslips were then washed six times with 1x PBS and mounted onto coverglass using ProLong Gold Antifade. Coverslips cured overnight and were sealed using clear nail polish.

GluA1 CHO cells were imaged by excitation with a light from a Sutter Lambda-LS illuminator (Sutter Instruments, Novato, CA,USA). A Nikon Eclipse Ti series microscope (Nikon Corps, Tokyo, Japan) with a CFI Plan Apo VC 60X 1.4 NA oil objective lens (Nikon) was employed for all imaging epifluorescence experiments. The

Cy-3 filter cue contained a 540/30 excitation filter, a 570 DRLP dichroic mirror, and 575 ALP emission filter (all from Omega Optical Corp., Brattleboro, VT, USA). Images were acquired using a Hamamatsu ORCA ER camera (Hamamatsu, Hamamatsu City, Japan) and NIS Elements BR 3.1 software (Nikon Corps, Melville, NY, USA).

Images were analyzed using ImageJ (U.S. National Institutes of Health, Bethesda, MD, USA). The mean of the minimum and maximum overall fluorescence values were set for all images collected from each of the coverslips.

4.4.10 Chemical Activity Based Protein Profiling of GluA1 CHO Cells

60 mm^2 petri dishes of GluA1 CHO cells and CHO cells were grown until they were 90% confluent. Petri dishes were washed three times with extracellular recording buffer. 5 mL of 10 µM of nanoprobe **3** in extracellular solution with 20 µM glutamate was applied for 5 minutes at room temperature. Cells were then irradiated with 365 nm light for 4 minutes. Control samples were prepared either by non-irradiation with UV light. Control non-transfected samples were treated for 5 minutes with TCEP and incubated with 10 µM malemide alkyne for 30 minutes at 37°C. Petri dishes were then washed three more times with extracellular solution. 1 mL of lysis solution (1 x PIC, 1x PBS) was added to each dish and cells were scrapped to remove cells from the bottom of the dish. Cells were lysed with a probe sonicator 30% power for 1 minute, and the membrane portions were spun down. The membrane pellet was lysed again using the same conditions and a BCA assay was run to quantitate protein concentrations. Master mixes for click solutions were set up with 1 mM CuSO$_4$*5H$_2$O (50 mM stock), 100 µM THPTA (1.7 mM stock), and freshly prepared 1 mM TCEP (50 mM stock). These incubated for 10 minutesutes and 10 µM of either rhodamine azide or biotin azide were then added. A separate control master mix was prepared by substituting deionized water in for the CuSO$_4$*5H$_2$O. 50 µL of cell lysate were removed and the appropriate master

mix was added to the tube with the reaction going for one hour. Samples were then

separated on a 10% SDS-PAGE gel. For Western blot experiments, proteins were

transferred to a nitrocellulose membrane and probed against streptavidin HRP. HRP was

activated using SuperSignal West Pico Chemiluminescent Substrate. Chemiluminescence

was measured using a BioRad imaging system.

4.5 References

1.(a) Stromgaard, K.; Mellor, I., AMPA receptor ligands: Synthetic and pharmacological studies of polyamines and polyamine toxins. *Medicinal Research Reviews* **2004,** *24* (5), 589-620; (b) Herlitze, S.; Raditsch, M.; Ruppersberg, J. P.; Jahn, W.; Monyer, H.; Schoepfer, R.; Witzemann, V., Argiotoxin detects molecular differences in AMPA receptor channels. *Neuron* **1993,** *10* (6), 1131-1140; (c) Blaschke, M.; Keller, B. U.; Rivosecchi, R.; Hollmann, M.; Heinemann, S.; Konnerth, A., A single amino-acid determines the subunit-specific spider toxin block of alpha-amino-3-hydroxy-5-methylisoxazole-4-propionate kainate receptor channels. *Proc. Natl. Acad. Sci. U. S. A.* **1993,** *90* (14), 6528-6532.

2.Brunner, J., New photolabeling and cross-linking methods. *Annual Review of Biochemistry* **1993,** *62*, 483-514.

3.Vodovozova, E. L., Photoaffinity labeling and its application in structural biology. *Biochemistry-Moscow* **2007,** *72* (1), 1-20.

4.(a) Schwyzer, R.; Caviezel, M., Para-azido-L- phenylalanine- photo-affinity probe related to tyrosine. *Helvetica Chimica Acta* **1971,** *54* (5), 1395-&; (b) Choi, S. K.; Kalivretenos, A. G.; Usherwood, P. N. R.; Nakanishi, K., Labeling studies of photolabile philanthotoxins with nicotinic acetylcholine-receptors - mode of interaction between toxin and receptor. *Chemistry & Biology* **1995,** *2* (1), 23-32.

5.Lin, J. W.; Ju, W.; Foster, K.; Lee, S. H.; Ahmadian, G.; Wyszynski, M.; Wang, Y. T.; Sheng, M., Distinct molecular mechanisms and divergent endocytotic pathways of AMPA receptors internalization. *Nature Neuroscience* **2000,** *3* (12), 1282-1290.

6.Uzunova, G.; Hollander, E.; Shepherd, J., The Role of Ionotropic Glutamate Receptors in Childhood Neurodevelopmental Disorders: Autism Spectrum Disorders and Fragile X Syndrome. *Current Neuropharmacology* **2014,** *12* (1), 71-98.

7.(a) Sobolevsky, A. I.; Rosconi, M. P.; Gouaux, E., X-ray structure, symmetry and mechanism of an AMPA-subtype glutamate receptor. *Nature* **2009,** *462* (7274), 745-U66; (b) Duerr, K. L.; Chen, L.; Stein, R. A.; De Zorzi, R.; Folea, I. M.; Walz, T.; McHaourab, H. S.; Gouaux, E., Structure and Dynamics of AMPA Receptor GluA2 in Resting, Pre-Open, and Desensitized States. *Cell* **2014,** *158* (4), 778-792.

8.Xu, B.; Huang, Z.; Liu, C.; Cai, Z.; Pan, W.; Cao, P.; Hao, X.; Liang, G., Synthesis and anti-hepatitis B virus activities of Matijing-Su derivatives. *Bioorganic & Medicinal Chemistry* **2009,** *17* (8), 3118-3125.

9.Iqbal, J.; Tangellamudi, N. D.; Dulla, B.; Balasubramanian, S., Sequential C-N and C-O Bond Formation in a Single Pot: Synthesis of 2H-Benzo b 1,4 oxazines from 2,5-Dihydroxybenzaldehyde and Amino acid Precursors. *Organic Letters* **2012,** *14* (2), 552-555.

10.Chambers, J. J.; Kramer, R. H., Light-Activated Ion Channels for Remote Control of Neural Activity. In *Methods in Nano Cell Biology*, Jena, B. P., Ed. 2008; Vol. 90, pp 217-+.

11.Bilimoria, P. M.; Bonni, A., Cultures of cerebellar granule neurons. *CSH protocols* **2008,** *2008*, pdb.prot5107-pdb.prot5107.

.

CHAPTER 4

LABELING OF BIOLOGICAL SYSTEMS USING PHOTOGENERATED DIAZONIUMS

5.1 Introduction

Understanding and visualizing how proteins react *in vivo* has become a popular topic in the past 15 years. Current methods for labeling biological systems involve either modifying the protein of interest with a fluorescent reporter or by targeting the protein using small-molecule probes which contain organic fluorophores. These organic fluorophores can more easily be changed out for different imaging experiments when compared to genetic manipulations. Further, one has the ability to modify biomolecules such as glycans and lipids using bioorthoginal strategies. A typical chemical probe contains a targeting ligand, a reactive partner for attachment, and a reporter tag for visualization. These probes are designed in such a way that is orthogonal to the function of the receptor, termed bioorthogonal chemistry. There are a number of reactions that fall under the term bioorthogonal chemistry, including 1,3-dipolar cycloadditions (click reactions), hydrazine/oxime formation from aldehydes and ketones, tetrazine ligation, isocyanide based click reactions, and quadricyclane ligation.[1] A full discussion of these can be found in section 1.3. Use of bioorthogonal probes is a two-step process in which the probe targets the protein of interest and then a reporter tag is added for visualization.

A well designed probe for bioorthogonal chemistry is one that will not interrupt function of the biomolecule target, can withstand the environment of the cell, yet can still react with its intended target, and the reaction does not produce a toxic byproduct.[2] One of the most common type of bioorthogonal reactions is the 1,3-dipolar cycloaddition. Click reactions involve the reaction of an azide labeled moiety forming a triazole with an alkyne labeled moiety. These reactions can be copper mediated or strain mediated. Strain mediated cycloadditions have been used in a variety of bio-systems such as proteins, live-cells, and living animals,[3] and are preferable over copper mediated

reactions as there is no introduction of toxic amounts of copper to promote triazole formation. However, when using strain-mediated cylcoadditions the biosystem of interest must be labeled with a bioorthogonal group, such as an azide. Most of the time, this means an azido sugar is fed to the organism, or the protein is covalently labeled with an azide. Also, the cylcooctyne containing reporter tag can undergo attack by thiols contained on the biosystem of interest, thus leading to conjugation in areas not targeted by the reporter.[2]

Another method of tagging a biosystem of interest is through the use of photoaffinity labeling. This includes the use of benzophenones, aryl azides, and 3-(trifluoromethyl)-3-phenyldiazirine.[4] Photoreactive probes can provide spatial information about how proteins interact with each other. This is due to the indiscriminate nature of the activated photophore, as it will react with the nearest neighboring molecule.[4] The aspects of a good photoprobe were covered in Section 4.1, and share overlap with the aspects of a good bioorthogonal probe listed above; chiefly, the probe not interfering with the mechanism of action of the protein of interest. An ideal probe for looking at protein interactions with high spatial-temporal resolution should then incorporate aspects from both photoaffinity labeling and bioorthoginal reactivity.

Aryl diazonium salts have been used to photolabel a number species due to their ability to undergo nucleophilic aromatic substitutions.[4-5] Upon photolysis, the aryl diazonium generates a highly reactive aryl cation, which is super-reactive and will not rearrange in the excited state. They also bind to the closest nucleophilic partner, including C-H bonds, quickly, so that there is little time for them to exit from the active site of the receptor of interest. [6]

A few attempts at this exact design have been produced and have been termed "photoclick" probes. Lin in 2008 [7] used terminal alkenes to induce photoactivated, nitrile imine mediated 1,3-dipolar cycloadditions in *E. coli.* Their method involved

incorporating *O*-allyl-tyrosine into *E.coli* Z-domain and applying probe molecules containing diaryl tetrazoles. After a 10 min irradiation with UV-light and SDS-PAGE analysis, they were able to tag their modified *E. coli* proteins. [7] In 2009, Poptik designed a photo-caged cyclooctyne by masking the alkyne as a photo-reactive cyclopropenone. Upon irradiation, the cyclopropenone transforms to the cyclooctyne which is ready for conjugation with an azide. In their cell experiments, CHO cells were grown with n-azidoacetylmannosamine to produce the metabolite n-azido-diacetyl-sialic acid. Their protected biotinylated probes were incubated with cells for an hour, irradiated with UV light for 1 minute, and then incubated for an additional hour to facilitate the cycloaddition reaction. CHO cells were then fixed and stained with avidin-FITC for detection.[8] This cyclopropenone protected cyclooctyne method was then further adapted for use with enzyme mediated azide ligation.[9]

These methods extend the idea of "photoclick" reaction, but still rely on the biosystem of interest being tagged in some fashion with the bioorthogonal group days beforehand. This is done by manipulation of the system with either a point mutation or by having the cell produce an azido metabolite. A probe which quickly targets a biomolecule of interest produces an active, targetable species upon irradiation, and specifically couples with an appropriate reporter is still desired.

5.2 Results

5.2.1 Live Cell Imaging of CHO Cells Using Oleic TBA and Cy-3 DHPP
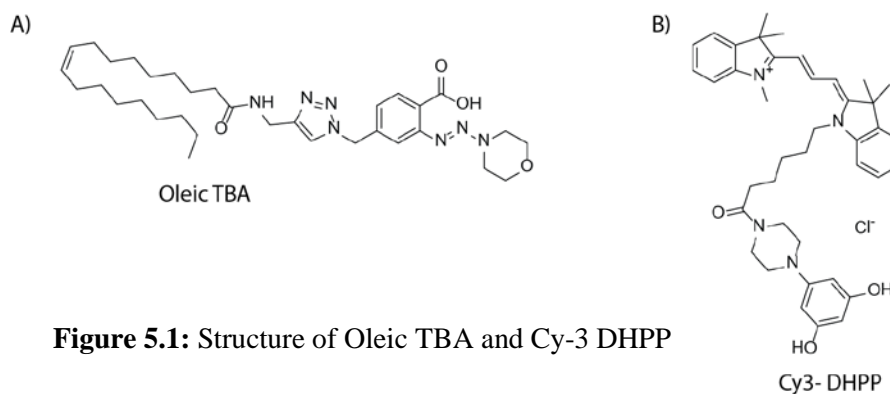
Figure 5.1: Structure of Oleic TBA and Cy-3 DHPP

Our new probe is based upon an oleic acid scaffold as it will partition into the cell membrane. (Figure 5.1) Other directly fluorescent probes have been made from this scaffold. [10] Our probe incorporates oleic acid so it contains an *ortho*-triazine benzonic acid head group which is able to undergo photochemistry yielding a diazonium carboxylate. Our targeting molecule is Cy-3 DHPP, (Cy-3 dihydroxyphenyl piperazine, Figure 5.1) which contains an electron rich aromatic ring for attachment to the photogenerated diazonium species. CHO cells were incubated with 10 µM oleic TBA for 15 minutes at 37°C in their home media. They were then washed via perfusion and photolysed. 1 µM Cy-3 DHPP was added for 15 seconds and cells were washed for 2 minutes before fluorescence images were captured. Controls were performed using DMSO as a sham treatment. We saw very little difference in the treated versus sham treated cells. (Figure 5.2)
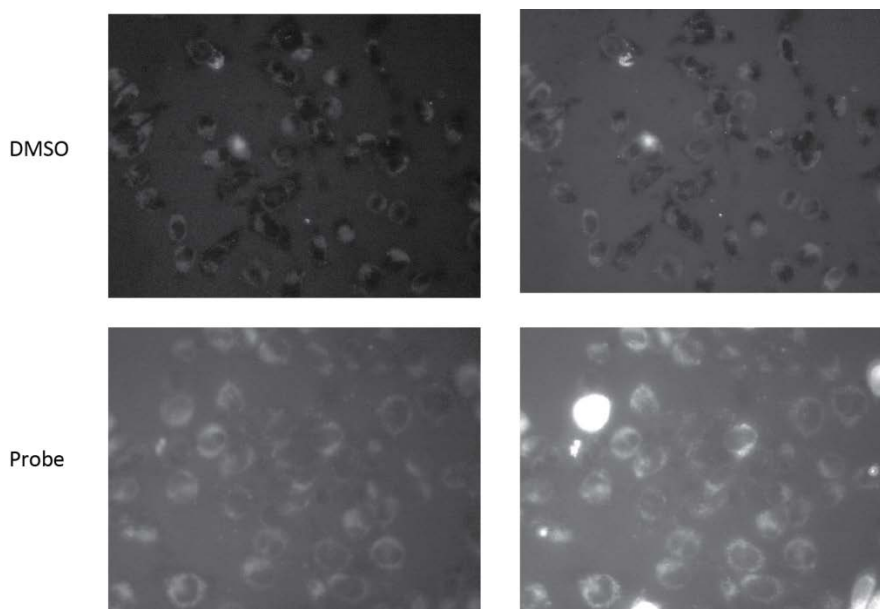
Figure 5.2: CHO cells labeled with oleic TBA and Cy-3 DHPP. CHO cells were incubated 10 µM oleic TBA for 15 min at 37°C and 1 µM Cy-3 DHPP for 15 seconds. Controls were done with DMSO. There was not a significant increase in fluorescence over the controls.

5.2.2 Live Cell Imaging of CHO Cells Using Oleic TBA and Cy-3 DMAPP
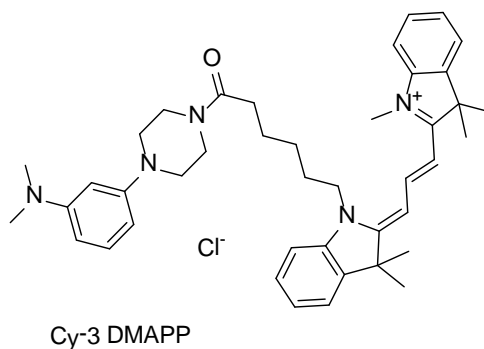
Cy-3 DMAPP

Figure 5.3: Structure of Cy-3 DMAPP

It was clear to us that the DHPP scaffold was far too reactive, so we decided to move to one that might be less so. Our new reporter tag was now Cy-3 DMAPP (dimethylaminophenyl piperazine, Figure 5.3) As before, CHO cells were incubated in their home media for 15 minutes with 1 µM oleic TBA, washed via perfusion, and photolysed for 15 seconds. Cy-3 DMAPP was applied for 15 seconds, and cells were

115

washed for 2 minutes. Fluorescence images were then collected. Sham DMSO treatments were also conducted as controls. Again, we only saw slight differences in the probed cells versus those that had the sham treatment. (Figure 5.4)
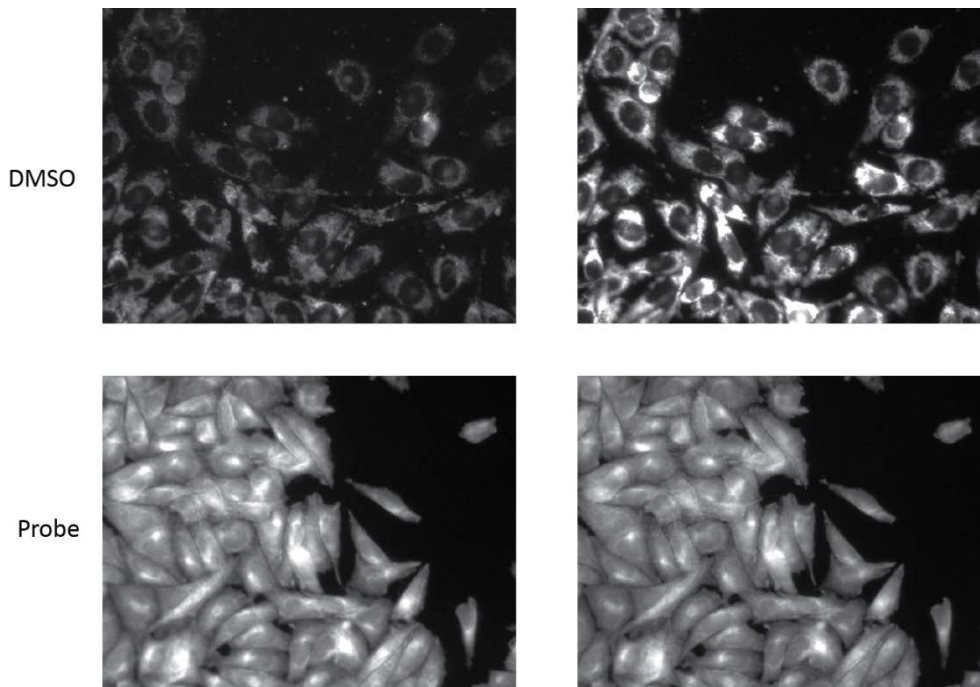
Figure 5.4: Live CHO cell imaging with Cy-3 DMAPP. CHO cells were incubated 1 µM oleic TBA for 15 min at 37°C and 1 µM Cy-3 DMAPP for 15 seconds. Controls were done with DMSO. There was not a significant increase in fluorescence over the controls.

5.2.3 Live Cell Imaging of CHO Cells Using Oleic TBA and Biotin-DMAPP
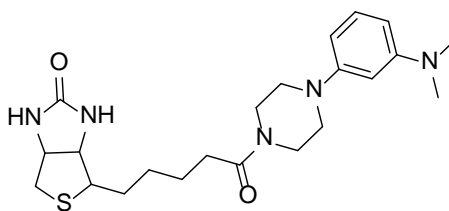
Biotin-DMAPP

Figure 5.5: Structure of biotin-DMAPP

We were not sure if it was our Cy-3 fluorophore itself that was crossing the membrane or otherwise being endocytosed by cells, so we decided to switch reporter

116

tags. Our new probe contained the same electron-rich targeting core (DMAPP), but now

had biotin installed for detection. (Figure 5.5) This allowed us to use an avidin-tagged

fluorophore for fluorescence reporting as excess avidin will be washed away by

perfusion.   CHO cells were incubated with 1 µM oleic-TBA for 15 minutes in their home

media and washed via perfusion. Cells were then irradiated with UV light for 15 sec, and

incubated with probe for 15 sec. Cells were then washed for 2 minutes, incubated with

1:100 avidin-FITC [11] washed for another 2 minutes, and imaged fluorescently. Controls

this time were a DMSO sham and non-irradiated samples containing the probe.

Fluorescent accumulation was seen along the cell membrane in irradiated cells, but not in

the control samples. (Figure 5.6)
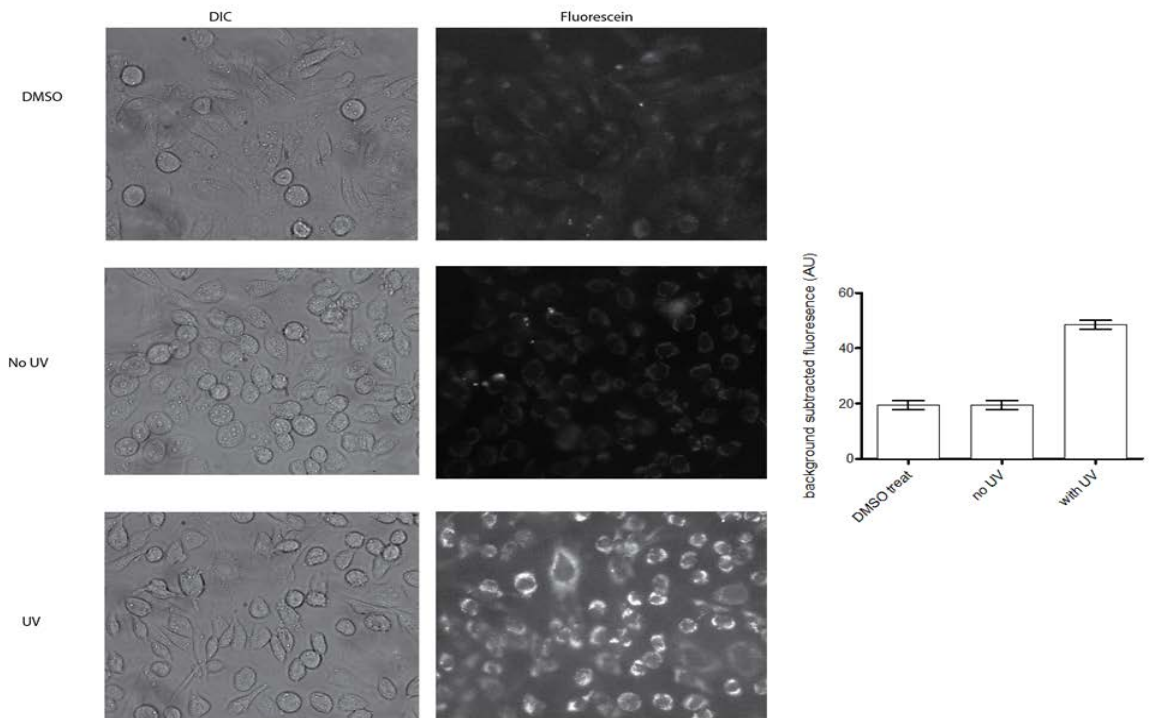
Figure 5.6: Live CHO cells imaged with oleic TBA and biotin-DMAPP. CHO cells were
incubated 1 µM oleic TBA for 15 min at 37°C ,1 µM biotin DMAPP for 15
seconds, and 1:100 FITC avidin for 2 min . Controls were done with DMSO and
non-irradiation of oleic-TBA. Cells treated with both UV-light and avidin-FITC
had an increase in fluorescence along membranes.

5.3 Discussion

Spatially and temporally controlled labeling of proteins using bioorthogonal methods is the future of where the field is heading in order to get real time information about protein dynamics and how cells function. Currently, there are a few methods available in order to be able to achieve this, but they suffer from the need of having an orthogonal reporter tag installed either genetically or metabolically prior to photo activation. Our approach is the first to develop a method that would allow for targeting a protein of interest target, then to target a photoactivated species with a reporter probe. To do so our targeting probe contained a triazine benzoic acid and our reporting probe containing an electron rich aromatic ring which attaches itself to a diazonium resulting from photolysis of the targeting probe.

The first version of the reporter probe contained a dihydroxyphenyl piperazine as our electron rich aromatic ring, conjugated to Cy-3 for visualization. Application of the probe targeted areas on the cell membrane, but sham controls with DMSO also demonstrated fluorescence accumulation in the membrane as well. The same effect of fluorescent accumulation in the sham samples was also seen when the electron rich aromatic targeting group was changed to dimethylaminophenyl piperazine. DMSO has been known to permeabilize membranes, [12] allowing for fluorophores to slowly leak in at higher concentrations of DMSO. Molecular dynamic simulations of lipid membranes with DMSO show that small pores can be formed in the dipalmitoyl-phosphatidylcholine bilayer, which could be a way for small molecules to get through the lipid bilayer. [12c, 13] It is also possible that the free fluorophore is diffusing across the cell membrane and accumulating in the cytosol. [14]

We decided to change our reporter tag to biotin so that we can then tag with an avidin labeled fluorophore. The avidin labeled fluorophore should not cross the cell membrane, thus any fluorescence accumulation would be from avidin labeling biotin. We see precisely this result in our biotin DMAPP probed cells. In control samples with DMSO, there was no fluorescence uptake. More importantly, there was no fluorescence accumulation when the oleic-TBA probe was not irradiated. This strongly suggests that there is only binding of the reporting probe, when the targeting probe has been photoactivated, indicating that our probe is capable of photoclick chemistry. This has also been confirmed in SDS-PAGE gels on acyl carrier protein (data not shown). Further probes would need to be ligand directed to confirm binding at specific sites, rather than global membrane binding.

5.4 Methods

5.4.1 General Imaging Methods

CHO cells were imaged by excitation with a light from a Sutter Lambda-LS illuminator (Sutter Instruments, Novato, CA,USA). A Nikon Eclipse Ti series microscope (Nikon Corps, Tokyo, Japan) with a CFI Plan Apo VC 40X objective lens (Nikon) was employed for all imaging epifluorescence experiments. The Cy-3 filter cube contained a 540/30 excitation filter, a 570 DRLP dichroic mirror, and 575 ALP emission filter (all from Omega Optical Corp., Brattleboro, VT, USA). The GFP filter cube contained a 470/40 excitation filter, 485 LP mirror, and a 525/50 emission filer (Filter series 49002, Chroma Corps, Bellows Falls, VT, USA). Images were acquired using a Hamamatsu ORCA ER camera (Hamamatsu, Hamamatsu City, Japan) and NIS Elements BR 3.1 software (Nikon Corps, Melville, NY, USA).

5.4.2 CHO Cell Culture

CHO cells were grown on coverglass (12.0 mm, size 1.0) until they were 70% confluent. They were maintained in Hams F-12 media containing 5% serum at 37 °C and 5% CO_2.

5.4.3 Live CHO Cell Imaging with Oleic TBA and Cy-3 DHPP

CHO cells were incubated in their home media with 10 µM Oleic TBA for 15 minutes at 37 °C. Cells were removed and then mounted in 12 mm perfusion apparatus (Warner Instruments, P-3, RC-25, Warner Instruments LLC, Hamden, CT, USA) and were bathed in extracellular recording buffer. Cells were irradiated with UV light for 15 seconds. After irradiation, 400 µL of a 1 µM Cy-3 DHPP for 30 seconds and then washed for 2 minutes with extracellular solution via perfusion. Fluorescence images were then taken using the Cy-3 filter cube. Controls were performed in the same way by using DMSO in place of Oleic TBA.

5.4.4 Live CHO Imaging with Oleic TBA and Cy-3 DMAPP

CHO cells were incubated in their home media with 10 µM Oleic TBA for 15 minutes at 37 °C. Cells were removed and then mounted in 12 mm perfusion apparatus (Warner Instruments, P-3, RC-25, Warner Instruments LLC, Hamden, CT, USA) and were bathed in extracellular recording buffer. Cells were irradiated with UV light for 15 seconds and 250 µL of 1µM Cy-3 DMAPP were applied for 30 seconds. Cells were then washed with extracellular solution via perfusion for 5 minutes. Fluorescence images were then taken using the Cy-3 filter cube. Controls were performed using DMSO in place of Oleic TBA.

5.4.5 Live CHO Cell Imaging with Oleic TBA and Biotin-DMAPP

CHO cells were incubated in their home media with 10 µM Oleic TBA for 15 minutes at 37 °C. Cells were removed and then mounted in 12 mm perfusion apparatus (Warner Instruments, P-3, RC-25, Warner Instruments LLC, Hamden, CT, USA) and were bathed in extracellular recording buffer. Cells were irradiated with UV light for 15 seconds, incubated with 250 µL of 1µM biotin DMAPP for 15 seconds, washed for 2 minutes with extracellular solution via perfusion, incubated with Avidin-FITC (BioLegend, San Diego, CA, USA) for 2 minutes, and washed for 2 minutes again with perfusion. Fluorescence images were then taken. Controls were performed with DMSO in place of the Oleic TBA and with no UV irradiation.

5.4.6 Image Analysis of Fluorescence Images

Images were analyzed using ImageJ (U.S. National Institutes of Health, Bethesda, MD, USA). Fluorescence was quantified using ROI (region of interest) analysis over the whole cell areas. The images were background subtracted and the data was quantified using GraphPad Prism (La Jolla, CA, USA).

5.5 References

1.Sletten, E. M.; Bertozzi, C. R., Bioorthogonal Chemistry: Fishing for Selectivity in a Sea of Functionality. *Angewandte Chemie-International Edition* **2009,** *48* (38), 6974-6998.

2.Patterson, D. M.; Nazarova, L. A.; Prescher, J. A., Finding the Right (Bioorthogonal) Chemistry. *ACS Chemical Biology* **2014,** *9* (3), 592-605.

3.(a) Dehnert, K. W.; Baskin, J. M.; Laughlin, S. T.; Beahm, B. J.; Naidu, N. N.; Amacher, S. L.; Bertozzi, C. R., Imaging the Sialome during Zebrafish Development with Copper-Free Click Chemistry. *Chembiochem* **2012,** *13* (3), 353-357; (b) Baskin, J. M.; Prescher, J. A.; Laughlin, S. T.; Agard, N. J.; Chang, P. V.; Miller, I. A.; Lo, A.; Codelli, J. A.; Bertozzi, C. R., Copper-free click chemistry for dynamic in vivo imaging. *Proc. Natl. Acad. Sci. U. S. A.* **2007,** *104* (43), 16793-16797; (c) Laughlin, S. T.; Baskin, J. M.; Amacher, S. L.; Bertozzi, C. R., In vivo imaging of membrane-associated glycans in developing zebrafish. *Science* **2008,** *320* (5876), 664-667.

4.Vodovozova, E. L., Photoaffinity labeling and its application in structural biology. *Biochemistry-Moscow* **2007,** *72* (1), 1-20.

5.Mahouche-Chergui, S.; Gam-Derouich, S.; Mangeney, C.; Chehimi, M. M., Aryl diazonium salts: a new class of coupling agents for bonding polymers, biomacromolecules and nanoparticles to surfaces. *Chemical Society Reviews* **2011,** *40* (7), 4143-4166.

6.Kieffer, B. L.; Goeldner, M. P.; Hirth, C. G., Aryldiazonium salts as photo-affinity labeling reagents for proteins. *Journal of the Chemical Society-Chemical Communications* **1981,** (9), 398-399.

7.Song, W.; Wang, Y.; Qu, J.; Lin, Q., Selective functionalization of a genetically encoded alkene-containing protein via "Photoclick Chemistry" in bacterial cells. *J. Am. Chem. Soc.* **2008,** *130* (30), 9654-+.

8.Poloukhtine, A. A.; Mbua, N. E.; Wolfert, M. A.; Boons, G.-J.; Popik, V. V., Selective Labeling of Living Cells by a Photo-Triggered Click Reaction. *J. Am. Chem. Soc.* **2009,** *131* (43), 15769-15776.

9.Yao, J. Z.; Uttamapinant, C.; Poloukhtine, A.; Baskin, J. M.; Codelli, J. A.; Sletten, E. M.; Bertozzi, C. R.; Popik, V. V.; Ting, A. Y., Fluorophore Targeting to Cellular Proteins via Enzyme-Mediated Azide Ligation and Strain-Promoted Cycloaddition. *J. Am. Chem. Soc.* **2012,** *134* (8), 3720-3728.

10.(a) Sklar, L. A.; Hudson, B. S.; Simoni, R. D., Conjugated polyene fatty-acids as fluorescent-probes - binding to bovine serum-albumin. *Biochemistry* **1977,** *16* (23), 5100-5108; (b) Wilton, D. C., The fatty-acid analog 11-(dansylamino)undecanoic acid is a fluorescent-probe for the bilirubin-binding sites of albumin and not for the high-affinity fatty acid-binding sites. *Biochemical Journal* **1990,** *270* (1), 163-166.

11.(a) Jeon, O.-H.; Kim, D.; Choi, Y.-J.; Kim, S.-H.; Choi, W.-S.; Kim, D.-S., Novel function of human ADAM15 disintegrin-like domain and its derivatives in platelet aggregation. *Thrombosis Research* **2007,** *119* (5), 609-619; (b) Lin, H.-Y.; Yang, Y.-T.; Yu, S.-L.; Hsiao, K.-N.; Liu, C.-C.; Sia, C.; Chow, Y.-H., Caveolar Endocytosis Is Required for Human PSGL-1-Mediated Enterovirus 71 Infection. *Journal of Virology* **2013,** *87* (16), 9064-9076.

12.(a) Anchordoguy, T. J.; Carpenter, J. F.; Crowe, J. H.; Crowe, L. M., Temperature-dependent perturbation of phosphlipid-bilayers by dimethylsulfoxide. *Biochimica et Biophysica Acta* **1992,** *1104* (1), 117-122; (b) Yu, Z. W.; Quinn, P. J., The modulation of membrane structure and stability by dimethyl sulphoxide (Review). *Molecular Membrane Biology* **1998,** *15* (2), 59-68; (c) Notman, R.; Noro, M.; O'Malley, B.; Anwar, J., Molecular basis for dimethylsulfoxide (DMSO) action on lipid membranes. *J. Am. Chem. Soc.* **2006,** *128* (43), 13982-13983.

13.Smondyrev, A. M.; Berkowitz, M. L., Molecular dynamics simulation of DPPC bilayer in DMSO. *Biophysical Journal* **1999,** *76* (5), 2472-2478.

14.(a) Cunningham, C. W.; Mukhopadhyay, A.; Lushington, G. H.; Blagg, B. S. J.; Prisinzano, T. E.; Krise, J. P., Uptake, Distribution and Diffusivity of Reactive Fluorophores in Cells: Implications toward Target Identification. *Molecular Pharmaceutics* **2010,** *7* (4), 1301-1310; (b) Baumgart, T.; Hunt, G.; Farkas, E. R.; Webb, W. W.; Feigenson, G. W., Fluorescence probe partitioning between L-o/L-d phases in lipid membranes. *Biochimica Et Biophysica Acta-Biomembranes* **2007,** *1768* (9), 2182-2194.

CHAPTER 5

FUTURE DIRECTIONS AND CONCLUSIONS

6.1 Conclusions for Nanoprobe Project

Our experiments with nanoprobe **1** suggest that this photolabile polyamine probe could be potentially targeting calcium permeable AMPARs. This was based on our promising imaging data which showed fluorescence accumulation in areas where AMPARs are known to aggregate and the fact that known AMPAR antagonists could block fluorescence accumulation. However, using SDS-PAGE analysis of neuronal cell lysate labeled with nanoprobe **1** multiple bands were observed (Section 2, Figure 2.9). Taken together, these results suggest that we needed to develop a probe that would be better targeted towards calcium permeable AMPARs.

To allow for identification of specific subunits, we developed nanoprobe **2** which simplified our synthetic design and resulted in a probe which more closely resembles the natural toxin. We also designed nanoprobe **2** so that it would be amendable for proteomic experiments. Nanoprobe **2**, much like nanoprobe **1**, relies on an acrylamide electrophile to bioconjugation to the surface of the receptor. In preliminary imaging experiments, we were able to target the same receptors as nanoprobe **1** as the fluorescence accumulation looked to be similar. We then moved into doing pull-down experiments with nanoprobe **2** labeled neuronal proteins. The result of the gels is that nanoprobe **2** did not label proteins like we saw with nanoprobe **1**. This could be due to the electrophile not being able to find a suitable nucleophillc partner to be able to bind on the surface of the protein.

We then decided to keep the same probe design, but swap out the electrophile for nanoprobe **3**. In this design, we used an aryl azide for our electrophile. The photoactivated aryl azide is more reactive than the acrylamide, [1] so finding a suitable nucleophilic partner should not be an issue. Initial testing of nanoprobe **3** in soluble protein showed that the photolysis and click chemistry conditions work. Moving into

124

neuronal proteins, nanoprobe **3** was, however, found to not bind either. Aryl azides are indiscriminate in their reactivity, and tend to react to their nearest neighbor. In this case, it is possible that the nearest neighbor was a water molecule inside the binding pocket and not the C-H of a proximal amino acid. Without the covalent attachment to the C-H of the nearest amino acid, nanoprobe **3** would simply be washed away by the many wash steps involved in the pull down experiment.

One of the main reasons for why neither nanoprobe **2** nor nanoprobe **3** was able to covalently conjugate to the receptor was mainly due to the position of the electrophile. In nanoprobe **1** the electrophile and the targeting polyamine ligand were separated far from each other as they were on either side of the ANI core. In both nanoprobe **2** and nanoprobe **3** the ligand and the electrophile are much closer to each other, as the ligand is eighteen bonds away from the electrophile in nanoprobe **1** and only nine in nanoprobe **2**, eight in nanoprobe **3**. This placed the electrophile closer into the ligand binding pocket, thus it might have not been able to find a good nucleophilic binding partner or would just bind to water. One way to remedy this would be to move the electrophile away from the targeting ligand.

6.2 Future Directions for Nanoprobes

One of the ways that our nanoprobes can be redesigned is already occurring in the Chambers lab. This is through the use of modular nanoprobes that are able to undergo click chemistry for ligand attachment. The core of these nanoprobes is the same as nanoprobe **1**, except there is an alkyne handle in the ligand attachment point. (Figure 6.1) Attachment of the targeting polyamine ligand has been a very tricky synthetic step in the synthesis of all nanoprobes, but there are other targeting ligands available. These ligands are not polyamine based but still act as use-dependent open ion channel blockers of AMPA receptors and they include molecules such as IEM 1925 and GYKI 52466

(Figure 6.1). These molecules both contain primary amines which could be modified

using a small acyl chain containing an azide for attachment to the nanoprobe scaffold

through click chemistry methods. This would provide us a few new targeting molecules

which keep the electrophile in the same position as nanoprobe **1**.
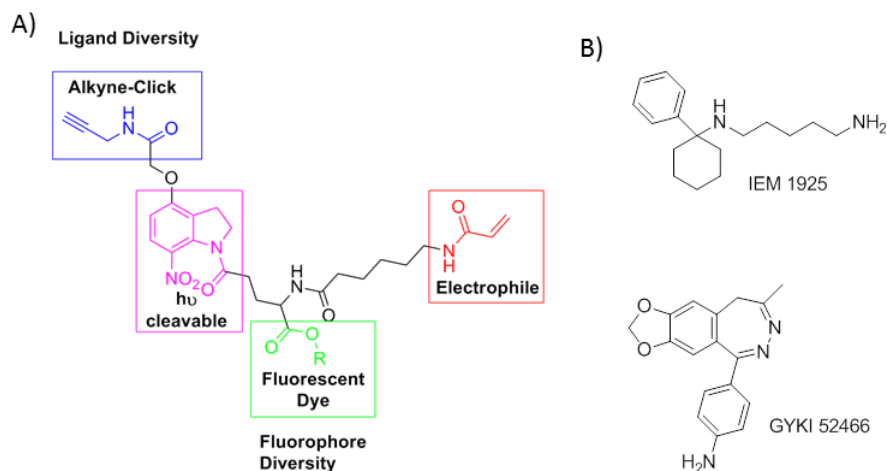
Figure 6.1: Structure of alkyne nanoprobe. A) Structure of alkyne nanoprobe, ANI core (pink) is attached to a carboxylic acid (green) for fluorophore diversity, and an acrylamide electrophile (red). The alkyne handle (blue) allows for ligand diversity. B) AMPA receptor antagonists IEM 1925 and GYKI 52466.

6.2.1 Probe Design of Nanoprobe 4

One of the main reasons we chose the polyamine targeting ligand was due to the

ability of the class of toxins to act as antagonists for calcium permeable AMPARs. A new

probe containing a polyamine would need to move the ligand away from the electrophile

in order for the electrophile to be able to explore similar chemical space to that of

nanoprobe **1**. One way of doing so is to use naphthaleneacetic acid as our core for

attachment of our electrophile, ligand, and reporter tag. (Scheme 6.1) Naphthaleneacetic

acid would first be nitrated and the nitro reduced to an amine for another attachment

point. TriBoc spermine can then be peptide coupled to the carboxylic acid. *Tert*-butyl 5-

((4-acrylamidobutyl)amino)-5-oxo-2-((prop-2-yn-1-ylamino)methyl)pentanoate would be

synthesized from Boc-Glu(OMe)-OH, propargyl bromide, and 6-acrylamidohexanoic

acid. This would then be peptide coupled to naphthaleneacetic acid to produce

nanoprobe **4**.
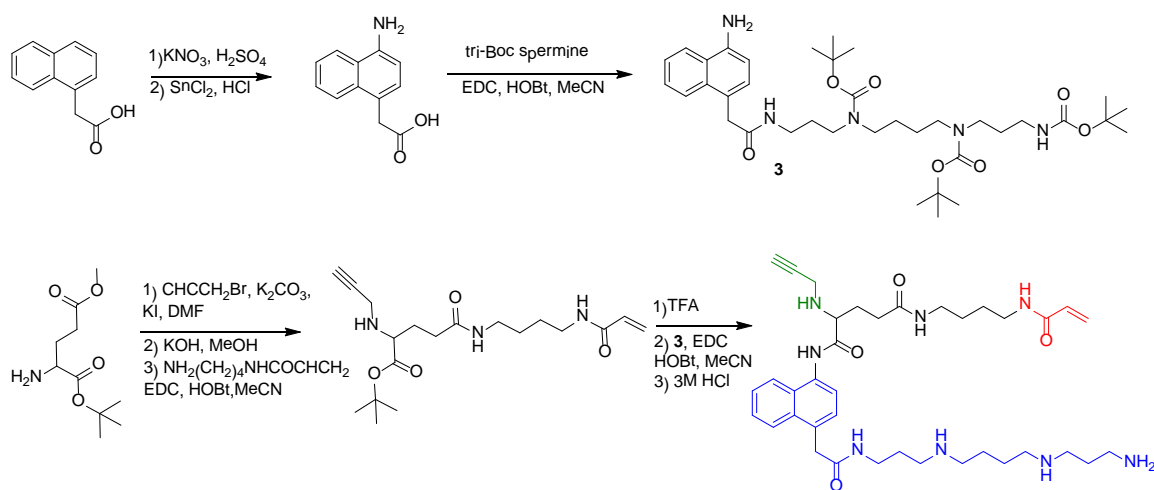
Scheme 6.1: Proposed synthesis for nanoprobe **5**

6.2.2 Quinoxaline Dione Probes for Calcium Permeable AMPAR Detection
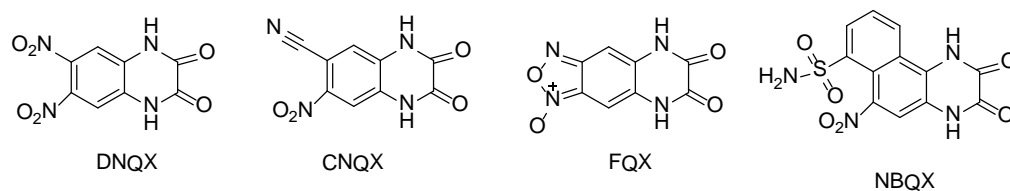
Figure 6.2: Quinoxaline diones

Quinoxaline diones are another class of AMPA receptor antagonists. These

include CBQX, DNQX, and NBQX. (Figure 6.2) Potential probes for the detection of

calcium permeable AMPARs could contain quinoxaline diones, specifically CBQX and

DNQX, as targeting ligands. One way of doing so, would be to attach an azide

containing alkyl chain to the quinoxaline dione and then attach that to either the

nanoprobe scaffold, or to the *ortho*-triazene benzoic acid scaffold.

6.3 Conclusions to the Photogenerated Diazonium Probes

With our photogenerated diazonium probes we wanted to target photolabile bioorthogonal probes to the cell membrane. This was done in an attempt to develop a probe that would have spatial and temporal control of reporter tag attachment to the probe in order to observe biological processes. We chose oleic acid conjugated to *ortho*-triazene benzoic acid to target towards biological membranes and an electron rich aromatic reporter tag. Our first version of the reporter tag used dihydroxyphenyl piperazine (DHPP) conjugated to Cy-3. This reporter tag proved to be membrane permeable as control samples that only contained DMSO also had fluorescence activity. We then altered the nucleophilic reporter to dimethylaminophenyl piperazine (DMAPP) conjugated to Cy-3 as our electron rich aromatic ring. As with the DHPP conjugated reporter tag, the DMAPP reporter tag also crossed the cell membrane in DMSO controls. This could be due to DMSO causing permeablization of cell membrane allowing for the reporter tag to cross the membrane.

We next decided to use a reporter tag that was conjugated with biotin in order to see if the initial concept of photoinducible cell tagging was occurring and was detectable. Biotin was chosen because it can be targeted with an avidin labeled fluorophore, which should not cross the cell membrane. When the targeting probe was photoactivated, the biotin reporter probe will bind, and then be targeted with the avidin-labeled fluorophore. We see this with the new version of the DMAPP probe. Fluorescence is seen only in the UV irradiated samples that contain the probe.

6.4 Future Directions for Photogenerated Probes

One of the main issues that needs to be perfected for the continued use of the photogenerated click probes is the targeting fluorophore. The two scaffolds that were tried were also taken up by the DMSO sham controls cells. These cells had fluorescence

accumulation that was equal to that of the ones that contained the targeting probe. If these probes are to be used further for imaging experiments, the use of a targeting probe that contains a fluorophore that does not cross the cell membrane would be crucial. One way to do so might be to use dyes that are more hydrophobic so they would have a harder time passing through the membrane.

The preliminary work with the photogenerated probes suggests that we can label live cells with our probes in a short time scale. The probes in this case are not ligand directed; rather they are attached to a long chain fatty acid for incorporation to the cell membrane. The next step for these probes would be to attach a targeting ligand to target fluorescence to a particular receptor.

Since we are interested in AMPARs in the Chambers lab, the logical targeting ligand would be one that targets towards AMPARs. The *ortho*-triazene benzoic acid portion of the targeting probe contains an alkyne handle for ligand attachment, so an azide labeled ligand can be attached. In this case, we would try the same panel of azide labeled ligands as listed in Section 6.2 and 6.2.2. (azido IEM 1925, azido GYKI 52466, or an azido containing quinoxaline dione (Figure 6.3)). The acyl azide chain attached to GYKI 52466 is to the pendant phenyl, or as the pharmacophore dictates. Once these probes are synthesized, they can be applied to GluA1 CHO cell and then neurons to see if we can use this new photoclick method to target receptors.
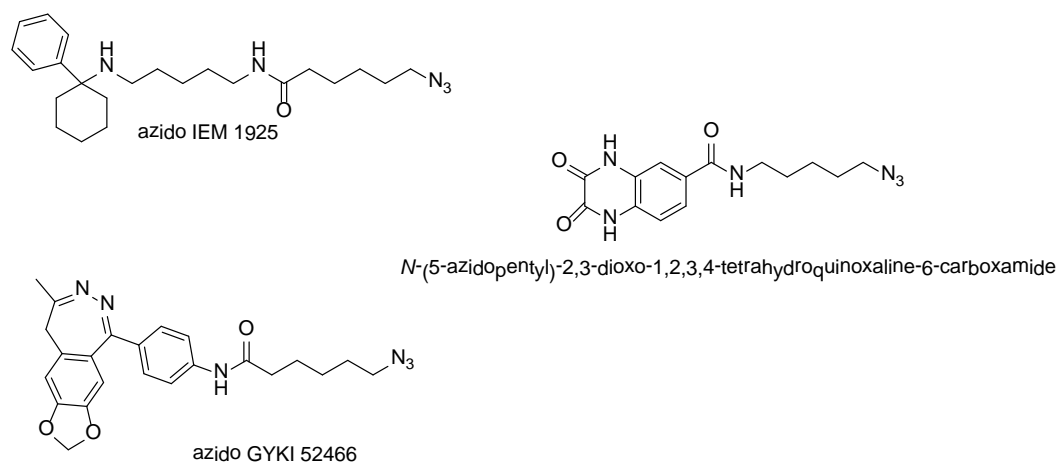
Figure 6.3: Azido functionalized AMPAR analogues,**.**

6.5 References
1.   Vodovozova, E. L., Photoaffinity labeling and its application in structural biology. *Biochemistry-Moscow* **2007,** *72* (1), 1-20.

BIBLIOGRAPHY

Adams, S. R.; Campbell, R. E.; Gross, L. A.; Martin, B. R.; Walkup, G. K.; Yao, Y.; Llopis, J.; Tsien, R. Y., New biarsenical ligands and tetracysteine motifs for protein labeling in vitro and in vivo: synthesis and biological application. *J. Am. Chem. Soc.* **2002,** *124*, 6063-6076.

Adesnik, H.; Nicoll, R. A.; England, P. M., Photoinactivation of native AMPA receptors reveals their real-time trafficking. *Neuron* **2005,** *48* (6), 977-985.

Alder, K.; Stein, G., The polymerisation of cyclic hydrocarbon. IV. About the stereoisomer forms of perhydrate naphto and anthrachinone. *Justus Liebigs Annalen Der Chemie* **1933,** *501*, 247-294.

Andersen, T. F.; Tikhonov, D. B.; Bolcho, U.; Bolshakov, K.; Nelson, J. K.; Pluteanu, F.; Mellor, I. R.; Egebjerg, J.; Stromgaard, K., Uncompetitive antagonism of AMPA receptors: Mechanistic insights from studies of polyamine toxin derivatives. *Journal of Medicinal Chemistry* **2006,** *49* (18), 5414-5423;

Anggono, V.; Huganir, R. L., Regulation of AMPA receptor trafficking and synaptic plasticity. *Current Opinion in Neurobiology* **2012,** *22* (3), 461-469.

Armstrong, N.; Gouaux, E., Mechanisms for activation and antagonism of an AMPA-Sensitive glutamate receptor: Crystal structures of the GluR2 ligand binding core. *Neuron* **2000,** *28* (1), 165-181.

Asami, T.; Kagechika, H.; Hashimoto, Y.; Shudo, K.; Miwa, A.; Kawai, N.; Nakajima, T., Acylpolyamines mimic the action of joro spider toxin (jstx) on crustacean muscle glutamate receptors. *Biomedical Research-Tokyo* **1989,** *10* (3), 185-189.

Auernheimer, J.; Dahmen, C.; Hersel, U.; Bausch, A.; Kessler, H., Photoswitched cell adhesion on surfaces with RGD peptides. *J. Am. Chem. Soc.* **2005,** *127* (46), 16107-16110.

Ban, N.; Escobar, C.; Garcia, R.; Hasel, K.; Day, J.; Greenwood, A.; McPherson, A., Crystal structure of an idiotype-anti-idiotype Fab complex. *Proc. Natl. Acad. Sci. U. S. A.* **1994,** *91*, 1604-1608.

Banke, T. G.; Bowie, D.; Lee, H. K.; Huganir, R. L.; Schousboe, A.; Traynelis, S. F., Control of GluR1 AMPA receptor function by cAMP-dependent protein kinase. *Journal of Neuroscience* **2000,** *20* (1), 89-102.

Bard, L.; Sainlos, M.; Bouchet, D.; Cousins, S. L.; Mikasova, L.; Breillat, C.; Stephenson, F. A.; Imperiali, B.; Choquet, D.; Groc, L., Dynamic and specific interaction between synaptic NR20NMDA receptor and PDZ proteins. *Proc. Natl. Acad. Sci. U. S. A.* **2010,** *107*, 19561-19566.

Barygin, O. I.; Grishin, E. V.; Tilchonov, D. B., Argiotoxin in the Closed AMPA Receptor Channel: Experimental and Modeling Study. *Biochemistry* **2011,** *50* (38), 8213-8220;

Baskin, J. M.; Prescher, J. A.; Laughlin, S. T.; Agard, N. J.; Chang, P. V.; Miller, I. A.; Lo, A.; Codelli, J. A.; Bertozzi, C. R., Copper-free click chemistry for dynamic in vivo imaging. *Proc. Natl. Acad. Sci. U. S. A.* **2007,** *104* (43), 16793-16797;

Bats, C.; Farrant, M.; Cull-Candy, S. G., A role of TARPs in the expression and plasticity of calcium-permeable AMPARs: Evidence from cerebellar neurons and glia. *Neuropharmacology* **2013**, *74*, 76-85;

Beattie, E. C.; Carroll, R. C.; Yu, X.; Morishita, W.; Yasuda, H.; von Zastrow, M.; Malenka, R. C., Regulation of AMPA receptor endocytosis by a signaling mechanism shared with LTD. *Nature Neuroscience* **2000**, *3* (12), 1291-1300;

Bellone, C.; Luscher, C., Cocaine triggered AMPA receptor redistribution is reversed in vivo by mGluR-dependent long-term depression. *Nature Neuroscience* **2006**, *9* (5), 636-641;

Benke, T. A.; Luthi, A.; Isaac, J. T. R.; Collingridge, G. L., Modulation of AMPA receptor unitary conductance by synaptic activity. *Nature* **1998,** *393* (6687), 793-797.

Bhunia, A. J.; Miller, S. C., Labeling tetracysteine-tagged proteins with a SplAsH of color: a modular approach to bis-arsenical flurophores. *Chembiochem* **2007,** *8*, 1642-1625.

Bilimoria, P. M.; Bonni, A., Cultures of cerebellar granule neurons. *CSH protocols* **2008,** *2008*, pdb.prot5107-pdb.prot5107.

Blagbrough, I. S.; Geall, A. J., Practical synthesis of unsymmetrical polyamine amides. *Tetrahedron Letters* **1998,** *39* (5-6), 439-442.

Blaschke, M.; Keller, B. U.; Rivosecchi, R.; Hollmann, M.; Heinemann, S.; Konnerth, A., A single amino-acid determines the subunit-specific spider toxin block of alpha-amino-3-hydroxy-5-methylisoxazole-4-propionate kainate receptor channels. *Proc. Natl. Acad. Sci. U. S. A.* **1993,** *90* (14), 6528-6532.

Bredt, D. S.; Nicoll, R. A., AMPA receptor trafficking at excitatory synapses. *Neuron* **2003,** *40* (2), 361-379.

Bruchez Jr., M.; Moronne, M.; Gin, P.; Weiss, S.; Alivisatos, A. P., Seminconducto nanocrystals as fluorescent biological labels. *Science* **1998,** *281* (5385), 2013-2016.

Brunner, J., New photolabeling and cross-linking methods. *Annual Review of Biochemistry* **1993,** *62*, 483-514.

Bowie, D.; Mayer, M. L., Inward rectification of both AMPA and kainate subtype glutamate receptors generated by polyamine-mediated ion-channel block. *Neuron* **1995,** *15* (2), 453-462.

Cartwright, I. L.; Hutchinson, D. W.; Armstrong, V. W., Reaction between thiols and 8-azidoadenosine derivatives. *Nucleic Acids Research* **1976,** *3* (9), 2331-2339;

Chan, J.; Dodani, S. C.; Chang, C. J., Reaction-based small-molecule fluorescent probes for chemoselective bioimagin. *Nature Chemistry* **2012,** *4*, 973-985.

Chambers, J. J.; Kramer, R. H., Light-Activated Ion Channels for Remote Control of Neural Activity. In *Methods in Nano Cell Biology*, Jena, B. P., Ed. 2008; Vol. 90, pp 217-+.

Chen, L.; Chetkovich, D. M.; Petralia, R. S.; Sweeney, N. T.; Kawasaki, Y.; Wenthold, R. J.; Bredt, D. S.; Nicoll, R. A., Stargazin regulates synaptic targeting of AMPA receptors by two distinct mechanisms. *Nature* **2000,** *408* (6815), 936-943

Choi, S. K.; Kalivretenos, A. G.; Usherwood, P. N. R.; Nakanishi, K., Labeling studies of photolabile philanthotoxins with nicotinic acetylcholine-receptors - mode of interaction between toxin and receptor. *Chemistry & Biology* **1995,** *2* (1), 23-32.

Chung, H. J.; Steinberg, J. P.; Huganir, R. L.; Linden, D. J., Requirement of AMPA receptor GluR2 phosphorylation for cerebellar long-term depression. *Science* **2003,** *300* (5626), 1751-1755.

Combs-Bachmann, R. E.; Johnson, J. N.; Vytla, D.; Hussey, A. M.; Kilfoil, M. L.; Chambers, J. J., Ligand-directed delivery of fluorophores to track native calcium-permeable AMPA receptors in neuronal cultures. *J. Neurochem.* **2015,** *133* (3), 320-329.

Correia, S. S.; Bassani, S.; Brown, T. C.; Lise, M.-F.; Backos, D. S.; El-Husseini, A.; Passafaro, M.; Esteban, J. A., Motor protein-dependent transport of AMPA receptors into spines during long-term potentiation. *Nature Neuroscience* **2008,** *11* (4), 457-466.

Dahan, M.; Lévi, S.; Luccardini, C.; Rostaing, P.; Riveau, B.; Triller, A., Diffusion dynamics of glycine receptors revealed by single-quantum dot tracking. *Science* **2003,** *302*, 442-445.

Dehnert, K. W.; Baskin, J. M.; Laughlin, S. T.; Beahm, B. J.; Naidu, N. N.; Amacher, S. L.; Bertozi, C. R., Imaging the Sialome during Zebrafish Development with Copper-Free Click Chemistry. *Chembiochem* **2012,** *13* (3), 353-357.

Duerr, K. L.; Chen, L.; Stein, R. A.; De Zorzi, R.; Folea, I. M.; Walz, T.; McHaourab, H. S.; Gouaux, E., Structure and Dynamics of AMPA Receptor GluA2 in Resting, Pre-Open, and Desensitized States. *Cell* **2014,** *158* (4), 778-792.

Ehlers, M. D., Reinsertion or degradation of AMPA receptors determined by activity-dependent endocytic sorting. *Neuron* **2000,** *28* (2), 511-525.

Eldefrawi, A. T.; Eldefrawi, M. E.; Konno, K.; Mansour, N. A.; Nakanishi, K.; Oltz, E.; Usherwood, P. N. R., Structure and synthesis of a potent glutamate receptor antagonist in wasp venom. *Proc. Natl. Acad. Sci. U. S. A.* **1988,** *85* (13), 4910-4913.

Eriksen, J.; Rasmussen, S. G. F.; Rasmussen, T. N.; Vaegter, C. B.; Cha, J. H.; Zou, M.-F.; Newman, A. H.; Gether, U., Visualization of dopamine transporter trafficking in live neurons by use of fluroescent cocain analogs. *The Journal of Neuroscience* **2009** *29* (21), 6794-6808.

Fernández-Suárez, M.; Ting, A. Y., Fluorecent probes for super-resolution imaging in living cells. *Nature* **2008,** *9*, 929-946.

Gallagher, S. S.; Jing, C.; Peterka, D. S.; Konate, M.; Wombacher, R.; Kaufman, L. J.; Yuste, R.; Cornish, V. W., A Trimethoprim-Based Chemical Tag for Live Cell Two-Photon Imaging. *Chembiochem* **2010,** *11* (6), 782-784.

Gautier, A.; Juillerat, A.; Heinis, C.; Corrêa Jr., I. R.; Kindermann, M.; Beufils, F.; Johnsson, K., An engineered protein tag for multiprotein labeling in lving cells. *Chemistry & Biology* **2008** *15*, 128-136.

Griffin, B. A.; Adams, S. R.; Jones, J.; Tsien, R. Y., Fluorescent labeling of recombinant proteins in living cells with FlAsH. *Methods Enzymol.* **2000,** *327*, 565-578.

Groc, L.; Heine, M.; Cousins, S. L.; Stephenson, F. A.; Lounis, B.; Cognet, L.; Choquet, D., NMDA receptor surface mobilty depends on NR2A-2B subunits. *Proc. Natl. Acad. Sci. U. S. A.* **2006,** *103* (49), 18769-18774.

Hangauer, M. J.; Bertozzi, C. R., A FRET-based fluorogenic phosphine for live-cell Imaging with the Staudinger ligation. *Angewandte Chemie-International Edition* **2008,** *47* (13), 2394-2397.

Hanley, J. G., PICK1: A multi-talented modulator of AMPA receptor trafficking. *Pharmacology & Therapeutics* **2008,** *118* (1), 152-160.

Hanley, J. G., Subunit-specific trafficking mechanisms regulating the synaptic expression of Ca2+-permeable AMPA receptors. *Seminars in Cell & Developmental Biology* **2014,** *27*, 14-22.

Heine, M.; Groc, L.; Frischknecht, R.; Béïque, J.-C.; Lounis, B.; Rumbaugh, G.; Hugnair, R. L.; Cognet, L.; Choquet, D., Surface mobilty of postsynaptic AMPARs tunes synaptic transmission. *Science* **2008,** *230*, 201-206.

Herlitze, S.; Raditsch, M.; Ruppersberg, J. P.; Jahn, W.; Monyer, H.; Schoepfer, R.; Witzemann, V., Argiotoxin detects molecular differences in AMPA receptor channels. *Neuron* **1993,** *10* (6), 1131-1140.

Higuchi, M.; Stefan, M.; Single, F. N.; Hartner, J.; Rozov, A.; Burnashev, N.; Feldmeyer, D.; Sprengel, R.; Seeburg, P. H., Point mutation in an AMPA receptor gene rescues lethality in mice deficient in the RNA-editing enzyme ADAR2. *Nature* **2000,** *406* (6791), 78-81.

Hollmann, M.; Hartley, M.; Heinemann, S., CA2+ permeability of KA-AMPA gated glutamate channels depends on subunit composition. *Science* **1991,** *252* (5007), 851-853

Hollmann, M.; Heinemann, S., Cloned glutamate receptors. *Annual Review of Neuroscience* **1994,** *17*, 31-108.

Huisgen, R., 1.3-Dipolare cycloadditione - ruckschau und ausblick. *Angewandte Chemie-International Edition* **1963,** *75* (13), 604-+.

Hussey, A. M.; Chambers, J. J., Methods To Locate and Track Ion Channels and Receptors Expressed in Live Neurons. *ACS Chemical Neuroscience* **2015,** *6* (1), 189-198.

Isaac, J. T. R.; Ashby, M.; McBain, C. J., The role of the GluR2 subunit in AMPA receptor function and synaptic plasticity. *Neuron* **2007,** *54* (6), 859-871.

Iqbal, J.; Tangellamudi, N. D.; Dulla, B.; Balasubramanian, S., Sequential C-N and C-O Bond Formation in a Single Pot: Synthesis of 2H-Benzo b 1,4 oxazines from 2,5-Dihydroxybenzaldehyde and Amino acid Precursors. *Organic Letters* **2012,** *14* (2), 552-555.

Jackson, A. C.; Nicoll, R. A., Stargazin (TARP γαμμα-2) is required for compartment-specific AMPA receptor trafficking and synaptic plasticity in cerebellar stellate cells. *The Journal of Neuroscience* **2011,** *31* (11), 3939-3952;

Jackson, A. C.; Nicoll, R. A., The Expanding Social Network of Ionotropic Glutamate Receptors: TARPs and Other Transmembrane Auxiliary Subunits. *Neuron* **2011,** *70* (2), 178-199.

Jewett, J. C.; Bertozzi, C. R., Cu-free click cycloaddition reactions in chemical biology. *Chemical Society Reviews* **2010,** *39* (4), 1272-1279.

Jonas, P.; Racca, C.; Sakmann, B.; Seeburg, P. H.; Monyer, H., Differences in Ca2+ permeablity of AMPA-type glutamate-receptor channels in neocortical neurons cuased by differential GluR-B subunit expression. *Neuron* **1994,** *12* (6), 1281-1289.

Ju, W.; Morishita, W.; Tsui, J.; Gaietta, G.; Deerinck, T. J.; Adams, S. R.; Garner, C. C.; Tsien, R. Y.; Malenka, R. C., Activity-dependant regulation of dendritic synthesis and trafficking of AMPA recepotrs. *Nature Neuroscience* **2004,** *7* (3), 244-254.

Kato, A. S.; Siuda, E. R.; Nisenbaum, E. S.; Bredt, D. S., AMPA receptor subunit-specific regulation by a distinct family of type II TARPs. *Neuron* **2008,** *59* (6), 986-996.

Keppler, A.; Gendreizig, S.; Gronemeyer, T.; Pick, H.; Vogel, H.; Johnsson, K., A general method for the covalent labeling of fusion proteins with small molecules *in vivo*. *Nature Biotechnology* **2003,** *21*, 86-90.

Kim, C. H.; Chung, H. J.; Lee, H. K.; Huganir, R. L., Interaction of the AMPA receptor subunit GluR2/3 with PDZ domains regulates hippocampal long-term depression. *Proc. Natl. Acad. Sci. U. S. A.* **2001,** *98* (20), 11725-11730.

Kobylecki, C.; Cenci, M. A.; Crossman, A. R.; Ravenscroft, P., Calcium-permeable AMPA receptors are involved in the induction and expression of l-DOPA-induced dyskinesia in Parkinson's disease. *J. Neurochem.* **2010,** *114* (2), 499-511.

Koike, M.; Iino, M.; Ozawa, S., Blocking effect of 1-naphthyl acetyl spermine on Ca^{2+} - permeable AMPA receptors in cultured rat hippocampal neurons. *Neuroscience Research* **1997,** *29*, 27-36.

Kostiainen, M. A.; Hardy, J. G.; Smith, D. K., High-affinity multivalent DNA binding by using low-molecular-weight dendrons. *Angewandte Chemie-International Edition* **2005,** *44* (17), 2556-2559.

Kumar, S. S.; Bacci, A.; Kharazia, V.; Huguenard, J. R., A developmental switch of AMPA receptor subunits in neocortical pyramidal neurons. *Journal of Neuroscience* **2002,** *22* (8), 3005-3015.

Kumar, V.; Rahbek-Clemmensen, T.; Billesbolle, C. B.; Jorgensen, T. N.; Gether, U.; Newman, A. H., Novel and High Affinity Fluorescent Ligands for the Serotonin Transporter Based on (S)-Citalopram. *ACS Med. Chem. Lett.* **2014,** *5* (6), 696-699.

Kwak, S.; Hideyama, T.; Yamashita, T.; Aizawa, H., AMPA receptor-mediated neuronal death in sporadic ALS. *Neuropathology* **2010,** *30* (2), 182-188.

Laughlin, S. T.; Baskin, J. M.; Amacher, S. L.; Bertozzi, C. R., In vivo imaging of membrane-associated glycans in developing zebrafish. *Science* **2008,** *320* (5876), 664-667.

Lee, H. K.; Takamiya, K.; Han, J. S.; Man, H. Y.; Kim, C. H.; Rumbaugh, G.; Yu, S.; Ding, L.; He, C.; Petralia, R. S.; Wenthold, R. J.; Gallagher, M.; Huganir, R. L., Phosphorylation of the AMPA receptor GluR1 subunit is required for synaptic plasticity and retention of spatial memory. *Cell* **2003,** *112* (5), 631-643.

Lemieux, G. A.; de Graffenried, C. L.; Bertozzi, C. R., A fluorogenic dye activated by the Staudinger ligation. *J. Am. Chem. Soc.* **2003,** *125* (16), 4708-4709.

Levitsky, K.; Boersma, M. D.; Ciolli, C. J.; Belshaw, P. J., Exo-mechanism proximity-accelerated alkylations: Investigations of linkers, electrophiles and surface mutations in engineered cyclophilin-cyclosporin systems. *Chembiochem* **2005,** *6* (5), 890-899.

Lin, J. W.; Ju, W.; Foster, K.; Lee, S. H.; Ahmadian, G.; Wyszynski, M.; Wang, Y. T.; Sheng, M., Distinct molecular mechanisms and divergent endocytotic pathways of AMPA receptors internalization. *Nature Neuroscience* **2000,** *3* (12), 1282-1290.

Lin, F. L.; Hoyt, H. M.; van Halbeek, H.; Bergman, R. G.; Bertozzi, C. R., Mechanistic investigation of the Staudinger ligation. *J. Am. Chem. Soc.* **2005,** *127* (8), 2686-2695.

Liu, S. H.; Lau, L.; Wei, J. S.; Zhu, D. Y.; Zou, S. W.; Sun, H. S.; Fu, Y. P.; Liu, F.; Lu, Y. M., Expression of Ca2+-Permeable AMPA receptor channels primes cell death in transient forebrain ischemia. *Neuron* **2004,** *43* (1), 43-55.

Liu, D. S.; Phipps, W. S.; Loh, K. H.; Howarth, M.; Ting, A. Y., Quantum Dot Targeting with Lipoic Acid Ligase and Halo Tag for Single-Molecule Imaging on Living Cells. *Acs Nano* **2012,** *6* (12), 11080-11087.

Livet, J.; Weissman, T. A.; Kang, H.; Draft, R. W.; Lu, J.; Bennis, R. A.; Sanes, J. R.; Lichtman, J. w., Transgenic strategies for combinatoral expression of fluorescent proteins in the neurvous system. *Nature* **2007,** *450*, 56-64;

Los, G. V.; Darzins, A.; Karassina, N.; Zimprich, C.; Learish, R.; McDougall, M. G.; Encell, L. P.; Ohana, R. F.; Wood, M. G.; Vidugiris, G.; Zimmerman, K.; Otto, P.; Klaubert, D. H.; Wood, K. V., HaloTag interchangeable labeling technology for cell imaging and protein capture. *Promega Cell Notes* **2005,** (11), 2-6.

Los, G. V.; Encell, L. P.; McDougall, M. G.; Hartzell, D. D.; Karassina, N.; Zimprich, C.; Wood, M. G.; Learish, R.; Ohana, R. F.; Ura, M.; Simpson, D.; Mendez, J.; Zimmerman, K.; Otto, P.; Vidugiris, G.; Zhu, J.; Darzins, A.; Klaubert, D. H.; Bulleit, R. F.; Wood, K. V., HaloTag:A novel protein labeling technology for cell imaging and protein analysis. *ACS Chemical Biology* **2008** *3*(6), 460-468.

Madani, F.; Lind, J.; Damberg, P.; Adams, S. R.; Tsien, R. Y.; Gräslund, A. O., Hairpin structure of biarsenical-tetracysteine motif determined by NMR spectroscopy. *J. Am. Chem. Soc.* **2009,** *131*, 4613-4615.

Mahajan, S. S.; Ziff, E. B., Novel toxicity of the unedited GluR2 AMPA receptor subunit dependent on surface trafficking and increased Ca2+-permeability. *Molecular and Cellular Neuroscience* **2007,** *35* (3), 470-481.

Man, H.-Y., GluA2-lacking, calcium permeable AMPA receptors-inducers of plasticity? *Current Opinion in Neurobiology* **2011,** *21*, 291-298.

Marek, K. W.; Davis, G. W., Transgenic encoded protein photoinactivation (FlAsH-FALI): accute inactivation of synaptotagmin I. *Neuron* **2002,** *36*, 805-813.

McKay, B. E.; Molineux, M. L.; Turner, R. W., Endogenous Biotin in Rat Brain. 2007; Vol. 418, pp 111-128.

Mellor, I. R.; Usherwood, P. N. R., Targeting ionotropic receptors with polyamine-containing toxins. *Toxicon* **2004,** *43* (5), 493-508.

Michalet, X.; Pinaud, F. F.; Bentolila, L. A.; Tsay, J. M.; Doose, S.; Li, J. J.; Sundaresan, G.; Wu, A. M.; Gambhir, S. S.; Weiss, S., Quantum dots for live cell, *in vivo* imagin, and diagnostics. *Science* **2005,** (307), 538-546.

Mok, S.-A.; Lund, K.; LaPointe, P.; Campenot, R. B., A HaloTag method for assesing the retrograde axonl transport of the p75 neurotrophin receptor and other proteins in compartmental cultures of rat sympathetic neurons. *Journal of Neuroscience Methods* **2013,** *241*, 91-104.

Mony, L.; Kew, J. N. C.; Gunthorpe, M. J.; Paoletti, P., Allosteric modulators of NR2B-containing NMDA receptors: molecular mechanisms and therapeutic potential. *British Journal of Pharmacology* **2009,** *157* (8), 1301-1317.

Nagarajan, N.; Quast, C.; Boxall, A. R.; Shahid, M.; Rosenmund, C., Mechanism and impact of allosteric AMPA receptor modulation by the Ampakine (TM) CX546. *Neuropharmacology* **2001,** *41* (6), 650-663.

Neumann, M.; Sampathu, D. M.; Kwong, L. K.; Truax, A. C.; Micsenyi, M. C.; Chou, T. T.; Bruce, J.; Schuck, T.; Grossman, M.; Clark, C. M.; McCluskey, L. F.; Miller, B. L.; Masliah, E.; Mackenzie, I. R.; Feldman, H.; Feiden, W.; Kretzschmar, H. A.; Trojanowski, J. Q.; Lee, V. M. Y., Ubiquitinated TDP-43 in frontotemporal lobar degeneration and amyotrophic lateral sclerosis. *Science* **2006,** *314* (5796), 130-133.

Niphakis, M. J.; Johnson, D. S.; Ballard, T. E.; Stiff, C.; Cravatt, B. F., O-hydroxyacetamide carbamates as highly potent and selective class of endocannabinoid hydrolase inhibitors. *ACS Chemical Neuroscience* **2012,** *3* (5), 418-426.

Nonaka, H.; Tsukiji, S.; Ojida, A.; Hamachi, I., Non-enzymatic covalent protein labeling using a reactive tag. *J. Am. Chem. Soc.* **2007,** *129*, 15777-15779.

Nørager, N. G.; Jensen, C. B.; Rathje, M.; Andersen, J.; Madsen, K. L.; Kristensen, A. S.; Strømgaard, K., Development of a potent fluorescent polyamine toxins and applications in labeling ionotropic glutamate receptors in hippocampal neurons. *ACS Chemical Biology* **2013** *8*(9), 2033-2041.

Ohana, R. F.; Encell, L. P.; Zhao, K.; Simpson, D.; Slater, M. R.; Urh., M.; Wood, K. V., HaloTag7: a genetically engineered tag that enhances bacterial expression of soluble proteins and improves protein purification. *Protein Expression and Purification* **2009,** *68* (1), 110-120.

Ostrowski, K.; Barnard, E. A., Application of isotopically-labelled specific inhibitors as a method in enzyme cytochemistry. *Experimental Cell Research* **1961,** *25* (2), 465-8

Piek, T.; Mantel, P.; Engels, E., Neuromuscular block in insects caused by the venom of the digger wasp philanthus-triangulum. *Comparative and General Pharmacology* **1971,** *2* (7), 317-331;

Piek, T.; Njio, K. D., Neuromuscular block in honeybees by venom of bee wolf wasp (philanthus-triangulum-f). *Toxicon* **1975,** *13* (3), 199-201.

Poulsen, M. H.; Lucas, S.; Stromgaard, K.; Kristensen, A. S., Evaluation of PhTX-74 as Subtype-Selective Inhibitor of GluA2-Containing AMPA Receptors. *Molecular Pharmacology* **2014,** *85* (2), 261-268.

Reardon, J. E.; Crouch, R. C.; Stjohnwilliams, L., Reduction of 3'-azido-3'-deoxythymidine (AZT) and AZT nucelotides by thiols - kinetics and product identification. *Journal of Biological Chemistry* **1994,** *269* (23), 15999-16008.

Richter, J. M.; Whitefield, B. W.; Maimone, T. J.; Lin, D. W.; Castroviejo, M. P.; Baran, P. S., Scope and mechanism of direct indole and pyrrole couplings adjacent to carbonyl compounds: Total synthesis of acremoauxin A and oxazinin 3. *J. Am. Chem. Soc.* **2007,** *129* (42), 12857-12869.

Roche, K. W.; Obrien, R. J.; Mammen, A. L.; Bernhardt, J.; Huganir, R. L., Characterization of multiple phosphorylation sites on the AMPA receptor GluR1 subunit. *Neuron* **1996,** *16* (6), 1179-1188.

Rosenthal, S. J.; Tomlinson, I. D.; Adkins, E. A.; Schroeter, S.; Adams, S.; Swafford, L.; McBride, J.; Wang, Y.; DeFelice, L. J.; Blakely, R. D., Targeting cell surface receptors with ligand-conjugated nanocrystals. *J. Am. Chem. Soc.* **2002,** *124* (12), 4586-4594.

Rostovtsev, V. V.; Green, L. G.; Fokin, V. V.; Sharpless, K. B., A stepwise Huisgen cycloaddition process: Copper(I)-catalyzed regioselective "ligation" of azides and terminal alkynes. *Angewandte Chemie-International Edition* **2002,** *41* (14), 2596-2604.

Sainlos, M.; Tigaret, C.; Poujol, C.; Olivier, N. B.; Bard, L.; Breillat, C.; Thiolon, K.; Choquet, D.; Imperiali, B., Biomimetic divalent ligands for the acute disruption of synaptic AMPAR stabilization. *Nature Chemical Biology* **2011,** *7*, 81-92.

Saxon, E.; Bertozzi, C. R., Cell surface engineering by a modified Staudinger reaction. *Science* **2000,** *287* (5460), 2007-2010.

Schwyzer, R.; Caviezel, M., Para-azido-L- phenylalanine- photo-affinity probe related to tyrosine. *Helvetica Chimica Acta* **1971,** *54* (5), 1395-1401.

Seidenman, K. J.; Steinberg, J. P.; Huganir, R.; Malinow, R., Glutamate receptor subunit 2 serine 880 phosphorylation modulates synaptic transmission and mediates plasticity in CA1 pyramidal cells. *Journal of Neuroscience* **2003,** *23* (27), 9220-9228.

Seki, T.; Yoshino, K.-i.; Tanaka, S.; Dohi, E.; Onji, T.; Yamamoto, K.; Hide, I.; Paulson, H. L.; Saito, N.; Sakai, N., Establishment of a novel fluorescence-based method to evaluate chaperone-mediated autophagy in a single neuron. *PlOs one* **2012,** *7* (2), e31232-e31243.

Shephard, J. D., Memory, plasticity, and sleep- a role for calcium-permeable AMPA receptors? *Frontiers in Molecular Neuroscience* **2012,** *5* (49), 1-5.

Shepherd, J. D.; Huganirl, R. L., The cell biology of synaptic plasticity: AMPA receptor trafficking. In *Annual Review of Cell and Developmental Biology*, 2007; Vol. 23, pp 613-643.

Sletten, E. M.; Bertozzi, C. R., Bioorthogonal Chemistry: Fishing for Selectivity in a Sea of Functionality. *Angewandte Chemie-International Edition* **2009,** *48* (38), 6974-6998.

Sobolevsky, A. I.; Rosconi, M. P.; Gouaux, E., X-ray structure, symmetry and mechanism of an AMPA-subtype glutamate receptor. *Nature* **2009,** *462* (7274), 745-66.

Soto, D.; Coombs, I. D.; Kelly, L.; Farrant, M.; Cull-Candy, S. G., Stargazin attenuates intracellular polyamine block of calcium-permeable AMPA receptors. *Nature Neuroscience* **2007,** *10* (10), 1260-1267.

Speers, A. E.; Cravatt, B. F., Profiling enzyme activities in vivo using click chemistry methods. *Chemistry & Biology* **2004,** *11* (4), 535-546.

 Speers, A. E.; Cravatt, B. F., A tandem orthogonal proteolysis strategy for high-content chemical proteomics. *J. Am. Chem. Soc.* **2005,** *127* (28), 10018-10019.

Squire, L. R.; Darwin, B.; Bloom, F. E.; su Lac, S.; Ghosh, A.; Spitzer, N. C., *Fundamental Neuroscience Third Edition*. 3 ed.; Elisver: Burlington, 2008.

Staudinger, H.; Meyer, J., On new organic phosphorus bonding III Phosphine methylene derivatives and phosphinimine. *Helvetica Chimica Acta* **1919,** *2*, 635-646.

Staros, J. V.; Bayley, H.; Standring, D. N.; Knowles, J. R., Reduction of aryl azides by thiols - implications for use of photoaffinity reagents. *Biochemical and Biophysical Research Communications* **1978,** *80* (3), 568-572.

Straub, C.; Tomita, S., The regulation of glutamate receptor trafficking and function by TARPs and other transmembrane auxiliary subunits. *Current Opinion in Neurobiology* **2012,** *22* (3), 488-495.

Stromgaard, K.; Mellor, I., AMPA receptor ligands: Synthetic and pharmacological studies of polyamines and polyamine toxins. *Medicinal Research Reviews* **2004,** *24* (5), 589-620.

Stromgaard, K.; Jensen, L. S.; Vogensen, S. B., Polyamine toxins: development of selective ligands for ionotropic receptors. *Toxicon* **2005,** *45* (3), 249-254.

Talos, D. M.; Fishman, R. E.; Park, H.; Rebecca, D. F.; Follett, P. L.; Volpe, J. J.; Jensen, F. E., Developmental regulation of alpha-amino-3-hydroxy-5-methyl-4-isoxazole-propionic acid receptor subunit expression in forebrain and relationship to regional susceptibility to hypoxic/ischemic injury. I. Rodent cerebral white matter and cortex. *Journal of Comparative Neurology* **2006,** *497* (1), 42-60.

Tateno, M.; Sadakata, H.; Tanaka, M.; Itohara, S.; Shin, R. M.; Miura, M.; Masuda, M.; Aosaki, T.; Urushitani, M.; Misawa, H.; Takahashi, R., Calcium-permeable AMPA receptors promote misfolding of mutant SOD1 protein and development of amyotrophic lateral sclerosis in a transgenic mouse model. *Hum. Mol. Genet.* **2004,** *13* (19), 2183-2196.

Thomas, G. M.; Huganir, R. L., Mapk cascade signalling and synaptic plasticity. *Nature Reviews Neuroscience* **2004,** *5* (3), 173-183.

Tikhonov, D. B., Ion channels of glutamate receptors: structural modeling. *Molecular Membrane Biology* **2007,** *24* (2), 135-64.

Tomita, S.; Chen, L.; Kawasaki, Y.; Petralia, R. S.; Wenthold, R. J.; Nicoll, R. A.; Bredt, D. S., Functional studies and distribution define a family of transmembrane AMPA receptor regulatory proteins. *Journal of Cell Biology* **2003,** *161* (4), 805-816.

Tomlinson, I. D.; Gies, A. P.; Gresch, P. J.; Dillard, J.; Orndorff, R. L.; Sanders-Bush, E.; Hercules, D. M.; Rosenthal, S. J., Universal polyethylene gycol linkers for attaching receptor ligands to quantum dots. *Bioorganic & Medicinal Chemistry Letters* **2006,** *16* (24), 6262-6266.

Tsien, R. Y., The green fluorescent protein. *Annual Review of Biochemistry* **1998,** *67*, 509-544.

Tully, S. E.; Cravatt, B. F., Activity-Based Probes That Target Functional Subclasses of Phospholipases in Proteomes. *J. Am. Chem. Soc.* **2010,** *132* (10), 3264-75.

Ungless, M. A.; Whistler, J. L.; Malenka, R. C.; Bonci, A., Single cocaine exposure in vivo induces long-term potentiation in dopamine neurons. *Nature* **2001,** *411* (6837), 583-587.

Uzunova, G.; Hollander, E.; Shepherd, J., The Role of Ionotropic Glutamate Receptors in Childhood Neurodevelopmental Disorders: Autism Spectrum Disorders and Fragile X Syndrome. *Current Neuropharmacology* **2014,** *12* (1), 71-98.

Vodovozova, E. L., Photoaffinity labeling and its application in structural biology. *Biochemistry-Moscow* **2007,** *72* (1), 1-20.

Vytla, D.; Combs-Bachmann, R. E.; Hussey, A. M.; Hafez, I.; Chambers, J. J., Silent, fluorescent labeling of native neuronal receptors. *Organic & Biomolecular Chemistry* **2011,** *21* (9), 7151-7161.

Weiss, J. H., Ca^{2+} permeable AMPA channels in disease of the nervous system. *Frontiers in Molecular Neuroscience* **2011,** *4* (42), 1-7.

Willems, L. I.; Overkleeft, H. S.; van Kasteren, S. I., Current Developments in Activity-Based Protein Profiling. *Bioconjugate Chemistry* **2014,** *25* (7), 1181-1191.

Wittig, G.; Krebs, A., *Chem. Ber.* **1961,** *94*, 3260.

Wright, A.; Vissel, B., The essential role of AMPA receptor GluA2 subunit RNA editing in the normal and diseased brain. *Frontiers in Molecular Neuroscience* **2012,** *5* (34), 1-13.

Wolf, M. E.; Tseng, K. Y., Calcium-permeable AMPA receptors in the VTA and the nucleus accumbens after cocaine exposure: when, how, and why? *Frontiers in Molecular Neuroscience* **2012,** *5* (72), 1-27.

Xiong, X.; Strømgaard, K., Polyamine Toxins from Spiders and Wasps. In *Polyamines*, Kusano, T.; Suzuki, H., Eds. Springer Japan: 2015; pp 201-214.

Xu, B.; Huang, Z.; Liu, C.; Cai, Z.; Pan, W.; Cao, P.; Hao, X.; Liang, G., Synthesis and anti-hepatitis B virus activities of Matijing-Su derivatives. *Bioorganic & Medicinal Chemistry* **2009,** *17* (8), 3118-3125.

Yin, H. Z.; Weiss, J. H., Zn2+ permeates Ca2+ permeable AMPA kainate channels and triggers selective neural injury. *Neuroreport* **1995,** *6* (18), 2553-2556.

Zach, G. W.; Rogers, W. E.; Latt, S. A., Automatic measurements of sister chromatid exchange frequencies. *J. Histochem. Cytochem.* **1977,** *25* (7), 741-53.

Zhang, P.; Jørgensen, T. N.; Loland, C. J.; Newman, A. H., A rhodamine-labeld citalopram analogue as a high-affinity fluorescent prove for the seratonin transporter. *Bioorganic & Medicinal Chemistry Letters* **2013,** *23*, 323-326.

Zuber, B.; Nikonenko, I.; Klauser, P.; Muller, D.; Dubochet, J., The mammalian central nervous synaptic cleft contains a high density of periodically organized complexes. *Proc. Natl. Acad. Sci. U. S. A.* **2005,** *102* (52), 19192-19197